Metabolism in Hepatocytes and Adipocytes under inhibition of carbonic anhydrases studied with multinuclear NMR-spectroscopy

DISSERTATION
Zur Erlangung des Grades eines
Doktors der Naturwissenschaften
-Dr. rer. nat-

Dem Fachbereich Biologie/Chemie der
Universität Bremen
vorgelegt von

Abolghasem Mohammadi

Bremen

Juni 2009

1. Gutachter: Prof. Dr. Dieter Leibfritz

2. Gutachter: Prof. Dr. Herbert Thiele

For my wife

Acknowledgement

I would like to acknowledge and extend my heartfelt gratitude to my supervisor Prof. Dr. Dieter Leibfritz, who introduced me into this interesting and exciting research project under exclusive working conditions for achievement of my thesis. I would like to mention his excellent efforts for providing me with the opportunity to present a part of my results in scientific journals and in European and international conferences.

I am indebted very much to Solvay Pharmaceuticals GmbH, who supported my thesis with a fellowship and supply of chemicals.

I also like to thank Prof. Dr. Herbert Thiele, Prof. Dr. Wolf-Dieter Stohrer, Dr. Wieland Willker, Miss Jane Mißler and Mr. Markus Plaumann to review this thesis and be member of the graduation committee.

I am very thankful to Dr. Claudia Zwingmann for the careful reading and review of my thesis.

I wish to thank Dr. Wieland Willker and Dipl.-Ing. Johannes Stelten for assistance with NMR spectroscopic problems and their friendly explanations.

My special thanks go to my wife Tayebeh for her moral support, advices, infinite patience and love in the time of my Ph.D. thesis. Without her, I would have been unable to overcome the time of my Ph.D. thesis.

I am very glad to thank Miss Ingrid Killer for organisation and preparation of materials, which I required in the cell labour.

Finally, I like to thank all my colleagues (Jessica Heins, Frauke Nehen, Michaela Hohnholt, Miriam Schwalbe-Herrmann, and others) in the department of chemistry for their continuous support and pleasant ambience.

ABBREVIATIONS

ACC	acetyl-CoA carboxylase
ACL	ATP-citrate lyase
ACT	acetazolamide
ADP	adenosinediphosphate
Ala	alanine
ALT	alanine aminotransferase
Asn	asparagine
ATP	adenosinetriphosphate
BSA	bovine serum albumine
CA	carbonic anhydrase
CAII	carboxyanhydrase subtype 2
CAIs	carbonic anhydrase inhibitors
CAV	carboxyanhydrase subtype 5
CS	calf serum
DHAP	dihydroxyacetone phosphate
DMEM	dulbecco´s modified eagle´s medium
DMSO	dimethylsulfoxid
DNL	*de novo* lipogenesis
EDTA	ethylendiaminetetraacetate
ETZ	ethoxyzolamide
FAS	fatty acid synthetase
FBS	fetal bovine serum
FID	free induction decay
FT	fourier transformation
Glc	glucose
Gln	glutamine
Glu	glutamate
Glyd	glyceraldehydes-3-phopsphate
His	histidine
HSQC	heteronuclear single quantum coherence
IC	inhibitory concentration
α-KG	α-ketoglutarate
Lac	lactate
LDH	lactate dehydrogenase
MCT1	monocarboxylic acid transporter 1
me	malic enzyme
n.a	natural abundance
n.d	not detectable
NMR	nuclear magnetic resonance
NDP	nucleosidediphosphate
NTP	nucleosidetriphosphate
OAA	oxaloacetate
P_i	inorganic phosphate
pc	pyruvate carboxylase
PCA	perchloric acid
PCr	phosphocreatine
pdh	pyruvate dehydrogenase
PEP	phosphoenolpyruvate
PK	pyruvate kinase
ppm	part per million
P/S	penicillin/streptomycine
Pyr	pyruvate
RF	radiofrequency
TCA	tricarboxylic acid
Thr	threonine
TPM	topiramate
TSP	trimethylsilylpropionic-2,2,3,3,-d_4-acid

Content

Chapter 1

1 SUMMARY 9

1 ZUSAMMENFASSUNG 13

Chapter 2

2 INTRODUCTION 17

2.1 Reversible hydration of CO_2 20

2.2 Carbonic anhydrases 21

2.2.1 Overview of the carbonic anhydrase isozymes and their functions 22

2.2.2 Structure and mechanism of CA 23

2.3 Carbonic anhydrase inhibitors (CAIs) 26

2.4 Use of carbonic anhydrase inhibitors for the inhibition of *de novo* fatty acid synthesis 27

2.5 Aims of the study 29

Chapter 3

3 RESULTS AND DISCUSSION 30

3.1 Introduction 30

3.2 Determination of IC50 of CAIs in first group for inhibition of DNL 31

3.3 Glucose metabolism in 3T3-L1 32

3.3.1 Introduction 32

3.3.2 Alteration of glutamate 33

3.3.3 ^{13}C-isotopomer pattern in glutamate (*pc* and *pdh*) 35

3.3.4 Effect of CAIs on lactate and alanine synthesises 36
3.4 The effect of CAIs on *de novo* lipogenesis in 3T3-L1 cells 38
3.5 Study of effect of CAIs on HEP-G2 cells 40
3.5.1. Introduction 40
3.5.2. Metabolites in HEP-G2 cells 40
3.5.2.1 Glucose metabolism in HEP-G2 cells 40
3.5.2.2. The effect of CAIs on DNL in HEP-G2 cells 41
3.5.2.3. Effect of compound **1** on alteration of the cellular energy status 42
3.5.3. Study of effect of compound **1** on HEP-G2 cells incubated with [2-^{13}C]- or [3-^{13}C]pyruvate and [2-^{13}C]acetate 45
3.5.3.1. Introduction 45
3.5.3.2. Effect of compound **1** on HEP-G2 cells, incubated with [2-^{13}C]- or [3-^{13}C]pyruvate 45
3.5.3.2.1 The effect of compound **1** on DNL in the presence of [2-^{13}C]- or [3-^{13}C]pyruvate 46
3.5.3.2.2 Effect of compound **1** on HEP-G2 cells incubated with [2-^{13}C]acetate 47
3.6. Discussion 49
3.7. Study of effect of new carbonic anhydrase inhibitors in in *de novo* lipid synthesis and TCA cycle-related amino acid glutamate with ^{13}C-NMR spectroscopy 52
3.7.1. Introduction 52
3.7.2 Determination of IC_{50} of CAIs in second group of CAIs 52
3.7.3. Cellular metabolism in HEP-G2 cells in the presence of new CAIs 54
3.7.4. Effect of CAIs on lactate and alanine synthesises 55
3.7.5. The effect of the new carbonic anhydrase inhibitors on DNL 56
3.8. Comparing the inhibitory effect of compound 5 and compound 1 58
3.8.1 Introduction 58
3.8.2 Comparing the inhibitory effect of CAIs on glucose metabolism 58
3.8.3 Comparing the effect of CAIs on acetate metabolism 60
3.8.4 Comparing the effect of compound **1** and compound **5** on DNL 61
3.8.5 Effect of compound **1** and compound **5** on the cellular energy status 62

Chapter 4

4 METHODS 63

Introduction 63

4.1 Cell culture 63

4.1.1 Definition 63

4.1.2 Preparation of cell cultures 63

4.2 Introduction to experimental procedures 64

4.2.1 Incubation procedure 64

4.2.2 Preparation of perchloric acid and lipid extracts 65

4.2.3 Determination of IC_{50}-values 66

4.3 Protein determination methods 67

4.3.1 UV/VIS spectroscopy 67

4.3.2 Biuret-method 67

4.3.3 Lowry-method 67

4.4 NMR spectroscopy 68

Introduction 68

4.4.1 Theory of NMR spectroscopy 69

4.4.2 Multinuclear high-resolution NMR spectroscopy 71

4.4.2.1 Preparation of samples 71

4.4.2.2 Acquisition- and processing parameter of NMR spectra 71

4.4.2.2.1 ^{1}H-NMR spectroscopy 71

4.4.2.2.2 ^{13}C-NMR spectroscopy 71

4.4.3 Identification of metabolites from 1H- and ^{13}C-NMR spectra 72

4.4.3.1 Analysis of ^{13}C isotopomer from ^{13}C-NMR spectra of cell extracts 73

- Metabolic fate of [U-^{13}C]glucose 74

- Metabolic fate of [2-^{13}C]pyruvate 74

- Metabolic fate of [3-^{13}C]pyruvate 75

- Metabolic fate of [2-^{13}C]acetate 76

4.4.3.2 Quantitative analysis of ^{13}C-NMR spectra 76

4.4.3.3 ^{13}C isotopomer analysis of ^{13}C-NMR spectra of lipid extracts 78

4.4.3.4 Determination of relative amount of metabolites using ^{13}C-NMR spectra 80

Chapter 5

5 REFERENCES 81

Chapter 6

6 APPENDIXES 90

6.1 Glial Metabolism of Isoleucine 91

6.2 Glial Metabolism of Valine 102

6.3 Molecular structure of sulphonamids with Carboanhydrase inhibitory effects 111

Chapter 1

Summary

Obesity is defined as an intense overweight condition and is an increasingly serious problem for the health of population, particularly in the modern Western countries. The excessive body weight is associated with various diseases, especially cardiovascular diseases, diabetes mellitus type 2, certain types of cancer, sleep apnea, and osteoarthritis. As a result, obesity is one of the primary avoidable reasons of death worldwide and with rates of adult and childhood obesity increasing, it can be viewed as one of the most serious public health problem of the 21st century. There are therefore already a number of therapeutic procedures aimed at the treatment or prophylaxis of obesity. Lipase-inhibitory compounds are one example to be mentioned, which reduce lipolysis in the intestinal tract and consequently cut down the energy yield from the food intake. The other novel therapeutic procedure for the treatment and/or prophylaxis of obesity, which can complement the previously known form of therapy, intends the inhibition of *de novo* lipogenesis (DNL). DNL means the synthesis of endogenous fatty acids from carbohydrate in the mammalian organism. DNL is a cytosolic process but it is based on the TCA cycle, a mitochondrial process. There are various conceivable possibilities to inhibite DNL in mammalian cells, all of which aim to reduce the turnover of the TCA cycle. The inhibition of carbonic anhydrases (CAs) isozymes involving in several steps of the *de novo* lipogenesis can inhibit the DNL. The CAs catalyze a very simple physiological reaction, the interconversion of carbon dioxide and bicarbonate. It is comprehensible that inhibition of mitochondrial CA (i.e. CA V) and/or cytosolic CA (i.e. CA II) subsequently affect pyruvate carboxylation. The carbohydrates are not only used to synthesis lipids, but also TCA cycle intermediates and TCA cycle related amino acids such as glutamate.

Sulphonamide/ Sulphamate are carbonic anhydrase inhibitors (CAIs) and good candidates to inhibit DNL on the step of pyruvate carboxylation in mitochondria and/or in cytosol. Inhibition of CA will reduce the influx into the anaplerotic activity of pyruvate carboxylase (*pc*) and subsequently into the citric acid (TCA) cycle, which will modify the intermediates of

the TCA cycle and its effluxes (in particular glutamate) and lipid synthesis. The inhibition of carboanhydrase affects also the synthesis of alanine and lactate.
To study the effect of CAIs upon the synthesis of lipids and other metabolites in HEP-G2 and 3T3-L1 cells multinuclear NMR spectroscopy was used. To investigate the effect of CAIs on the cellular metabolism, the HEP-G2 and 3T3-L1 cells were incubated for 6, 12, or 24h in the presence or absence of CAIs, and metabolic alterations of labeled substrates (i.e. [U-^{13}C]glucose , [3-^{13}C]- and [2-^{13}C]pyruvate) were followed up using NMR spectroscopy.

The data of the present study clearly show that topiramate (TPM) and acetazolamide (ACT) are nonspecific inhibitors of CA isozymes ($IC_{50} \geq 1000$ μM), but DNL in the presence of lower concentrations of ethoxyzolamide (ETZ) (13-100 μM) is more effectively inhibited ($IC_{50} \approx 120$ μM). The results also show that compound **1** (a newly synthesised sulfonamide) is a very efficient candidate ($IC_{50} \approx 50$μM) to inhibit CA II and CA V and possibly also other CA isozymes.
After incubation of HEP-G2 and 3T3-L1 cells with ^{13}C-labelled substrates (i.e. glucose, pyruvate, and acetate) the ^{13}C-label of these tracers was found mainly in glutamate within cell extracts and media, whether CAI was present or not. Inhibition of CA II and CA V decreases the anaplerotic influx of labelled glucose and labelled pyruvate into the TCA cycle. The reduced influx of labelled tracers via *pc* leads to a decrease of *de novo* synthesis of glutamate. The results of this study show that the influx of labelled glucose into the TCA cycle via *pc* is strongly reduced in the presence of compound **1**. The results of the study show also that the influx of labelled glucose into the TCA cycle via pyruvate dehydrogenase (*pdh*) is reduced in the presence of compound **1**.

To investigate the effect of compound **1** on *pdh*, the HEP-G2 cells were incubated with [2-^{13}C]acetate in the presence or absence of compound **1** for 6h and the metabolic alteration were determined using NMR spectroscopy. Acetate enters the TCA cycle independent of *pdh*. The data of this study show that in the cell extract analysis of the C4-gultamate signal surprisingly shows a 70% increase of labelled glutamate in the presence of 50μM compound **1** as compared to control. These results suggest that compound **1** has a direct inhibitory effect on *pdh.*

The data of this study show also that compound **1** has no effect on DNL, if labelled acetate is used as tracer. Therefore, the effect of compound **1** on DNL operates at the level of CA V and/or CA II and not at the level of acetyl-CoA carboxylase (ACC).

The results of the study with [U-^{13}C]glucose confirm the very high susceptibility of the energy-status in HEP-G2 cells to compound **1** as concluded from the decreased high energy phosphates using ^{31}P-NMR spectroscopy. 100 µM compound **1** lead to an increase of lactate to 1300-3500% of control in HEP-G2 cells. This result indicates that the cells use glycolysis to produce more ATP, since 100 µM compound **1** also lead to a 100% reduction of *pc* activity.

HEP-G2 cells were also incubated for 6h with compound **5** (another newly synthesised sulfonamide) and three follower compounds of compound **1** (i.e. compound **2**, compound **3**, compound **4**) or drug vehicle (0.1% DMSO) to study the CA inhibitory effect on bicarbonate fixation in cultured HEP-G2 cells. The results of this study clearly show that compound **5** is the most efficient CAI whereas the followers of compound **1** are mediocer CAIs for DNL.
DNL is inhibited to 100% in the presence of 50 µM compound **5** or 100 µM compound **1**, thus the effects of 50 µM compound **5** on bicarbonate fixation in cultured HEP-G2 cells is comparable with the inhibitory effect of 100 µM compound **1**. The HEP-G2 cells were incubated in the presence of CAIs or drug vehicle (0.1% DMSO) for control with [U-^{13}C]glucose for 6 or 24h. The results of this study show that after 6h the effect of 50 µM compound **5** and 100 µM compound **1** on the glucose influx into the TCA cycle via *pc* and on *pdh* are similar. However after 24h in the presence of 50 µM compound **5**, the influx of labelled glucose into the TCA cycle via *pc* is decreased by only 20% and *pdh* activity is not affected, whereas after 24h the *pc* and *pdh* activities are reduced in the presence of 100 µM compound **1** to 100% and 80% of control respectively.

The results of experiments with [2-^{13}C]acetate in the presence of compound **5** show that compound **5** has possibly an indirect inhibitory effect on *pdh*. The results of this study also show that, similar to compound **1**, the effect of compound **5** on DNL is at the level of CA and not at the level of acetyl-CoA carboxylase.

To study the effect of compound **5** on the energy status of HEP-G2 cells, the cells were incubated with labelled glucose in the presence of compound **5** for 24h. The results of this study indicate also that the decrease in TCA cycle intermediates in the presence of compound **5** is not strong enough to change the energy charge of these cells after 24 hours. Thus, sufficient ATP for ATP citrate-lyase seems to be present in these cells after 24h treatment with compound **5**.

Kapitel 1

Zusammenfassung

Adipositas ist definiert als ein Zustand intensiven Übergewichts und ist insbesondere in den entwickelten Industrienationen ein zunehmend ernsthaftes Problem für die Gesundheit der Bevölkerung. Übermäßiges Körpergewicht steht im Zusammenhang mit verschiedenen Krankheiten, insbesondere Herz-Kreislauf-Erkrankungen, Diabetes mellitus Typ II, bestimmte Arten von Neoplasien, Schlafapnoe und Arthrose. Des Weiteren zählt Adipositas zu den wichtigsten vermeidbaren Todesursachen in der Welt. Mit der Zunahme des prozentualen Bevölkerungsanteils übergewichtiger Erwachsener und Kinder, kann es als eines der wichtigsten Probleme für die Gesundheit der Nationen im 21. Jahrhundert angesehen werden. Es gibt bereits eine Reihe von therapeutischen Verfahren zur Behandlung und/oder zur Prophylaxe von Adipositas. So sind z.B. Lipase hemmende Verbindungen bekannt, die die Fähigkeit besitzen, die Fettspaltung im Darmtrakt zu reduzieren und auf diese Weise den Energiegewinn aus der aufgenommenen Nahrung zu erniedrigen. Ein anderes neuartiges therapeutisches Verfahren zur Behandlung und/oder zur Prophylaxe von Adipositas ist die Verwendung von *de novo* Lipogenese (DNL) hemmenden Verbindungen, so dass der Aufbau von Fettsäuren aus Kohlenhydraten im Organismus verringert wird. Die DNL ist eine Aufbaureaktion, die im Cytosol der Körperzellen stattfindet und auf den Citratzyklus basiert, welcher wiederum in den Mitochondrien stattfindet. Damit sind verschiedene Möglichkeiten denkbar, die DNL in Säugetierzellen zu hemmen. Diese zielen alle darauf ab, den im Citrat Zyklus anfallenden Stoffumsatz herabzusetzen. So kann die Inhibierung von Carboanhydrase (CA) Isozymen, welche an den verschiedenen Schritten der DNL beteiligt sind, zur Reduzierung der DNL führen. Carboanhydrasen katalysieren ein sehr einfaches Gleichgewicht zwischen Kohlendioxid und Hydrogencarbonat. Anschließend beeinflussen die mitochondriale Carboanhydrase, der Subtypen V (CA V) sowie cytosolische Carboanhydrase, der Subtypen II (CA II), die Carboxylierung von Pyruvat. Carboanhydrasen sind nicht nur zur DNL notwendig, sondern auch zur Produktion von Zwischenprodukten des Citratzyklus und zur Synthese Citratzyklus-abhängiger Aminosäuren, besonders Glutamat.

Sulfonamide und Sulfamate sind Carboanhydrase-Inhibitoren (CAIs) und bieten sich für die Unterbindung der Pyruvat Carboxylierung und damit für die Hemmung der DNL an. Die Inhibierung von CA führt zu einer Verminderung der anaplerotischen Aktivität der Pyruvat Carboxylase (*pc*), wodurch es zu einer Verringerung der Zwischenprodukte des Citratzyklus kommt und damit auch zu geringeren Gehalten an Citratzyklus-abhängigen Aminosäuren (insbesondere Glutamat), sowie einer verminderten Lipid-Synthese. Die Hemmung von Carboanhydrasen beeinflusst außerdem die Bildung von Lactat und Alanin.

Zur Untersuchung der Wirkung von CAIs auf die Synthese von Lipiden und anderen Metaboliten in HEP-G2 und 3T3-L1 Zellen wurde die multinukleare NMR-Spektroskopie verwendet. Um die Effekte von CAIs auf den Zellstoffwechsel zu untersuchen, wurden die HEP-G2 und 3T3-L1 Zellen für 6, 12 und 24 Stunden in der Anwesenheit oder Abwesenheit von CAIs inkubiert und metabolische Änderungen mit Hilfe markierter Substratmoleküle z.B. [U-^{13}C]Glukose, [3-^{13}C] - und [2-^{13}C]Pyruvat mit Hilfe der NMR-Spektroskopie analysiert.
Um die Effekte von CAIs allein auf die Pyruvat Dehydrogenase (*pdh*) zu untersuchen, wurden die HEP-G2 Zellen für 6 Stunden mit [2-^{13}C]Acetat in der Anwesenheit oder Abwesenheit von CAIs inkubiert und die Änderung der Metabolite des [2-^{13}C]Acetats ebenfalls mit Hilfe der NMR-Spektroskopie festgestellt.
Die Ergebnisse der vorliegenden Studie zeigen deutlich, dass Topiramat und Acetazolamid unspezifische CA-Iinhibitoren sind (IC_{50} über 1000 μM), während Ethoxyzolamid in wesentlich niedrigeren Konzentrationen (13-100 μM) die DNL effektiv hemmt (IC_{50} ≈120 μM). Die Ergebnisse zeigen auch, dass Verbindung **1** (ein neues synthetisches Sulfonamid) ein sehr wirksamer Kandidat (IC_{50} ≈ 50μM) für die Hemmung der CA II und CA V und möglicherweise auch andere CA Isoenzyme ist.

Die Folgeprodukte der verwendeten ^{13}C-makierten Substrate zum Nachweis der TCA Zyklus-Aktivität in Anwesenheit bzw. Abwesenheit von CAIs wurden vorwiegend in den gebildeten Isotopomeren des Glutamats untersucht. Wird die Pyruvatcarboxylase (*pc*) gehemmt, führt dies zu einem Rückgang der *de-novo*-Synthese von Glutamat. Die Ergebnisse dieser Studie zeigen, dass der Eintritt der Abbauprodukte markierter Glucose in den TCA-Zyklus über *pc* in Anwesenheit von Verbindung **1** stark abnimmt, ebenso wie über die Pyruvatdehydrogenase (*pdh*). Um zu untersuchen ob Verbindung **1** direkt oder indirekt auf *pdh* wirkt, wurden die metabolischen Änderungen in HEP-G2 Zellen nach 6 Stunden Inkubation mit [2-^{13}C]Acetat

untersucht, denn Acetat gelangt unabhängig von *pdh* in den TCA Zyklus. Die Ergebnisse der Experimente mit Acetat zeigen, dass in Anwesenheit von Verbindung **1** sogar 70% mehr markiertes Glutamat produziert wurde als in der Kontrolle. Verbindung **1** wirkt sich daher direkt auf die *pdh* Aktivität aus.
Darüber hinaus bestätigten die Ergebnisse, dass Verbindung **1** keinen Effekt auf die DNL hat, wenn Acetat als markierte Substanz aufgenommen wurde. Daher erfolgt die Wirkung von Verbindung **1** auf die DNL auf der Stufe von CA V und/oder CA II und nicht auf der Stufe von Acetyl-CoA Carboxylase (ACC).

Darüber hinaus belegen die Ergebnisse eine höhere Anfälligkeit des Energiestatus in HEP-G2 Zellen gegenüber Verbindung **1**. Dies wurde aus der Abnahme der energiereichen Phosphate mit Hilfe der ^{31}P-NMR-Spektroskopie ermittelt. Ferner führen 100 µM Verbindung **1** zu einem Anstieg von Lactat auf 1300-3500% in HEP-G2 Zellen. Dies deutet darauf hin, dass die Zellen diesen Weg zur Produktion von ATP einsetzen, zumal 100 µM Verbindung **1** zu einer 100 %igen Hemmung von *pc* führen.

Zur vergleichenden Untersuchung der inhibitorischen Wirkung von Verbindung **5** und von drei synthetischen Folgeprodukten von Verbindung **1** (d.h. Verbindung **2**, Verbindung **3** und Verbindung **4**) auf die Bikarbonat-Fixierung in kultivierten HEP-G2-Zellen wurden die Zellen mit den verschiedenen CAIs oder DMSO (0,1%) für 6 Stunden inkubiert. Die Ergebnisse dieser Untersuchungen zeigen deutlich, dass Verbindung **5** der bei weitem wirksamste CA-Inhibitor ist, während die Folgeprodukte von Verbindung **1** eher konventionelle CAI-Wirkstärke erreichen.

Ferner wurden die Auswirkungen von 50 µM Verbindung **5** mit 100 µM Verbindung **1** auf die Bikarbonat-Fixierung bzw. die DNL in HEP-G2 Zellen nach 6 bzw. 24 Stunden Inkubation [U-^{13}C]Glucose verglichen. Die Ergebnisse dieser Untersuchungen zeigen, dass nach 6-stündiger Inkubation die Wirkung von 50 µM Verbindung **5** und 100 µM Verbindung **1** auf die Verstoffwechslung von Glucose via *pc* und auf *pdh* ähnlich sind. Während nach 24 Stunden in Anwesenheit von 50 µM Verbindung **5** die Folgeprodukte des *pc* Weges um 20% reduziert wurden und *pdh* Aktivität nicht betroffen ist. Entgegen nehmen die Aktivitäten von *pc* und *pdh* nach 24 Stunden in Anwesenheit von 100 µM Verbindung **1** um 100% bzw. 80% ab.

Die Ergebnisse der Experimente mit [2-^{13}C]Acetat in Anwesenheit von Verbindung **5** zeigen, dass Verbindung **5** möglicherweise eine indirekte Hemmwirkung auf *pdh* besitzt. Die Ergebnisse dieser Studie zeigen auch, dass die Wirkung von Verbindung **5** auf die DNL (ähnlich wie Verbindung **1**) auf der Ebene der CA und nicht auf der Ebene des ACC erfolgt.

Zur Untersuchung der Wirkung von Verbindung **5** auf Energie-Status von HEP-G2-Zellen wurden die Zellen für 24 Stunden mit markierter Glucose in Gegenwart von Verbindung **5** inkubiert. Die Ergebnisse dieser Studie zeigen, dass Energiezustand der Zellen nach 24 Stunden nicht verändert ist. Demzufolge wird in den Zellen für 24 Stunden immer noch ausreichend ATP für die ATP-Citratlyase produziert.

Chapter 2

2 Introduction

Obesity is a disease, which affects over 300 million [1] people both in developed and developing countries. Obesity likely is caused by incorrect and very high-fat diet, although other reasons are discussed. The increase in the proportion of overweight people in the population will be accompanied by an epidemical increase of obesity, with complications ranging from personal dissatisfaction to heart disease or certain forms of diabetes. Motivated patients can achieve remarkable degrees of sustained weight loss with dietary change and exercise alone [2]. However, successful maintenance of the lifestyle changes which is needed for optimal bodyweight is uncommon [3, 4] and the current methods for lifestyle modification alone are widely regarded as ineffective [5]. For the enormous number of patients who are not able to reduce weight by means of nonpharmacological measures due to different reasons, drug therapy offers a reasonable option to overcome obesity. Drug therapy may be effective if given without lifestyle modification [6, 7], but is most effective when combined with diet, increased physical activity, and behaviour modification [7]. Therefore, weight-loss drugs should only be used as part of a comprehensive weight loss regimen [8]. Thus, pharmacological interventions are necessary, and suitable compounds for the treatment and/or prophylaxis of obesity have to be discovered. Many of these compounds have been developed towards an inhibition of *de novo* lipogenesis (DNL). DNL means the synthesis of fatty acids from carbohydrates, which can then be stored in fat cells (adipocytes). Few pharmacological approaches for the treatment of obesity exist so far, and most of them are unsatisfactory. A possible new intervention for the treatment and prophylaxis of obesity is based on the inhibition of carbonic anhydrases (CAs, EC 4.2.1.1), which are involved in

several metabolic steps of *de novo* lipogenesis, both in the mitochondria and the cytosol of cells.

The conversion of carbohydrates to fatty acids involves the oxidation of pyruvate to acetyl-CoA via pyruvate dehydrogenase (*pdh*). This is an intramitochondrial process, while fatty acid synthesis occurs extramitochondrially. Acetyl-CoA itself cannot pass the mitochondrial membrane. Its transport into the cytosol for fatty acid synthesis is mediated by the citrate shuttle. After condensation of acetyl-CoA with oxaloacetate via citrate synthase, acetyl units are transported into the cytosol as citrate. In the cytosol, citrate undergoes ATP-dependent cleavage to yield acetyl-CoA and oxaloacetate [9] (Figure2.1). Citrate is also an important intermediate of the mitochondrial tricarboxylic acid (TCA) cycle.

Supplementary to *pdh*, the replenishment of citrate in the mitochondria requires an anaplerotic mechanism. In most organs and cells, the continuous supply of oxaloacetate is mediated by pyruvate carboxylase (*pc*), an enzyme that catalyses the irreversible carboxylation of pyruvate (eq. 1 and 2).

$$ATP + HCO_3^- + \text{Enz-biotin} \xrightleftharpoons{Mg^{2+},\ \text{acetyl-CoA}} \text{Enz-biotin-}CO_2 + ADP + P_i \quad (1)$$

$$\text{Pyruvate} + \text{Enz-biotin-}CO_2 \rightleftharpoons \text{Enz-biotin} + \text{Oxaloacetate} \quad (2)$$

The condensation of pyruvate and bicarbonate to oxaloacetate is an important anaplerotic reaction, replenishing oxaloacetate loss from the TCA cycle for several biosynthetic purposes such as the synthesis of amino acids, as well as for lipogenesis and gluconeogenesis [10,11] (Figure 2.1).

For the conversion of pyruvate to oxaloacetate via *pc*, adequate amounts of bicarbonate are essential. The production of bicarbonate from carbon dioxide in the mitochondria is mediated by carbonic anhydrase (CA). Among the known CAs, in mammals, CA II and CA V contribute predominantly to the provision of bicarbonate for the *pc* reaction [12].

For the treatment of obesity, there are various conceivable possibilities to inhibit DNL in mammalian cells, which aim to reduce the amount of citrate needed for fatty acid synthesis in the cytosol. One of these possibilities is to inhibit CAs.

Figure 2.1 Anaplerotic role of cellular pc.

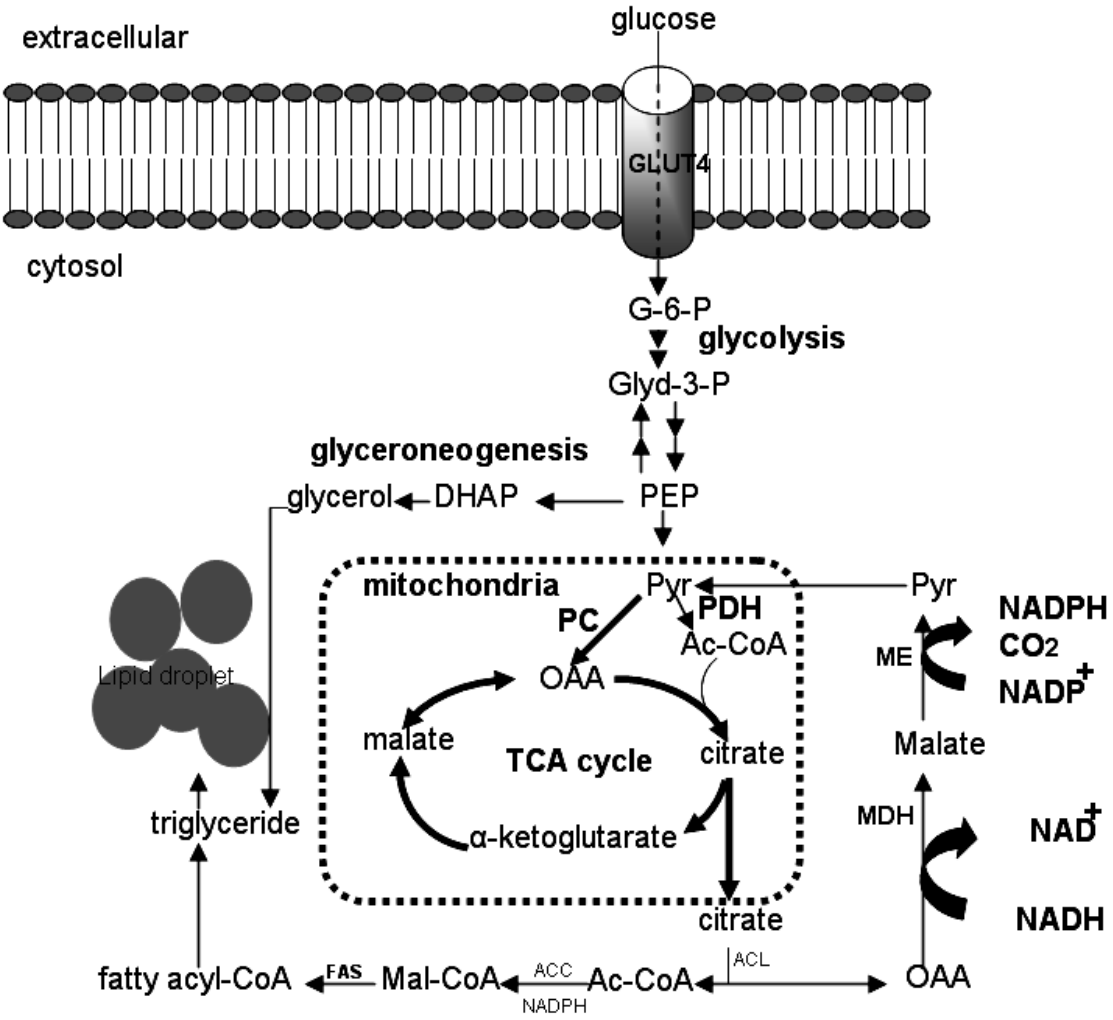

Oxaloacetate formed by mitochondrial pc condenses with acetyl-CoA to citrate by citrate synthase. Citrate is converted to oxaloacetate and acetyl-CoA by ACL, and acetyl-CoA is then carboxylated by ACC to malonyl-CoA in the cytosol. Condensation of acetyl-CoA units from malonyl-CoA by FBS produces long-chain fatty acyl-CoA in the cytosol (as part of the de novo fatty acid synthesis). Oxaloacetate is subsequently converted back to pyruvate by cytosolic MDH and ME before re-entering in the mitochondria (known as pyruvate recycling). ME, malic enzyme; MDH, malic dehydrogenase; OAA, oxaloacetate; Pyr, pyruvate; pc, pyruvate carboxylase; pdh, pyruvate dehydrogenase; ACC, acetyl-CoA carboxylase; ACL, ATP-citrate lyase; FAS, fatty acid synthetase; G-6-P, glucose-6-phosphate; Glyd, glyceraldehyde-3-phopsphate; DHAP, dihydroxyacetone phosphate; PEP, phosphoenolpyruvate.

To understand the normal functions of the CAs and how the isozymes are affected by carbonic anhydrase inhibitors (CAIs), it is essential to consider the chemical structure of CAs and their biochemical interaction with CAIs. This chapter concentrates mainly on CO_2

hydration, functions and structures of CAs, e.g. CA II and CA V in adipocytes, hepatocytes and other tissues/cells e.g. the brain, as well as on the effect of CAIs in DNL and TCA cycle-related amino acid synthesis.

2.1 Reversible hydration of CO_2

In the first step, CO_2 undergoes the simple but very important reaction for the respiratory control in mammals:

$$CO_2 + H_2O \underset{K_{-1}}{\overset{K_{+1}}{\rightleftharpoons}} H_2CO_3 \underset{K_{-2}}{\overset{K_{+2}}{\rightleftharpoons}} H^+ + HCO_3^- \qquad (3)$$

In the reaction (3), $K_{+1}$and K_{-1} are the velocity constants of hydration and dehydration reaction, respectively, given in s^{-1}. These are K_{+1} = 0.18 and K_{-1} = 64 s^{-1} at 37°C in physiological saline [13]. The hydration is a bimolecular reaction but the omnipresent [HOH] is absorbed in the hydration rate constant. K_{+2} and K_{-2} are the reaction constants of the ionization and protonation of carbonic acid, about 4.7×10^{10} and 8×10^6 [13] in s^{-1} and M^{-1} s^{-1}, respectively. The second reaction, that is an equilibrium reaction, can be represented by the ionization equilibrium constant

$$K_A = \frac{[H^+]\,[HCO_3^-]}{[H_2CO_3]} \qquad (4)$$

K_A = 3.4 × 10^{-4}M [14]. At chemical equilibrium the complete reaction in Eq. (3) can be expressed as:

$$K' = \frac{[H^+]\,[HCO_3^-]}{[CO_2]} \qquad (5)$$

Where $K'=K_{A^*}(K_{+1}/K_{-1})$, K' is not an appropriate equilibrium constant but includes two reactions. It equals $10^{-6.07}$ at physiological ionic strength (0.150) and 37°C. The value of K' shows that, the interconversion between CO_2 and HCO_3^- is very slow without catalyst.

2.2 Carbonic anhydrases

CAs belong to a widespread family of zinc metalloenzymes consisting of a single polypeptide chain (Mr ~ 29-35 kDa) complexed to one zinc atom. The CAs are found in a diversity of organisms including higher vertebrates, green plants, algae, bacteria, and archaea. They play crucial and essential physiological roles in these organisms. The primary function of the CAs in animals is to interconvert carbon dioxide and bicarbonate, (H_2O + CO_2 $\leftrightarrow$ HCO_3^- + H^+), to maintain acid-base balance in blood and other tissues, a.o. in brain [15], and to help to transport carbon dioxide out of tissues. These enzymes are involved in many biosynthetic reactions e.g. gluconeogenesis [16], lipogenesis [17], ureagenesis [18], bone resorption, calcification, tumorigenicity, and many other physiologic or pathologic processes too [19].

Sixteen isozymes of the zinc-binding CA enzyme have been characterised in mammals, which differ in their enzymatic properties, specific tissue localisations, functions [20], and susceptibility to different classes of inhibitors [21]. Some of these isozymes are cytosolic (CA I, CA II, CA III, CA VII and CA XIII), others are membrane bound (CA IV, CA IX, CA XII and CA XIV), two are mitochondrial (CA VA and CA VB) and CA VI is secreted in saliva [11]. Three catalytic forms are also known, which are denominated CA related proteins (CARP), CARP VIII, CARP X, and CARP XI [22]. More detailed depictions of the roles of mammalian carbonic anhydrases II, IV and V are given in table 2.1. The associations of CAs with lipogenesis, gluconeogenesis, ureagenesis, and carbon dioxide in liver mitochondria are shown in Figure 2.2 [23].

Table 2.1 Functions (established and putative) of the α-carbonic anhydrases in mammals

Isozyme	Function
CA II	***Respiration and acid/base regulation*** Hydration of CO_2 to HCO_3^- in peripheral tissue/ Elimination of H^+ in kidney ***Vision*** Production of aqueous humour (ciliary body) ***Bone development and function*** Differentiation of osteoclasts and provision of H^+ in osteoclasts for bone resorption ***Metabolic processes*** Provision of HCO_3^- for pyrimidine synthesis
CA IV	***Respiration and acid/base regulation*** Dehydration of HCO_3^- to CO_2 at lungs/ Reabsorption of HCO_3^- ***Vision*** Production of aqueous humour (ciliary body)
CA V	***Metabolic processes*** Provision of HCO_3^- for gluconeogenesis and ureogenesis Provision of HCO_3^- for fatty acid synthesis (possibly CA II)

2.2.1 Overview of the carbonic anhydrase isozymes and their functions

Until the early 1960s, CA was thought to exist in only one form. Tashian, R.E. and Carter, N. D. have reviewed the difference between the two major erythrocyte isozymes CA I and CA II in 1976 [24]. The CA I has a higher concentration in the erythrocyte than CA II, but CA II is much more active (table 2.2) [23]. CA II is one of the fastest enzymes known with a K_{cat} exceeding a million per second while CA III possesses less than one hundredth of CA II activity (table 2.2).

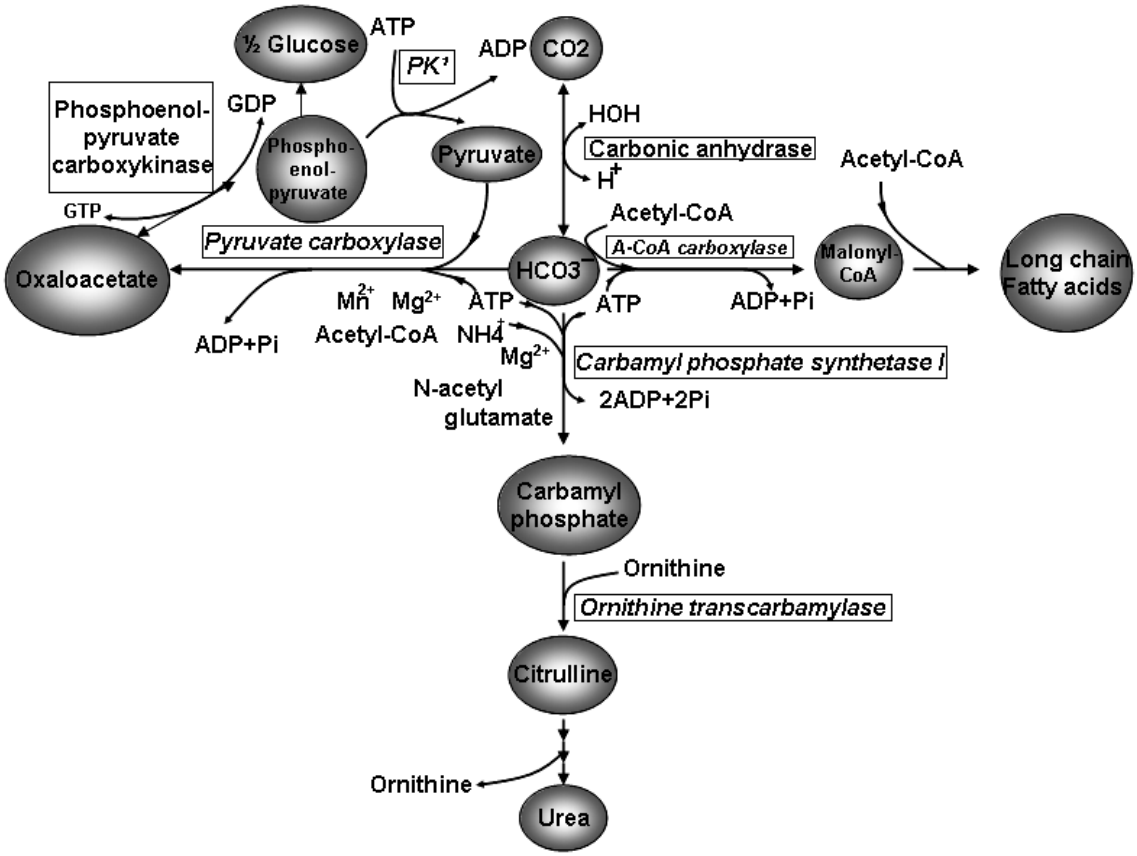

Figure 2.2. *Reactions of HCO_3^- in liver mitochondria. HCO_3^- is required in the three metabolic pathways.*
1) PK: pyruvate kinase

2.2.2 Structure and mechanism of CAs

It has been known for long that the zinc ion in CA is necessary for its catalytic activity [25]. X-ray crystallographic data showed that the metal ion is coordinated by three histidine residues (His 94, His 96, and His 119) and a water molecule/ hydroxide ion [26, 27]. The zinc ligands and a number of amino acids residues connected to the zinc ion by hydrogen-bond network are conserved in all sequenced animal carbonic anhydrases (Figure 2.3).

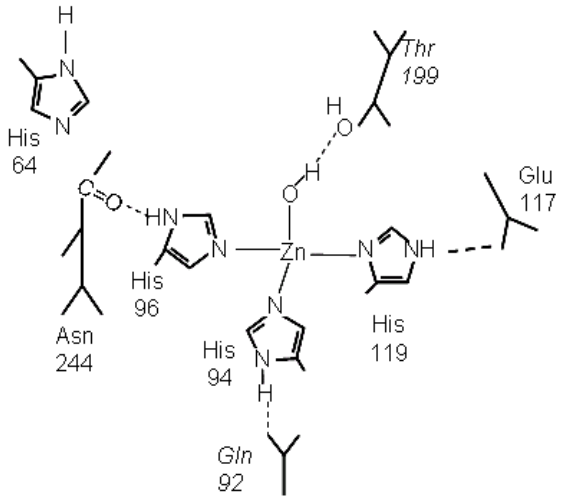

Figure 2.3. *The active site of a CA. Zn^{2+} ion is coordinated by three histidine ligands (His 94, His 96 and His 119), shuttle residue His 64 as well as other residues that are important for catalytic cycle are shown.*

One fundamental characteristic of this environment is a metal-bound water molecule ionizing to OH^- with a pK_a between 5 and 7.5, depending upon the isozyme type. Despite the fact that the metal-bound OH^- has relatively low basicity, it seems to be a good nucleophile and the current mechanistic hypothesis involves a nucleophilic attack of this OH^- on CO_2 to form metal-bound HCO_3^- as the central catalytic step (fig. 2.4, step 1).

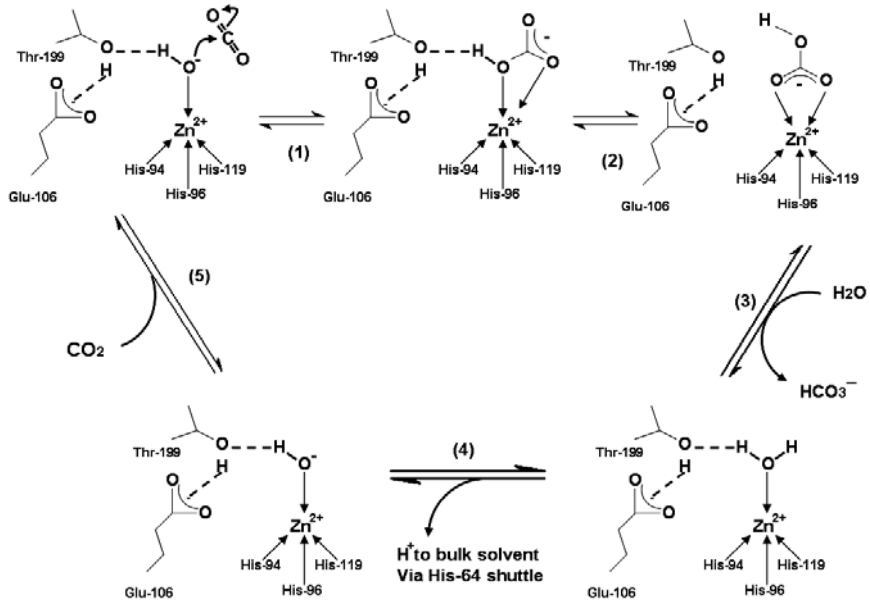

Figure 2.4. *Schematic representation of the catalytic mechanism for CA II catalysed CO_2 hydration.*

As shown in figure 2.4, CO_2 reacts with a Zn-OH (a strong nucleophile) intermediate at the active site of the enzyme (step 1) in the hydration reaction. The bicarbonate ion is displaced by a water molecule and librated into solution (step 3), leading to the acid form of the enzyme (in the reverse dehydration direction, HCO_3^- reacts with Zn-H_2O). In step 4, i.e. the proton transfer reaction from the active site to the environment, the basic form of the enzyme is regenerated. The transfer of a proton to the environment is supported either by the active site residue (His 64 e.g. in CA II) or by the buffer in the reaction medium. The catalytic cycle can be summarized in equations (6) and (7).

$$\mathbf{EZn^{2+}\text{-}OH^- + CO_2 \leftrightarrow EZn^{2+}\text{-}HCO_3^- \leftrightarrow EZn^{2+}\text{-}OH_2 + HCO_3^-} \quad (6)$$

$$\mathbf{EZn^{2+}\text{-}OH_2 \leftrightarrow EZn^{2+}\text{-}OH^- + H^+} \quad (7)$$

Equation (7) is the rate limiting step in the catalytic cycle, i.e. the proton transfer that regenerate the basic form of the enzyme [28]. As outlined above, for the catalytically very active isozymes, such as CA II, CA IV, CA V, CA VII, and CA IX, this process is supported by a histidine residue located at the entrance of the active site (His 64) [29]. These reactions have been studied extensively, particularly with CA enzymes from animal sources [30].

2.3 Carbonic anhydrase inhibitors (CAIs)

CAIs differ in their power to inhibit CAs. The relative CA activities, affinities for sulfonamide inhibitors and their sub-cellular localizations are shown in table 2.2 [31]. The CAIs can be categorised into two main classes: the metal complexing anions and the unsubstituted sulfonamides, which bind to the Zn^{2+} ion of the enzyme either by substituting the non-protein zinc ligand (equation 8), or add to the metal coordination sphere (equation 9), generating trigonal-bipyramidal species [26, 32, 33, 34].

$$\mathbf{EZn^{2+}\text{-}OH_2 + I \leftrightarrow EZn^{2+}\text{-}I + H_2O} \quad \text{Substitution} \quad (8)$$

$$\mathbf{EZn^{2+}\text{-}OH_2 + I \leftrightarrow EZn^{2+}\text{-}OH_2(I)} \quad \text{Addition} \quad (9)$$

The mechanism of inhibition by sulphonamide and anionic inhibitors are shown schematically in figure 2.5 [31]. In 1940, Mann and Keilin have discovered the CA inhibitory effect by sulphanilamide [35] and it was the beginning of an enormous scientific activity that led to important drugs, such as the antihypertensive benzothiadiazine. The sulfonamides with CA inhibitory properties are mainly used as antiglaucoma agents [36, 37], some of them are anti-thyroid drugs [36], the hypoglycemic sulfonamides [38], and some are novel types of anticancer agents [39]. The new substances and three CAIs have been used in this work and belong to sulfonamides class (see below).

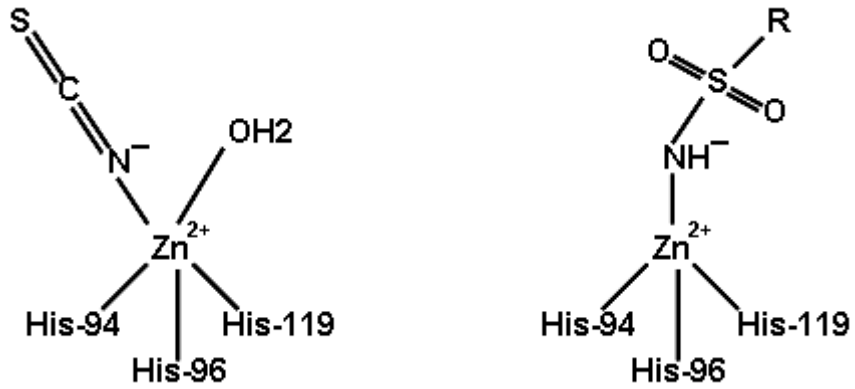

Trigonal-biipiramidal adduct (Thiocianate)

Tetrahedraladduct (Sulfonamide)

Figure 2.5. *The mechanism of carbonic anhydrase inhibition by sulphonamide and anionic inhibitors.*

Table 2.2 The relative CA activity, affinity for sulfonamide inhibitors, and their sub-cellular localization

Isozyme	*Catalytic activity (CO_2 hydration)*	*Affinity for sulfonamides*	*Sub-Cellular localization*
CA I	Low (10% of that of CA II)	Medium	Cytosol
CA II	High	Very high	Cytosol
CA III	Very low (0.3% of that of CA II)	Very low	Cytosol
CA IV	High	High	Membrane-bound
CA V	Moderate-high	High	Mitochondria
CA VI	Moderate	Medium-low	Secreted into saliva
CA VII	High	Very high	Cytosol

Table 2.2 Continue

Isozyme	*Catalytic activity (CO_2 hydration)*	*Affinity for sulfonamides*	*Sub-Cellular localization*
CARP VIII	Acatalytic	*	Probably cytosolic
CA IX	High	High	Membrane-bound
CARP X	Acatalytic	*	Unknown
CARP XI	Acatalytic	*	Unknown
CA XII	Active (not quantitative data)	Unknown	Membrane-bound
CA XIII	Probably active	Unknown	Unknown
CA IV	Low	Unknown	Membrane-bound

2.4 Use of carbonic anhydrase inhibitors for the inhibition of de novo fatty acid synthesis

Topiramate (TPM) [2,3:4,5-bis-O-(1methylethylidene)-β-D-fructopyranose sulfamate] (figure 2.6) is a structurally novel neurotherapeutic agent synthesised from D-fructose. It contains a sulphamate moiety that is essential for its pharmacological activity [40]. TPM has been developed initially to treat of epilepsy, but it is discovered recently as a drug for a wide variety of other indications including obesity, neuropathic pain, bipolar disorder and migraine. The potency of TPM for the treatment of obesity was discovered by chance as a side effect in long-term studies of epileptic patients and has been recently shown to act as CAI. It has been suggested that the weight loss may be due to the inhibition of the mitochondrial isozymes CA VA and CA VB involved in metabolic processes, such as lipid biosynthesis [41, 42]. It is comprehensible that CA V participates in pyruvate carboxylation, but the role of CA II an extramitochondrial CA should not be discounted. Exogenous bicarbonate in mitochondria is rapidly incorporated into TCA cycle intermediates in cells. This indicates that mitochondrial CO_2 production is not the only source of bicarbonate for pyruvate carboxylation. Despite the fact that bicarbonate cannot pass through the mitochondrial membrane, the bicarbonate must be converted into CO_2. This transmembrane motion into the mitochondrial matrix undoubtedly involves extramitochondrial CA, i.e. CA II [43].

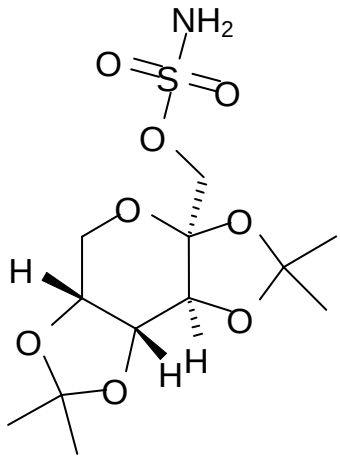

Figure 2.6. *Structure of Topiramate.*

Figure 2.7 represents schematically the effect of CAIs on CAs in hepatocytes and their potential effect on *de novo* lipid synthesis as well as glutamate synthesis through TCA cycle activity [44].

Figure 2.7. Putative mechanism of de novo lipogenesis in adipocytes [44]

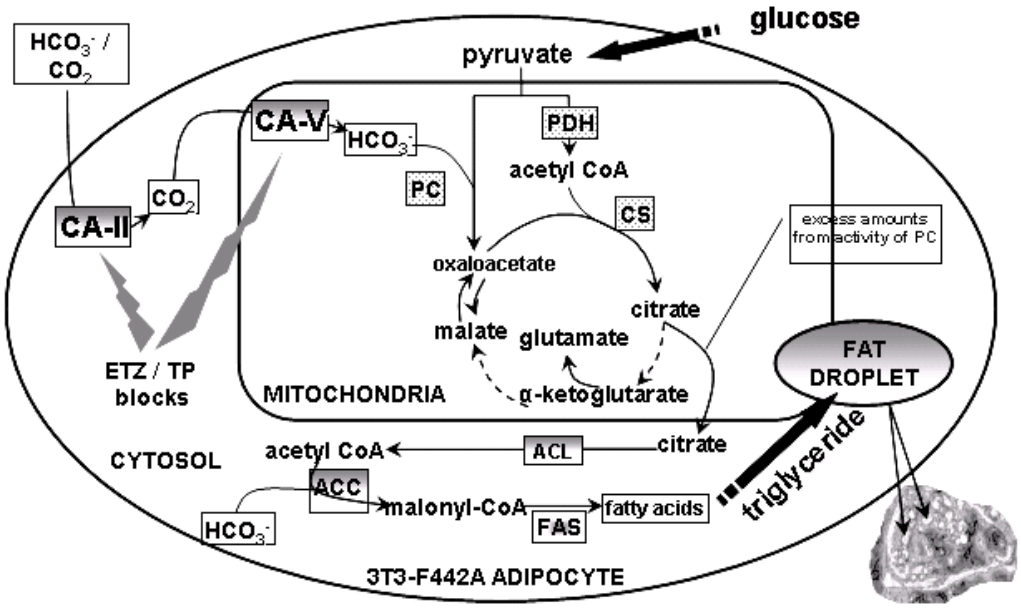

Proposed role of carbonic anhydrase activity for de novo lipid synthesis in adipocytes. Inhibition of CA II and CA V can lead to a reduction in citrate production resulting in the inhibition of DNL.

2.5 Aims of the study

The central aim of this study was to investigate the metabolic effects of new CAIs and three known CAIs, i.e. TPM, acetazolamide (AZM) and ethoxyzolamide (ETZ) on *de novo* lipid synthesis and TCA cycle related amino acid, i.e. glutamine. For this purpose, HEP-G2 cells and 3T3-L1 were incubated with [U-^{13}C]glucose, [2-^{13}C]pyruvate, or [3-^{13}C]pyruvate, in the presence of various CAIs. Multinuclear NMR spectroscopy (^{1}H, ^{13}C and ^{31}P) was used to follow up various metabolites and their synthesis from tracers.

To obtain more detailed information on the involved metabolic pathways, i.e. on flux through *pdh* and related fatty acid synthetic pathways in the cytosol, [2-^{13}C]acetate was used as an additional tracer.

Chapter 3

3 Results and Discussion

3.1 Introduction

As obesity is a widespread disease, various pharmacological approaches to treat this disease are followed presented. One example are lipase-inhibitory substances. Orlistat is an example for this group of inhibitors [45]. These substances reduce the lipolysis in the intestine and in that way decrease the energy yield from the food intake. It is desirable to have other new therapeutic approaches for the treatment and/or prophylaxis of obesity which can complement the previously known form of therapy. A new strategy might be the inhibition of DNL from carbohydrate in the mammalian organism. Sulphonamides as carbonic anhydrase inhibitors are good candidates for treatment of obesity. In this study we have investigated the effect of eight CAIs on DNL and TCA-related amino acid i.e. glutamate in two groups. The first group contained TPM, ETZ, ACT, and a new candidate as CAI i.e. compound **1** (see Appendix 6.3, page 111). The second group contains four new substances as CAIs. As the compound **5** is not patented yet, the molecular structure of this compound is not shown in appendix 6.3. In this study the 3T3-L1 (clonal mouse fibroblasts) and HEP-G2 (clonal hepatocytes) were chosen (see 4.1.2, page 63). The effects of CAIs on bicarbonate fixation in cultured 3T3-L1 cells and HEP-G2 cells were examined by incubating the cells with CAIs or drug vehicle (DMSO) (0,1%) in the presence of various ^{13}C-labelled substrates, i.e. [U-^{13}C]glucose, [2-^{13}C]pyruvate, [3-^{13}C]pyruvate or [2-^{13}C]acetate as tracer. After incubation of

the cells with a tracer in the presence or absence of a CAI, perchloric acid (PCA) extracts were obtained (see 4.2.2, page 65) and subsequently analysed by multinuclear NMR.

3.2 Determination of IC_{50} of CAIs in first group for inhibition of DNL

The total IC_{50} (Inhibitory Concentration) value for each CAI of the first group, i.e. TPM, ETZ, ACT and compound **1** (for molecular structure of sulphonamides with carboanhydrase inhibitory effects see page 111), was determined by incubation of HEP-G2 cells with 5mM [U-^{13}C]glucose in the presence of varying concentration of CAI (table 4.1) or drug vehicle (DMSO) as control using NMR spectroscopy. The ratio of doublet spectra of $\mathbf{F}_{\omega}$ (terminal carbon of fatty acid residues) to spectrum of natural abundance after 6h incubation in the presence of various carbonic anhydrase inhibitors or only DMSO (control) was used as an indicator for determination of IC_{50} of CAIs.

Figure 3.1 Effect of CAIs on total lipid synthesis

(A) ***(B)***

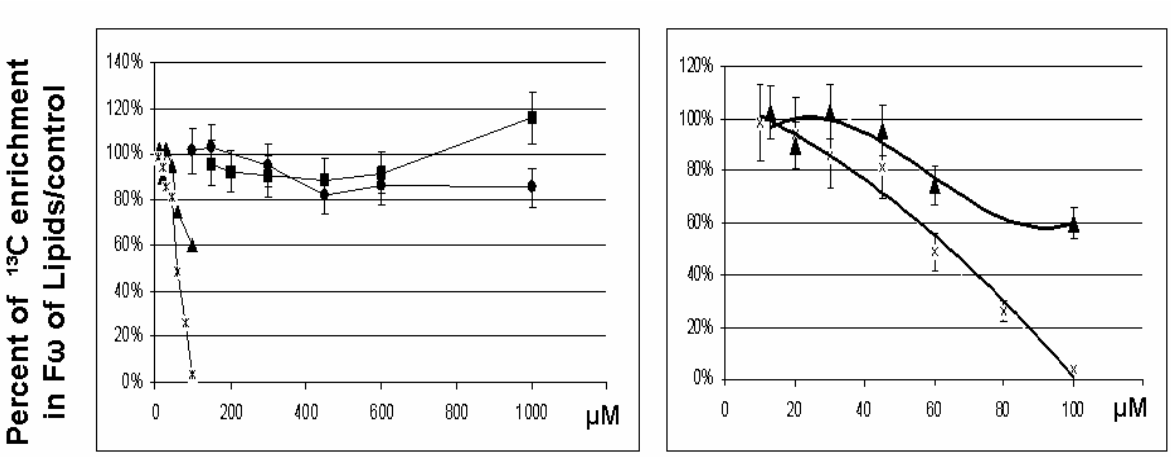

*The effect of CAIs i.e. TPM, ACT, compound **1**, and ETZ on total lipid synthesis in HEP-G2 cells. HEP-G2 cells were incubated for 6h with various concentrations of CAIs or drug vehicle (0.1% DMSO). (●) TPM; (■) ACT; (x) compound **1**; (▲) ETZ.*

The data of this study (Figure 3.1, A) show that the IC_{50} of TPM is over 1000 μM. Dodgson et. al. have shown that TPM weakly inhibited CAs and TPM is more potent as an inhibitor of human CA II (HCA II) and HCA IV than of other CA forms [46]. The results also show that ACT is a nonspecific inhibitor of CA isozymes (IC_{50} over 1000 μM) [47]. As is shown in figure 3.1 A and B, *de novo* lipogenesis in the presence of lower concentrations of ETZ (13-100 μM) is more effectively inhibited (40% of control in the presence of 100 μM of ETZ). Thus it can be expected that IC_{50} of ETZ for this inhibition is around 120 μM. Simone et al. [48] and Nishimori et al. [49] showed that ETZ indiscriminately inhibits all CA isozymes except CA III, which is in good agreement with our result. The IC_{50} values for TPM, ACT and ETZ are different from the IC_{50} values in the literature. These differences are due to 1) different cell types, 2). The IC_{50} values in the literature are specific for a special CA e.g. CA II, while we have determined the total IC_{50}, 3) we have incubated the cells for a long time in the presence of CAIs i.e. 6 hours, while the IC_{50} for CAIs in the literature are all determined for short incubation times i.e. 15-30 minutes. The new CAI (compound **1**), (figure 3.1, B), is a remarkable candidate for the inhibition of CA II and CA V and possibly other CA isozymes. IC_{50} value for this CA lies between 50-55 μM. The hypotheses of selective inhibition of CA V, or the dual inhibition of CA II and CA V, may lead to the development of new pharmacological applications for such CAIs, e.g. in the treatment/prevention of obesity [50].

3.3 Glucose metabolism in 3T3-L1

3.3.1 Introduction

Based on previous investigations, CAIs are used as an inhibitor for CO_2-fixing enzymes. One of these enzymes is pyruvate carboxylase [51, 52]. Pyruvate carboxylase is an anaplerotic enzyme that replenishes TCA cycle intermediates when these are consumed in anabolic pathways, such as DNL [44] and glutamate synthesis [53]. For years sulphonamide carbonic anhydrase inhibitors are used as an adjuvant treatment for childhood epilepsy, especially so-called absence seizures [54, 55, 56, 57] and it is well known that the neuronal excitability and seizure susceptibility vary inversely with concentration of free divalent cations, Ca^{2+} and Zn^{2+}. Secreted abundances citrate from mitochondria into the extracellular space [58] can chelate free Ca^{2+} cations and result in either seizure or increased seizure susceptibility[59,

60, 61, 62]. Thus inhibition of *de novo* synthesis of citrate via CAIs may lead to increased free divalent cation concentration in the brain, and thereby to decreased seizure susceptibility [63].

3.3.2 Alteration of glutamate

As *pc* is a requirement for *de novo* synthesis of glutamate and glutamine, inhibition of *pc* leads to a decrease of *de novo* synthesis of glutamate and glutamine [53].

The data of this study show that the ^{13}C-label from [U-^{13}C]glucose in cell extracts and media was found mainly in glutamate, whether CAI was presented or not. Typical ^{13}C-NMR spectrum of 3T3-L1 cells (cell extract) is shown in figure 3.2. The results show that after 24h exposure of 3T3-L1 cells to 100 µM TPM, 150 µM ACT, and 13 µM ETZ, resulted in a decrease of anaplerotic entrance of [U-^{13}C]glucose into TCA cycle to 70%, 60%, and 60% of control respectively (table 3.1). However, incubation of the 3T3-L1 cells with [U-^{13}C]glucose in the presence of 10 µM compound **1**, the entrance of labelled glucose via *pc* into TCA cycle is undetectable. This result shows that compound **1** is a superior inhibitor for inhibition of CA V, or the dual inhibition of CA II and CA V. The *pdh* activity in the presence of TPM is nearly not affected but the other CAIs have a negative effect on this pathway. This effect might be a direct effect of CAIs on *pdh* or a result of inhibitory effect of *pc* (see 4.4.3.1, metabolic fate of [2-^{13}C]acetate, page 76). 100 µM TPM leads to nearly 30% reduction of *pc* activity in 3T3-L1 cells whereas 150 µM ACT leads to 40% reduction of *pc* activity. TPM is more effective as an inhibitor of CA II and CA IV than of CA V, CA I, CA III. ACT is usually 10-100 times more potent than TPM as a nonspecific inhibitor of CA isozymes [46]. These results show that TPM and ACT are nonspecific CAIs. Results from incubation in the presence of ETZ are in good agreement with the results from Hazen et al. [63]. 13 µM from ETZ caused a 40% decrease of *pc* activity. This decrease can be attributed to the inhibition of intramitochondrial CA, i.e. CA V and cytosolic CA II. 10 µM from compound **1** caused a nearly 100% decrease of the anaplerotic entry of [U-^{13}C]glucose into the TCA cycle and a 70% decrease of entrance of [U-^{13}C]glucose via *pdh* into the TCA cycle shown in cell extracts.

Figure 3.2. ^{13}C-NMR spectrum of 3T3-L1 cells

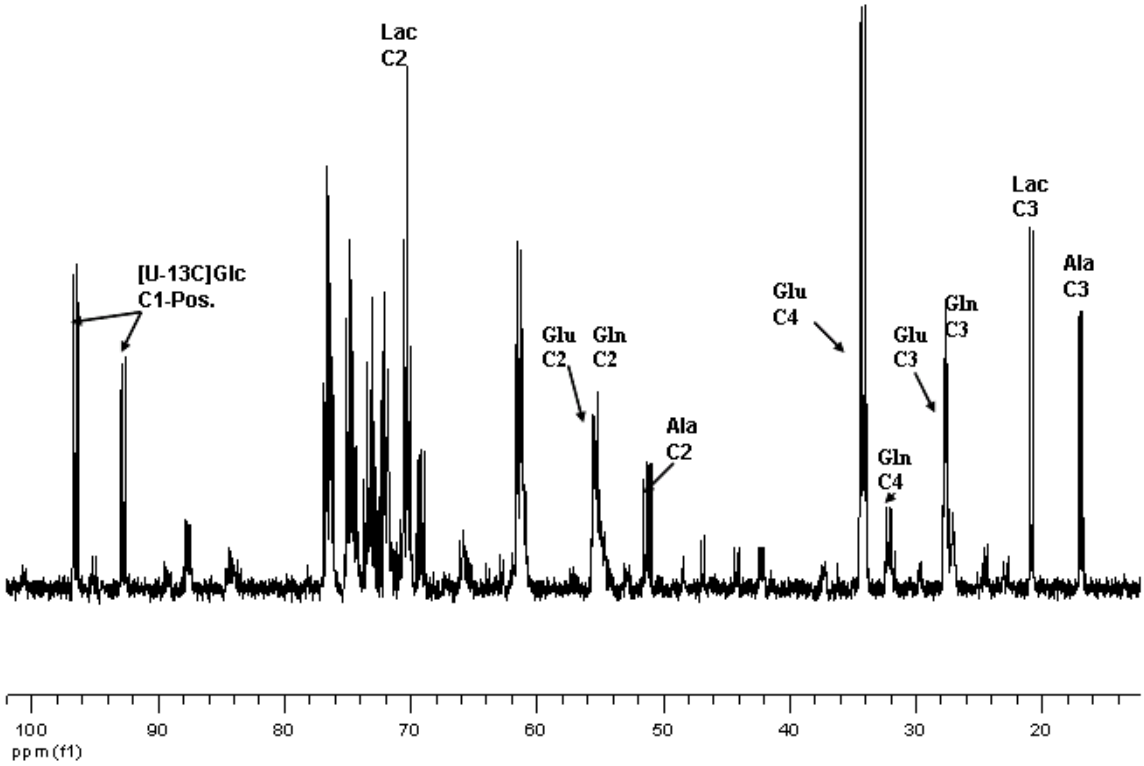

^{13}C-NMR spectra of perchloric acid (PCA) extracts of 3T3-L1 cells, obtained after 24h incubation in DMEM medium containing 4mM glutamine, 5mM [U-^{13}C]glucose and 1,5.10^{-4} M acetazolamide. Peak assignments: Ala, alanine; Glc, glucose; Gln, glutamine; Glu, glutamate.

Table 3.1. ^{13}C-labelled glutamate after incubation with [U-^{13}C]glucose

	TPM 100µM,24h	ACT 150 µM,24h	compound **1** 97µM,24h	ETZ 13µM,24h	compound **1** 10 µM,24h	compound **1** 10 µM,12h
[4,5-^{13}C]glu	122.7±19.7	67.7±8.2	31.9±2.9	73.7±4.4	27.4±3.3	76.1±4.1
[3,4,5-^{13}C]glu	70.3±11.7	58.7±7.8	n.d.	57.5±4.9	n.d.	n.d.

*The percentage ^{13}C-enrichment in specific carbon positions of glutamate were calculated by integration of the respective signals in ^{13}C-NMR spectra obtained from cell extract after 24hour (12 hour) incubation of 3T3-L1 cells with 5 mM glutamine and 5 mM [U-^{13}C]glucose as tracer in the presence of various CAIs or drug vehicle (DMSO 0.1%). Abbreviations: TPM, topiramate; ACT, acetazolamide; compound **1**, the new CAI; ETZ, ethoxyzolamide. The values are given as percentage of control and represent mean ± SD of 3-5 experiments.*

In 3T3-L1 cells, the decreasing influence of [U-^{13}C]pyruvate into the TCA cycle can be a secondary effect of CAI on *pc* activity and/or a direct effect on *pdh* activity. This new CAI, compound **1**, is a very good candidate to inhibit the CA II and CA V. Typical ^{13}C-NMR signals of C-4 glutamate in the presence or absence of various CAIs i.e. TPM, ACT, ETZ, and compound **1** are shown in figure 3.3.

3.3.3 ^{13}C-isotopomer pattern in glutamate (pc and pdh)

The percentage of ^{13}C-enrichments in fourfold labelled C-2,3,4,5 glutamate and double-labelled C-4,5 glutamate (table 3.1), depend on the relative fluxes through TCA cylce-releated enzymes. *pdh* transforms [U-^{13}C]glucose into [1,2-^{13}C]acetyl-CoA and by this means into the TCA-cycle intermediate [4,5-^{13}C]α-ketoglutarate. *pdh* is active in all mammalian cells and plays a major role in the regulation of glucose oxidation and mitochondrial energy production in cells. The predominance of [4, 5-^{13}C]glutamate under both experimental conditions shows that *pdh* is very active in our cultured cells (figure 3.4). [U-^{13}C]glucose can be transformed also to [2, 3, 4, 5-^{13}C]glutamate or [U-^{13}C]glutamate via *pc*, the main anaplerotic enzyme in the cells [64]. Intensity of fourfold labelled glutamate at C-4, therefore indicates the *pc* activity in our cultured cells.

Figure 3.3 Typical ^{13}C-NMR signals at C4 from Glu.

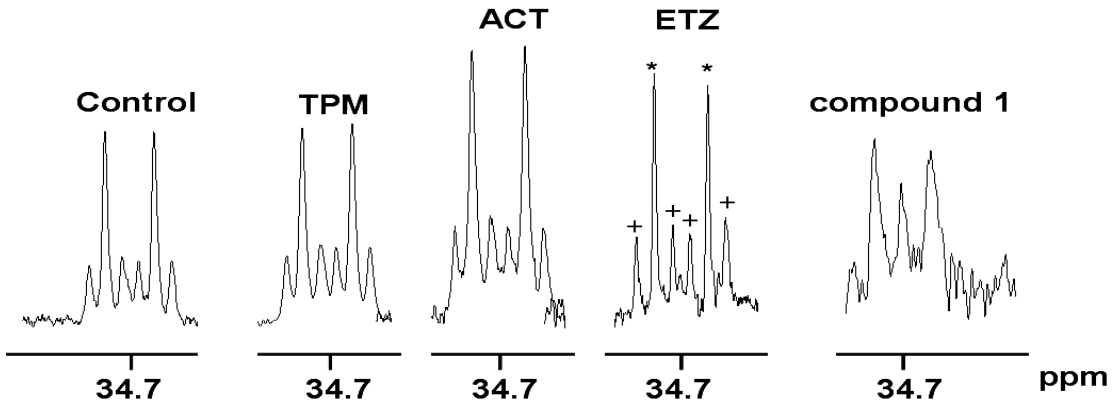

*^{13}C-NMR signals at C-4 from glutamate in the presence or absence of various carbonic anhydrase inhibitors i.e. topiramate, acetazolamide, ethoxyzolamide, and compound **1** (97 µM) incubated for 24 h.*

**: [4, 5-13C] glutamate, +: [2,3, 4, 5-13C]-, [U-^{13}C]glutamate.*

3.3.4 Effect of CAIs on lactate and alanine synthesis

The fractional ^{13}C-enrichments of intracellular and extracellular lactate in 3T3-L1 cells in the presence of various CAIs are given in Table 3.2. CAIs-induced increase intra-, and extracellular lactate concentration indicates a higher glycolytic activity compared to control, which can be upregulated under inhibition of CAs for anaerobic generation of ATP [65]. The exposure of 3T3-L1 cells for 24 hours to CAIs, i.e. TPM, ACT, and compound **1** (97 μM), resulted in significant increases of lactate concentrations in cell extracts to 175%, 305%, and 1280% of controls respectively, whereas this values in media were 107%, 104%, and 546% of control respectively. ETZ has no effect on the concentration of lactate in the cell extract but the concentration of lactate in the medium is increased to 193% of control. Inhibition of lactate transport in the presence of ACT or TPM in extracellular space of 3T3-L1 cells is possibly due to an inhibition of lactate transport or a result of CA inhibition.

Figure 3.4 Segment ^{13}C-NMR spectrum of cell extract of 3T3-L1 cells

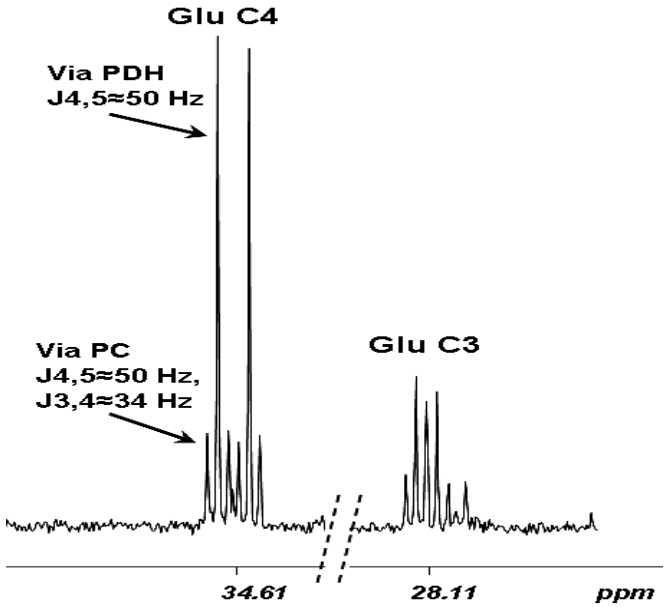

Section of ^{13}C-NMR spectrum of lyophilised cell extract of 3T3-L1 cells after 24h incubation with DMEM containing 5 mM [U-^{13}C]glucose and 0.1% DMSO as drug vehicle and absence of CAI. The expanded spectrum shows the C4 and C3 resonances of glutamate. The doubled signal at C4 of glu is appeared only via pdh activity after first turn of TCA cycle but fourfold labelled glu at C4 is appeared via pc activity. Peak assignments: DMSO, Dimethylsulfoxid; Glu, glutamate; $J_{4,5}$, coupling constant between C4 and C5; $J_{3,4}$, coupling constant between C3 and C4.

Camerino et al. have shown that acetazolamide prevented inhibited efflux of lactate from muscle of K^+-depleted rats and this effect was associated with inhibition of lactate transport, rather than inhibition of CA [66]. Lactate can be transported in the extracellular space via monocarboxylic acid transporter 1 (MCT1). Deitmer et al. have shown that 10 µM ETZ has no effect on MCT1 activity [67]. The present data also show that ETZ has no effect on the concentration on lactate in cell extract (table 3.2) and this is in a good agreement with the results of Deitmer et al. These results show that compound **1** may has an inhibitory effect on lactate transport in the extracellular (table 3.2). The fractional ^{13}C-enrichments of intracellular and extracellular alanine in 3T3-L1 cells in the presence of various CAIs are given in table 3.3. These results show that the *de novo* synthesis of ^{13}C-labelled alanine from [U-^{13}C]glucose in the presence of various CAIs, especially compound **1** (97µM, 24h), are remarkably increased in media or cell extracts. These results indicate a predominant cellular ammonia detoxification processes via ALAT, whereas in astrocytes the main pathway to detoxify excess intracellular ammonia is GS [68, 69].

Table 3.2 Percentage ^{13}C-enrichments of intra- and extracellular lactate

	TPM 100µM,24h	ACT 150 µM,24h	Compound **1** 97µM,24h	ETZ 13µM,24h	compound **1** 10 µM,24h	compound **1** 10 µM,12h
Lac,C3 MED	107.7±12.8	104.0±14.3	546.0±14.0	193.0±9.0	386.5±8.5	323.5±9.5
Lac,C3 CE	175.5±11.6	305.3±13.5	1280.0±30.2	96.8±11.3	714.0±16.1	374.1±14.1

The percentage ^{13}C-enrichment in lactate was calculated by integration of the areas of ^{1}H-^{13}C peaks in ^{1}H-NMR spectra of cell extracts and media after 24hours (12 hours) incubation of 3T3-L1 cells with 5 mM glutamine and 5 mM [U-^{13}C]glucose as tracer in the presence of various CAIs. Values represent means± SD. Abbreviations: see table 3.1.

Table 3.3 Percentage ^{13}C-enrichments of intra- and extracellular alanine

	TPM 100µM,24h	ACT 150 µM,24h	compound **1** 97µM,24h	ETZ 13µM,24h	compound **1** 10 µM,24h	compound **1** 10 µM,12h
Ala,C3 MED	129.2±10.8	93.5±5.5	106.5±3.5	175.3±4.8	124.5±1.5	175.0±6.9
Ala,C3 CE	202.3±16.2	186.7±9.5	396.6±13.3	105.8±11.0	267.1±7.3	251.0±12.5

The percentage ^{13}C-enrichment alanine was calculated by integration of the C3-signal of alanine in ^{13}C-NMR spectra obtained from cell extracts after 24hours (12 hours) incubation of 3T3-L1 cells with 5 mM glutamine and 5 mM [U-^{13}C]glucose as tracer in the presence of various CAIs. Abbreviations: see table 3.1.

3.4 The effect of CAIs on de novo lipogenesis in 3T3-L1 cells

De novo lipogenesis means the synthesis of endogenous fatty acids from carbohydrates in the mammalian organism. The enzymatic pathway for synthesis of fatty acids from acetyl-coenzyme A, or *de novo* lipogenesis (DNL), is present in human liver and, to a lesser extent, in adipose [70]. The effect of CAIs on DNL can be studied with ^{13}C-NMR spectra of lipid extracts from cells (Table 3.4). Typical ^{13}C-NMR spectra of lipid extract of 3T3-L1 cells, after incubation with [U-^{13}C]glucose in the presence and absence of compound **1**, are shown in figure 3.5.

***Table 3.4 Percentage ^{13}C-enrichments in* F_ω of lipids of 3T3-L1 cells**

	TPM 100µM,24h	ACT 150 µM,24h	compound **1** 97µM,24h	ETZ 13µM,24h	compound **1** 10 µM,24h	compound **1** 10 µM,12h
F_ω	76.6±4.8	67.1±16	n.d.	73.8±11	n.d.	n.d.

Percentage ^{13}C-enrichments in F_ω of lipids were calculated by integration of the signal of the terminal carbon in lipid chain (Fω) in ^{13}C-NMR spectra obtained from lipid extracts after 24hours (12 hours) incubation of 3T3-L1 cells with 5 mM glutamine and 5 mM [U-^{13}C]glucose as tracer in the presence of various CAIs. DNL synthesis in the presence of [U- ^{13}C]glucose will label all carbons or at least pairwise odd/even numbered carbons and the terminal carbon will show a doublet or a singlet (nat. abundance). Fractional enrichments are obtained by referring the area of doublet spectra of $\boldsymbol{F}_\omega$ to the area of natural abundance singlet peak of $\boldsymbol{F}_\omega$ /control. Abbreviations: see table 3.1; n.d., not detectable.

Figure 3.5 Segment of ^{13}C-NMR spectra of lipid extracts

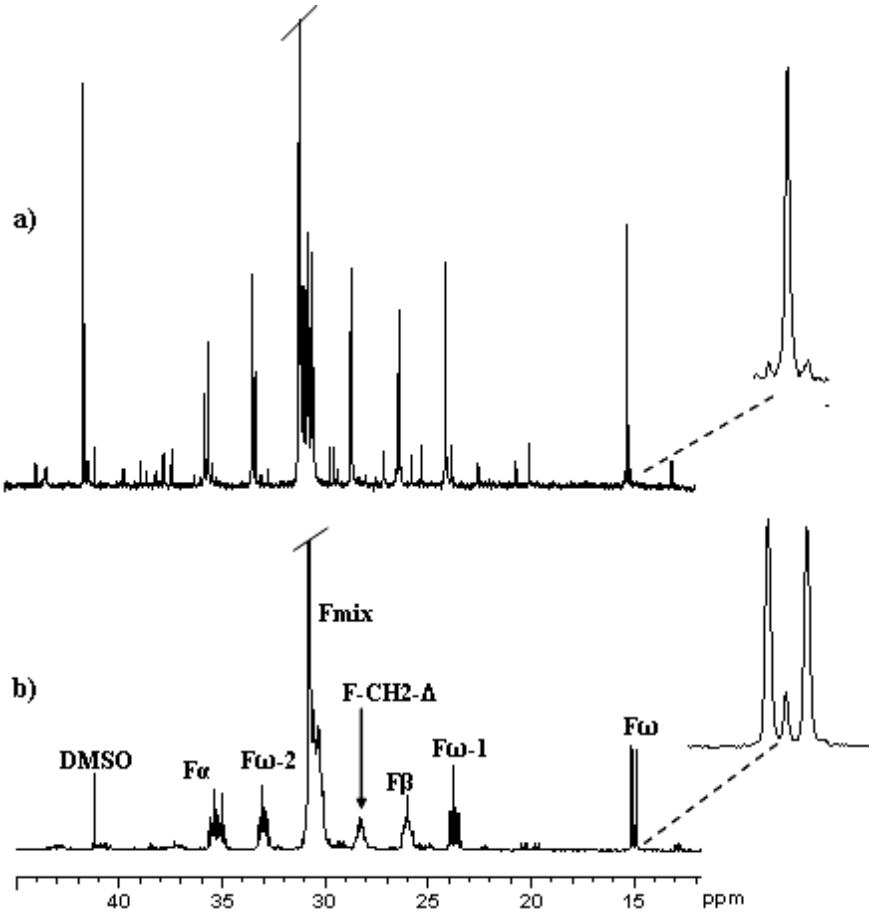

*The 3T3-L1 cells were incubated in the presence of 4 mM glutamate and 5 mM [U-^{13}C]glucose and 97 µM compound **1** (a) or absence of any CAI (b) for 24 hours.*

As can be seen from the data, DNL in the presence of TPM, ACT, and ETZ is not effectively blocked but large reduction of DNL synthesis was observed in the presence of compound **1** with various concentrations and various incubations time, which might be attributed to inhibition of CA V and CA II.

Dodgson et al. [43] and Waheed et al. [44] have shown that in freshly isolated rat hepatocytes and 3T3 cells the inhibitory effect of ETZ on DNL acts via inhibition of *pc* and not by inhibition of acetyl-CoA carboxylase, a cytosolic enzyme, because CAIs inhibit also *de novo* synthesis of non-saponifiable lipids, which does not require acetyl-CoA carboxylase activity but dose share other earlier metabolic steps with *de novo* fatty acid synthesis, i.e. CA [43]. This finding suggests that this effect arises from an inhibition of pyruvate carboxylation.

3.5 Study of effect of CAIs on HEP-G2 cells

3.5.1 Introduction

HEP-G2, a liver cell line derived from a human hepatoblastoma, has been found to express a wide variety of liver-specific metabolic functions. Among these functions are those related to fatty acid metabolism [71]. Hepatocytes contain a relatively high specific activity of CA due to the presence of a mitochondrial matrix isozyme CA V [72, 73, 74] and two cytosolic forms (CA II and CA III) [75, 76, 77]. In this study we have used HEP-G2 cells a model for Hepatocytes to investigate the effect of CAIs, i.e. TPM, ACT, ETZ, and compound **1**, on the *de novo* synthesis of glycolytic- and TCA-cycle related metabolite synthetic and DNL.

3.5.2 Metabolites in HEP-G2 cells

The most important metabolites in HEP-G2 cells after incubation with a ^{13}C-labelled precursor, e.g. [U-^{13}C]glucose, are glutamate, lactate, and alanine which are detected in ^{13}C-NMR spectra of cell extracts. In this study we have investigated the effect of eight CAIs on DNL and TCA-related amino acid i.e. glutamate in two groups. The first group contained TPM, ETZ, ACT, and a new candidate as CAI i.e. compound **1**. The second group contain four new substances as CAIs.

3.5.2.1 Glucose metabolism in HEP-G2 cells

In this study the HEP-G2 cells were incubated for 24h with 5 mM [U-^{13}C]glucose. The relative amount of metabolites from HEP-G2 cells in the presence of various CAIs, i.e. TPM (100µM), ACT (150µM), ETZ (13µM), and compound **1** (97µM), are shown in figure 3.5. Exposure of HEP-G2 cells to 100µM TPM, 150µM ACT, and 13µM ETZ for 24 hours resulted no change of cellular metabolites. This means these CAIs are not specific for CA V and CA II. In contrast, 97µM compound **1** shows a considerable decrease of the anaplerotic entry of [U-^{13}C]glucose into TCA cycle to 14% of control. This strong inhibitory effect of compound **1** on *pc* activity can be interpreted as an effect of CAI inhibition of CA V and/or CA II [63]. The absence of any glucose in cell extracts or media (figure 3.6), after 24h indicates a very high glycolysis rate in this cell line.

Figure 3.6 The percentage ^{13}C-enrichment of metabolites in cell extracts of HEP-G2 cells

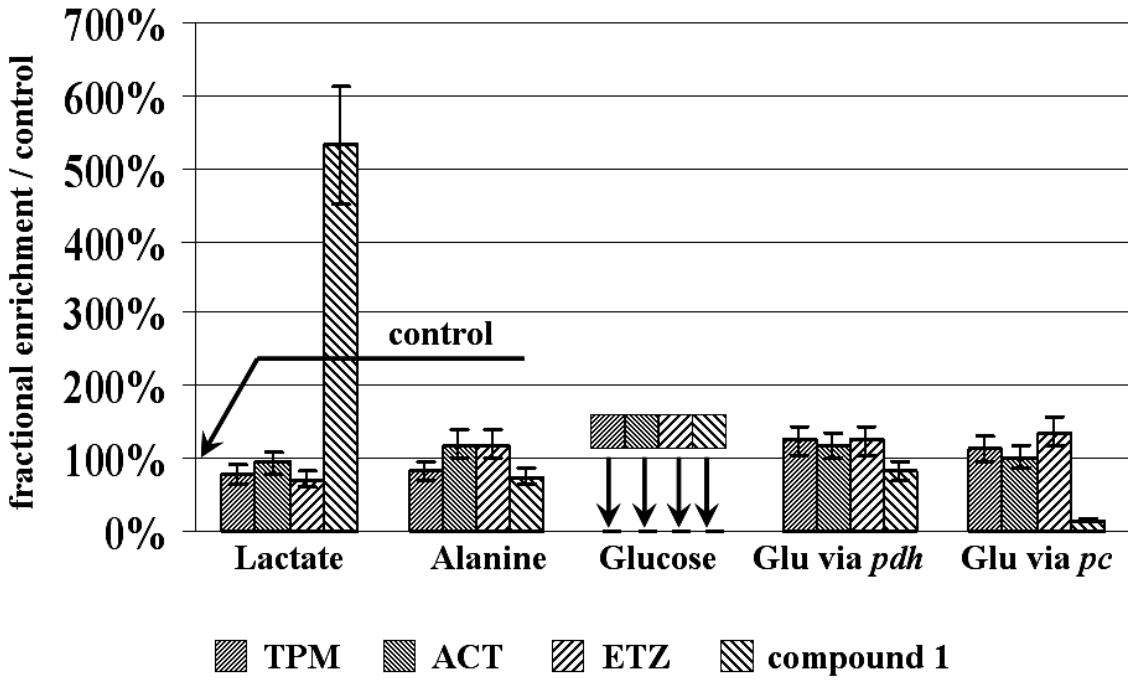

*The percentage ^{13}C-enrichment in lactate was calculated by integration of the areas of ^{1}H-^{13}C peaks in ^{1}H-NMR spectra of cell extracts, and the percentage ^{13}C-enrichment in specific carbon position of glutamate, alanine, and glucose were calculated by integration of the respective signals in ^{13}C-NMR spectra obtained from cell extract after 24 hours incubation of HEP-G2 cells with 5 mM glutamine and 5 mM [U-^{13}C]glucose as tracer in the presence of various CAIs. Abbreviations: TPM, topiramate; ACT, acetazolamide; ETZ, ethoxyzolamide; compound **1**, the new CAI.*

3.5.2.2 The effect of CAIs on DNL in HEP-G2 cells

Figure 3.7 shows the ^{13}C -NMR spectra of F_{ω} in lipids from HEP-G2 cells. The ^{13}C-enrichment in F_{ω} of lipids from HEP-G2 cells are shown in figures 3.7 and 3.8. The data show that TPM, ACT and ETZ have no effect on inhibition of *de novo* lipogenesis after 24h incubation, whereas 97 µM compound **1** leads to fast 100% decrease on DNL in HEP-G2 c ells after 24h incubation with [U-^{13}C]glucose.

Figure 3.7 ^{13}C-NMR spectra of F_ω of lipids extracts of HEP-G2 cells

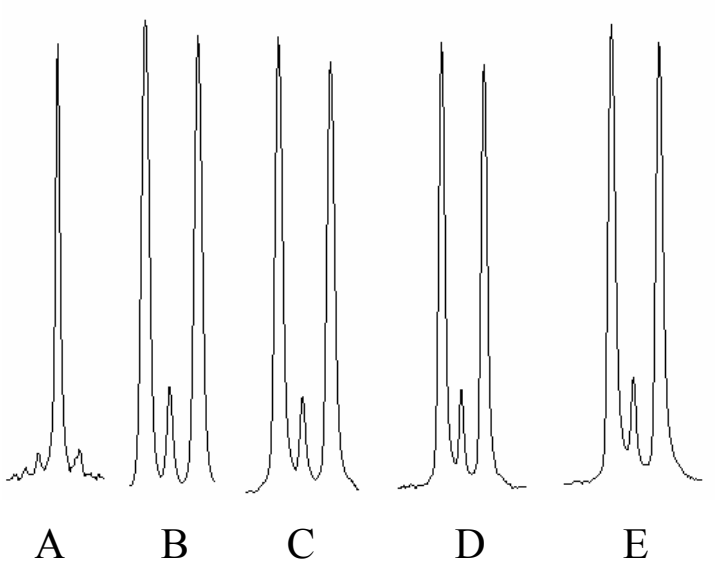

*The HEP-G2 cells were incubated for 24 h with 5mM [U-^{13}C]glucose under control conditions and in the presence of various CAIs. The doubled signals (in B-E) of Fω are from [U^{13}C]glucose. ^{13}C-NMR spectrum after 24h incubation in the presence of, A, 97 µM compound **1**; B, 100 µM TPM; C, 150 µM ACT; D, 13 µM ETZ, and E, control.*

Figure 3.8 ^{13}C-enrichment in F_ω of lipids from HEP-G2 cells

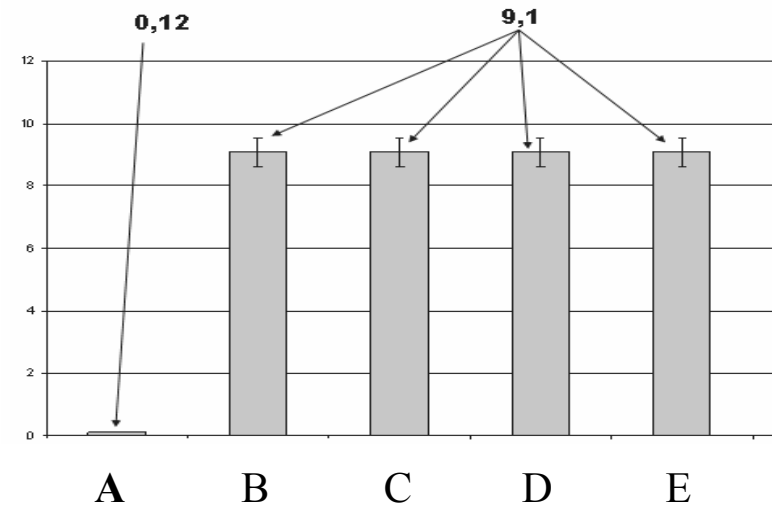

*The columns show the ratio of doublet spectra of F_ω (terminal carbon of fatty acid residue) to spectrum of natural abundance after 24 h incubation with [U-^{13}C]glucose in the presence of various carbonic anhydrase inhibitors, i.e. TPM, ACT, ETZ, and compound **1** or absence of CAI (control). The columns represent the ratio of the area of doublet spectra of F_ω to the F_ω area of natural abundance singlet peak. A, 97 µM compound **1**; B, 100 µM TPM; C, 150 µM ACT; D, 13 µM ETZ, and E, control.*

3.5.2.3 Effect of compound 1 on alteration of the cellular energy status

The energy state of cells is reflected by the concentrations of high energy phosphates such as nucleoside di- and triphosphates (NDP´s, NTP´s), in particular ADP and ATP (adenosine di- and triphosphate), and phosphocreatine (PCr). These substances can be quantified from ^{31}P-NMR spectra of PCA extracts of HEP-G2 cells.

The relative amount of NTP, and PCr in the presence of 100 µM compound **1** after 6, and 24h incubation and typical ^{31}P-NMR spectra are shown in figures 3.9 and 3.10 respectively. The data show that exposure of HEP-G2 cells to 100 µM compound **1** for 6 hours decreased NTP and PCr considerably. 100 µM compound **1** caused a 33% and 66% decreases of NTP and PCr after 6h respectively (figure 3.9). Under control conditions, the PCr/NTP ratio was 0.250, whereas this ratio was reduced to 0.125 after exposure of HEP-G2 cells to 100 µM compound **1** for 6h. This behaviour of HEP-G2 cells reflects the buffering of the NTP level at the expense of PCr, although the NTP level was reduced. The incubation of cells for 24h caused an undetectable level of NTP and PCr (figure 3.10). This indicates a strong reduction of the energy status in HEP-G2 cells. It may be partly due to a more efficient glucose metabolism through glycolysis and subsequent lactate production in these cells under inhibition of CA V and/or CA II.

Figure 3.9 Effect of compound 1 on high-energy phosphates

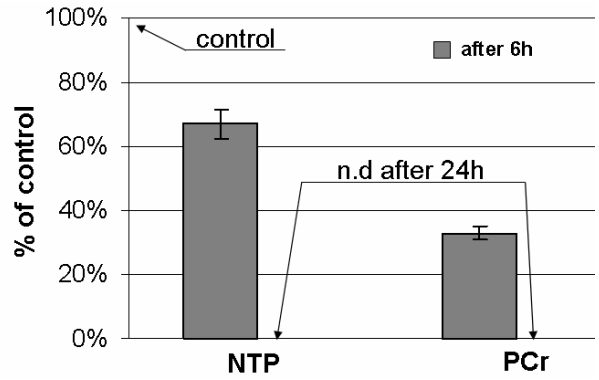

*The concentrations of high-energy phosphates were calculated by integration of the respective signals in ^{31}P- and ^{1}H-NMR spectra after 6 h and 24 h incubation of HEP-G2 cells with media containing 5 mM [U-^{13}C]glucose and 4 mM glutamine in the presence or absence (control) of 100µM compound **1**. The values are given in % of controls and represent means ± SD of three individual experiments, n.d: not detectable.*

Figure 3.10 ^{31}P-NMR spectra of HEP-G2 cells

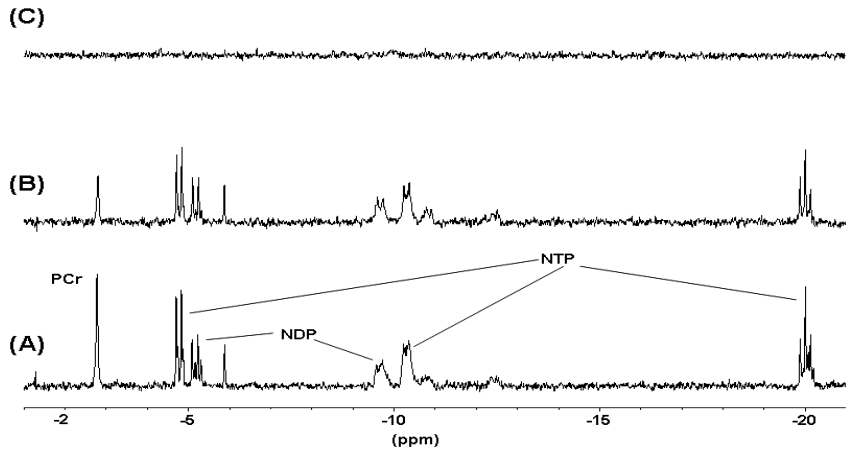

*^{31}P-NMR spectra of perchloric acid extracts of HEP-G2 cells incubated for 6 hours (A and B) and 24 hours (C) with media containing 5 mM [U-^{13}C]glucose and 4 mM unlabelled glutamine in the presence (B and C) or absence (A) of 100 µM compound **1**. Peak assignments: NTP, nucleoside triphosphate; NDP, nucleoside diphosphate; PCr, phosphocreatine.*

3.5.3 Study of effect of compound 1 on HEP-G2 cells incubated with [2-^{13}C]- and [3-^{13}C]pyruvate and [2-^{13}C]acetate

3.5.3.1 Introduction

It is well known that glucose is the main substrate for cells, especially for the brain energy metabolism [78, 79, 80, 81]. Pyruvate is the last product of glycolysis. Thus incubation of cells with pyruvate as tracer is a well suited method to study the effect of CAIs of glycolyse and pyruvate metabolism, while labelled acetate was used to study the effect of compound **1** on *pdh* and on DNL. Hazen et al. [44] demonstrated that ETZ did not inhibit *de novo* lipogenesis from [^{14}C]glutamine in 3T3 cells. This suggests that ETZ inhibits lipogenesis by an inhibitory effect on pyruvate carboxylase as opposed to acetyl CoA carboxylase, because the incorporation of glutamine into lipids does not involve pyruvate carboxylase. Lipogenesis from acetate requires the activity of acetyl-CoA carboxylase, but not pyruvate

carboxylase (see metabolic fate of [2-^{13}C]acetate, page 76). For this propose the HEP-G2 cells were incubated with 2.5 mM [2-^{13}C]acetate in the presence of 50 µM compound **1** for 6h.

3.5.3.2 Effect of compound 1 on HEP-G2 cells, incubated with [2-^{13}C]- or [3-^{13}C]pyruvate

The relative portion of newly synthesised ^{13}C-labelled glutamate (Figure 3.11) decreases to 60%-70% of control after compound **1** treatment, due to the decrease of anaplerotic entries of [2-^{13}C]pyruvate into TCA cycle. The relative portion of [2,3,4-^{13}C]glutamate synthesised from [3-^{13}C]pyruvate was reduced to 60%-70% of control after treatment with 50 µM compound **1**, due to decreases of anaplerotic entries of [3-^{13}C]pyruvate into TCA cycle (data not shown). Since the incorporation of ^{13}C from [2-^{13}C]pyruvate into the C2 and C3 of glutamate (see metabolic fate of [2-^{13}C]pyruvate, page 74) and the incorporation of ^{13}C from [3-^{13}C]pyruvate into [2,3,4-^{13}C]glutamate (see metabolic fate of [3-^{13}C]pyruvate, page 75) can only occur as the result of pyruvate carboxylase activity and subsequent conversion of ^{13}C-labelled oxaloacetate into ^{13}C-labelled glutamate. This result is consistent with experimental inhibition of pyruvate carboxylation in astrocytes [63] and in hepatocytes and adipocytes [16, 43, 44, 82, 83], demonstrating that CAIs inhibit pyruvate carboxylation. Dodgson and Forster [16] reported that the ability of these drugs (CAIs) to inhibit *pc* was not due to direct inhibition of the enzyme since purified *pc* activity was unaffected by supramaximal concentrations of ACT. Since *pc* uses bicarbonate, instead of CO_2, as the preferred substrate [84] it can be proposed that CA V increased the availability of bicarbonate for oxaloacetate production (figure 2.7, page 28).

Figure 3.11 Fractional ^{13}C-enrichment per control in individual carbon of glutamate

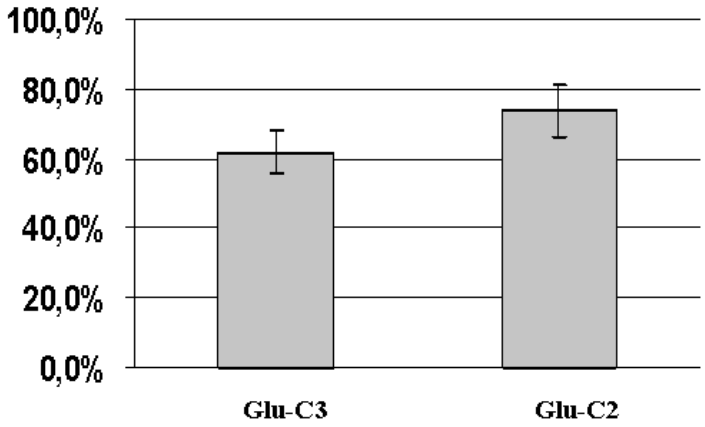

*The HEP-G2 cells were incubated in Dulbecco's modified Eagle's medium (DMEM) supplemented with 5 mM [2-^{13}C]pyruvate as tracer and 50 µM compound **1** for 6h. Values are means ± SD for n=3*

Thus inhibition of influx of pyruvate into TCA cycle via *pc* in the presence of compound **1**, a sulphonamide, suggests that compound **1** inhibits CA V and /or CA II.

3.5.3.2.1 The effect of compound 1 on DNL in the presence of [2-^{13}C]- or [3-^{13}C]pyruvate

In HEP-G2 cells, 50 µM compound **1** caused a nearly 50% decrease of DNL after 6h incubation with [2-^{13}C]-, [3-^{13}C]pyruvate. Fractional ^{13}C-enrichment/control in F_{ω}, $F_{\omega-1}$, $F_{\omega-2}$, F_{α}, and F_{β} of lipids of HEP-G2 cells are shown in table 3.5. After incubation of cells with [3-^{13}C]pyruvate, only even numbered carbons will be labelled in the synthesised lipids, i.e. $F_{\omega-1}$, and F_{β}, while odd numbered carbons will be labelled in the synthesised lipids after incubation of cells with [2-^{13}C]pyruvate.

Table 3.5 Fractional ^{13} C-enrichment/control in F_{ω}, $F_{\omega-2}$, F_{β} and F_{α} of lipids

Incubation with	F_{ω}	$F_{\omega-1}$	$F_{\omega-2}$	F_{β}	F_{α}
[2-^{13}C]pyruvate	**100±3.5**	**56±7.4**	**98±5.7**	**53±6.4**	**96±9.7**
[3-^{13}C]pyruvate	**45±8.1**	**98±4.7**	**42±6.3**	**95±9.7**	**26±5.8**

*The percentage ^{13}C-enrichments in specific carbon position of lipids were calculated by integration of the respective signals in ^{13}C-NMR spectra obtained from lipid extracts after 6h incubation HEP-G2 cells with media containing 5 mM [2-^{13}C]pyruvate or [3-^{13}C]pyruvate under control conditions or treatment with 50 µM compound **1**. The values are given in percent of control and represent means ± SD for n=3.*

The data show that exposure of HEP-G2 cells to 50 µM compound **1** for 6 hours resulted in a considerable decrease of DNL to 50% of control. CAIs have been reported to inhibit DNL in hepatocytes [85] and human adipose tissue [86]. CA II and CA V have been shown to be important and specific isozymes in DNL [43]. CAIs have been observed to inhibit urea synthesis [73, 74, 82, 87, 88] and gluconeogenesis [16] from pyruvate and these inhibitions were at the level of CA V, which provides additional bicarbonate for carbamoylphosphate synthesis and *pc*. The strong inhibitory effect of compound **1** on DNL (figure 3.6 and table 3.5) at the level of CA V/ CA II indicates that this CAI is a very potent candidate to inhibit DNL and eventually for treatment of obesity.

3.5.3.2.2 Effect of compound 1 on HEP-G2 cells incubated with [2-^{13}C]acetate

Effect on *pdh* activity

^{13}C-isotopomer pattern in glutamate after incubation with [2-^{13}C]acetate : *pdh* activity decreased to 30% of control in HEP-G2 cells in the presence of 50 µM compound **1** using [U-^{13}C]glucose as substrate. This may be due to an immediate drop of *pdh* activity by *pdh* inhibition or compound **1** inhibits *pc* and by this means *pdh* indirectly. To test both hypnotization the same experiment was repeated using [2-^{13}C]acetate as substrate, since acetate forms acetyl-CoA independently of *pdh*. As noted before, the main entry point for acetate into metabolism in

vertebrates is its conversion to acetyl-CoA by acetyl-CoA synthetase [89]. The labelled acetyl-CoA then enters the TCA cycle by reaction with oxaloacetate to form citrate. Carbon label from [2-^{13}C]acetate reaches [4-^{13}C]glutamate by transamination of [4-^{13}C]α-ketoglutarate formed in the TCA cycle, after the first turn and after second turn of TCA cycle [2(3)-^{13}C]glutamate will appear (upon equilibration with fumarate). The relative portions of newly synthesised ^{13}C-labelled glutamate are shown in figure 3.12. In the cell extract analysis of the C4-gultamate signal surprisingly shows a 77% increase of labelled glutamate in the presence of 50μM compound **1** as compared to control. Experiments with [U-^{13}C]glucose have shown that the newly synthesised glutamate from labelled glucose via *pdh* activity was reduced to 68% of control in 3T3-L1 cells (table 3.1) and to nearly 30% of control in HEP-G2 cells (figure 3.6). Taguci et al have shown that 25 mM bicarbonate in liver cells causes a 16% increase in the *pdh* activity, whereas the activity of *pc* is increased to 300% of control [90]. This means (a) compound **1** has a direct inhibitory effect on *pdh* as glucose is not as efficiently recruited as in control and (b) anaplerotic pathways other than *pc* provide sufficient oxaloacetate as substrate for the TCA cycle.

Figure 3.12 Fractional^{13}C-enrichment per control in individual carbon of glutamate

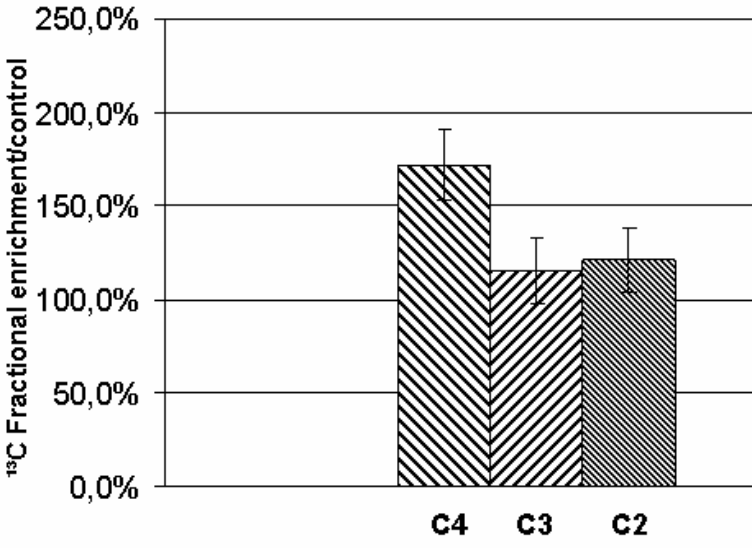

The effect of carbonic anhydrase inhibitor, compound ***1****, on the pdh pathway. The HEP-G2 cells were incubated for 6h in the presence of compound* ***1*** *or 0.1 % of DMSO as drug vehicle and 4 mM glutamine and 5 mM glucose and 2.5 mM [2-^{13}C]acetate as tracer.*

Effect on *DNL*

As noted above, CAIs are good candidates to inhibit DNL. In 1984, Herbert and Coulson have hypothesized that the inhibitory effect of CAI on DNL might represent an interaction between acetyl-CoA carboxylase, a bicarbonate requiring enzyme, and the cytosolic carbonic anhydrases [85]. This idea stemmed from the in vitro inhibition of acetyl-CoA carboxylase by CAIs reported earlier by Cao and Rouse [91]. The results of experiments with labelled glutamine have shown that CAIs have no effect on DNL [44], on urea synthesis and gluconeogenesis. Thus it is good evidence that the effect of CAIs on urea synthesis and gluconeogenesis were at the level of CA V [16, 74, 82, 83, 88, 92]. To examine, whereas the effect of compound **1** on DNL is at the level of CA V and/or CA II or at the level of the acetyl-CoA carboxylase, the newly synthesised lipids in the lipid fractions of experiment with [2-^{13}C]acetate in the presence or absence of 50 μM compound **1** were investigated using NMR spectroscopy. The data show that compound **1** has no effect of DNL, if labelled acetate is used as tracer (data not shown). Therefore, the effect of compound **1** on DNL is at the level of CAV and/or CA II and not at the level of acetyl-CoA carboxylase. If the effect of compound **1** on DNL was at the level of acetyl-CoA carboxylase, a large reduction in DNL must be seen in the presence of compound **1** but no direct effect of compound **1** could be observed on DNL in the presence of labelled acetate.

3.6 DISCUSSION

Pyruvate carboxylase has a peripheral role in DNL. It provides a 4-carbon intermediate in the mitochondria for the synthesis of citrate required for the cytosolic enzyme, ATP-citrate lyase. In several tissues it has been proposed that CA V and/or CA II may help maintain adequate rates of pyruvate carboxylation. Because 3T3-L1 and HEP-G2 cells contain relatively high concentration of *pc* and CA activity, we examined the influence of CA activity on pyruvate carboxylation and DNL in 3T3-L1 and HEP-G2 cells.

The CAIs, i.e. TPM, ETZ, and ACT caused a 30-40% decrease of the incorporation of [U-^{13}C]glucose into TCA cycle via *pc* and a 30-40% decrease of DNL in 3T3-L1 cells. A decrease of incorporation of labelled glucose into the TCA cycle via *pc* can lead to reduction in the citrate concentration. Thus export of surplus mitochondrial citrate will be reduced and it may explain the reduction in DNL observed in cells incubated with CAIs. The decrease of labelled glucose incorporation into the TCA cycle via *pc* and into DNL in HEP-G2 cells was not significant in the presence of TPM, ETZ, and ACT.

The inhibitory effect of CAIs on DNL must be associated with a decrease of the cellular energy state since the synthesis of fatty acids is ATP requiring. Waheed et al. [44] and Hazen et al. [43] have shown that the concentrations of citrate and malate were reduced in the presence of ETZ without a concomitant decrease of ATP concentration but the reduction of TCA cycle intermediates were associated with a decrease of DNL from [^{14}C]glucose. The inhibitory effect of 100 µM compound **1** on DNL is strongly associated with a decrease of the cellular energy state in HEP-G2 cells (figures 3.9 and 3.10, page 40). This implies that the decrease of mitochondrial intermediates is sufficient to inhibit ATP synthesis [44]. In addition, it may also cause a decreasing export of mitochondrial citrate to the cytosol. A strong decrease of the newly synthesised glutamate via *pc* in the presence of compound **1** is a result of strong decrease of the mitochondrial citrate with a concomitant decrease in ATP concentration. Decreased export of excess mitochondrial citrate and decrease in ATP concentration may explain the significant reduction of DNL observed in the 3T3-L1 and HEP-G2 cells incubated with compound **1**, because citrate is used by cytosolic ATP citrate-lyase to produce acetyl-CoA, the precursor for DNL. The strong effect of 100 µM compound **1** on high energy level of cells also suggests that compound **1** inhibits *pc* non-specifically by a toxic effect on the cells (high level of lactate in CE or media).

Several reports have hypothesised that the effects of CAIs on *de novo* lipogenesis might be associated with acetyl-CoA carboxylase, in the sense that cytosolic carbonic anhydrases provides bicarbonate to that enzyme [85, 86, 91]. If acetyl-CoA carboxylase alone was inhibited, an increase or no change of newly synthesised glutamate would be expected. However, glutamate concentrations were depressed in 3T3-L1 and HEP-G2 cells and the reduction appears to be of sufficient magnitude to cause the decrease of DNL.

Furthermore, if another source of citrate was provided in the form of acetate, compound **1** had no effect in the experiment where DNL from [2-^{13}C]acetate was measured. As acetate is not metabolized via *pc*, it is consistent with the hypothesis that compound **1** inhibits DNL via a decreasing substrate availability (bicarbonate) to *pc* rather than via acetyl-CoA carboxylase or another enzyme step distal to oxaloacetate.

As the CA III has only 0.3% activity compared to CA II, the low IC_{50} in figure 3.1 and the lack of a second component of inhibition at higher doses suggest that CA III is not involved in the effects of CAIs on pyruvate carboxylase activity in HEP-G2 cells.

It has been demonstrated clearly that CAIs do not inhibit the purified *pc* directly [16]. Thus studies of the interaction between carbonic anhydrase and pyruvate carboxylase should focus on the mechanism by which CAIs inhibit *pc*. One hypothesis is that bicarbonate levels may be limiting in the mitochondria and that CA V provides the bicarbonate for *pc*. This hypothesis is supported by several observations. Bicarbonate, not CO_2, is required as a substrate by *pc* [84]. CO_2, not bicarbonate, is produced by all mitochondrial decarboxylases [84]. Different to CO_2, bicarbonate does not readily cross biological membranes such as the inner mitochondrial membrane [93]. Thus most of the bicarbonate needed to synthesize oxaloacetate in the mitochondria must be formed within the mitochondria by hydration of CO_2. CA V may be necessary to produce this. Because CA V and pyruvate carboxylase are present in the mitochondria, it seems most likely that they are primarily affected by CAIs. Several groups have reported that the cytosolic CA can facilitate the diffusion of bicarbonate/CO_2 (for review, see [92]). Forster's group have shown that carbonic anhydrase can increase the rate of diffusion of bicarbonate/CO_2 in solutions in vitro [94]. CA II may facilitate the diffusion of exogenous bicarbonate/CO_2 through the cytosol to the mitochondrial matrix to maintain pyruvate carboxylase activity at levels required to fulfil its anaplerotic role (providing citrate) in DNL. Bicarbonate/CO_2 would have to cross the inner mitochondrial membrane as CO_2, because the membrane is poorly permeable for bicarbonate (for review, see [93]).

Overall, our findings suggest that the major indirect target of compound **1** to inhibit DNL could be ATP-citrate lyase due to a decline of citrate concentration. Because most cellular citrate is cytosolic, the reduced cytosolic citrate concentration would decrease ATP-citrate lyase activity and reduce the supply of acetyl-CoA, a substrate for DNL.

3.7 Study of effect of new carbonic anhydrase inhibitors in in de novo lipid synthesis and TCA cycle-related amino acid glutamate with ^{13}C-NMR spectroscopy

3.7.1 Introduction

In this study we have examined the effect of four new CAIs on DNL and cell metabolisms. The compounds of the new CAIs are unknown for us. Thus these CAIs are given only with codes i.e. compound **2**, compound **3**, compound **4**, and compound **5**. The first three are follower of compound **1**. The effects of CAIs on bicarbonate fixation in cultured HEP-G2 cells were examined by incubating cells with CAIs or drug vehicle (DMSO) (0.1%) in the presence of various substrates for 6h.

3.7.2 Determination of IC_{50} of CAIs in second group of CAIs

The IC_{50} values of compound **2**, compound **3**, compound **4**, and compound **5**, were determined by incubation of HEP-G2 cells with 5 mM [U-^{13}C]glucose in the presence of various concentrations of CAIs or drug vehicle (DMSO) as control with NMR spectroscopy. The intensity of triplet spectra of C-3 of newly synthesised glutamate from [U-^{13}C]glucose after 6h incubation in the presence of various carbonic anhydrase inhibitors or only DMSO (control) were used as an indicator to determine the IC_{50} values of CAIs.

The data (figure 3.13 A) show that the IC_{50} of compound **2** and compound **3** are 62 µM and 52 µM respectively and IC_{50} value of compound **4** lie over 200 µM whereas the IC_{50} of compound **5** is 10 µM (figure 3.13 B).

The data show that compound **5** is an extremely potent candidate for inhibition of CA V and/or CA II and this CAI is very effective for inhibition of DNL. The inhibitory data show that the three followers of compound **1** have distinctly weaker potency to inhibit isoforms CA V and/or CA II. Inhibition constants for DNL are over 300 µM.

Figure 3.13 Effect of CAIs on HCO_3^- fixation

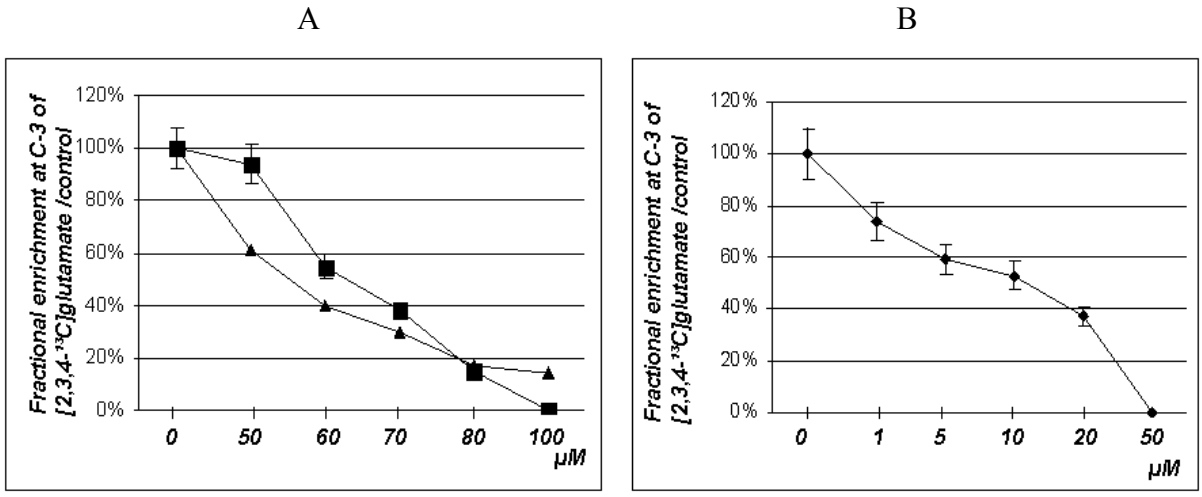

*The HEP-G2 cells were incubated for 6h with various concentrations of CAIs or drug vehicle (0.1% DMSO). (■),compound **2**; (▲),compound **3**; (●),compound **5**.*

In figure 3.14 [95], two very closely structurally related CAIs are shown. The compound with R=Cl, is a rather efficient inhibitor of the isoforms CA I, CA II, and CA IV. Even small structural changes in the benzothiadiazine scaffold (compound in figure 3.14) such as the substitution of the chlorine atom ortho to the sulfamoyl moiety by a trifluoromethyl group, have dramatic consequences for the CA inhibitory properties of the two compounds.

Figure 3.14 Inhibition data of two structurally very closely related sulphonamides.

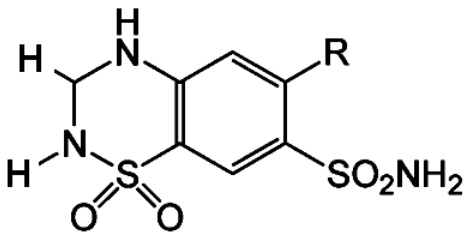

Isozyme	R=Cl	$R=CF_3$
hCA I	328	2840
hCA II	290	435
hCA IV	427	4780

The data are from [95] and the values are the concentrations of CAIs (nM). CAs will be 50% inhibited by each concentration. The values show that small structural changes can have dramatic effect on the CA inhibitory properties of these compounds.

Thus it can be concluded that structural changes in the followers of compound **1** may strongly modify the CA inhibitory properties of these compounds on DNL. Because the followers of compound **1** are much less potent for DNL inhibition, their inhibitory effect on newly synthesised glutamate were also tested.

3.7.3 Cellular metabolism in HEP-G2 cells in the presence of new CAIs

HEP-G2 cells were incubated for 6h, with serum-free DMEM culture medium containing 4 mM glutamine in the presence of 5 mM [U-^{13}C]glucose, and various carbonic anhydrase inhibitors (CAIs) i.e. 50 μM compound **2**, 50 μM compound **3**, 50 μM compound **4**, and 1μM, 10 μM, and 50 μM compound **5**.

[U-^{13}C]glucose metabolism: The results of the present study using NMR spectroscopy show that in HEP-G2 cells influx of [U-^{13}C]glucose via *pc* into the TCA cycle forming [2,3,4-^{13}C]glu decreased to 94%, 60%, and 75% compared to controls after 6 hours exposure of 50 μM compound **2**, 50 μM compound **3** and 50 μM compound **4** respectively. Typical ^{13}C-NMR spectra of PCA extracts of HEP-G2 cells incubated with [U-^{13}C]glucose in the presence of 50 μM compound **5** and drug vehicle (control) for 6h are shown in figure 3.15. The 1μM, 10 μM and 50 μM compound **5** decrease the anaplerotic entry of [U-^{13}C]glucose into the TCA cycle to a 70%, 65% and nearly 100% of control (table 3.6 and figure 3.15). The results of this study show that 50 μM compound **2** is not sufficient to inhibit the entrance of glucose via *pc* whereas compound **3** and compound **4** show higher inhibition of glucose influx into the TCA cycle via *pc*. Particularly striking is the CA inhibitory effect from compound **5**. As is shown in table 3.6, 1 μM compound **5** leads to 30% decrease in the synthesis of [2, 3, 4-^{13}C]glucose, which is produced via *pc* activity. Thus compound **5** might be a good candidate to inhibit CA V and/or CA II. The inhibitory effect of compound **5** and compound **1** are comparative but as will be shown, the effects of these two CAIs on DNL and *pdh* activity are different (see 3.8, page 58).

Figure 3.15 Segment ^{13}C-NMR spectra of cell extract of HEP-G2 cells

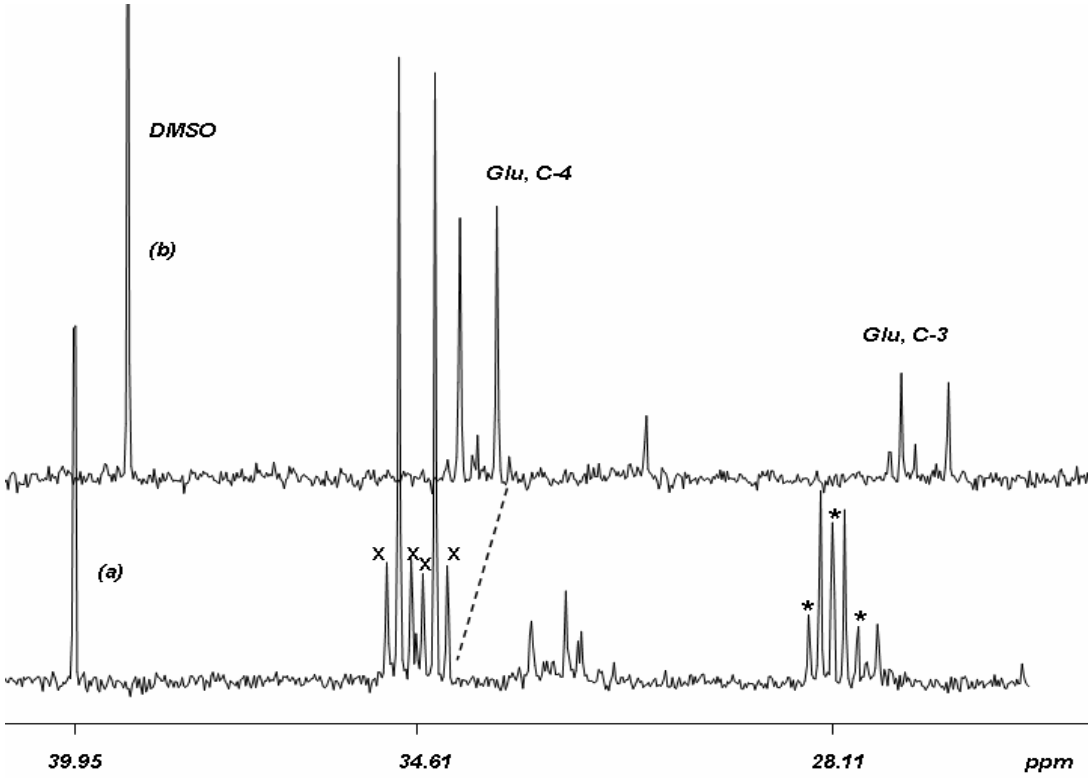

*Section of ^{13}C-NMR spectra of lyophilized cell extract of HEP-G2 cells after 6h incubation with DMEM containing 5 mM [U-^{13}C]glucose in the presence of 0.1% DMSO as drug vehicle for control(a) and 50 µM compound **5** (b). The expanded spectra show the C4 and C3 resonances of glutamate. The doublet signal at C4 of Glu represents only the pdh activity after the first turn of TCA cycle while the fourfold labelled Glu C4 and the triplet at C3 reflect the pc activity. Peak assignments: DMSO, Dimethylsulfoxid; Glu, glutamate, *: [2, 3, 4-^{13}C]Glu; x:[3,4,5-^{13}C]Glu.*

Table 3.6 ^{13}C-fractional enrichment (%) versus control of metabolites within the cell extracts of HEP-G2 cells.

				compound **5**		
	compound **2**	compound **3**	compound **4**	(1 µM)	(10 µM)	(50µM)
[2,3,4-^{13}C]glu	93.8 ± 0.5	60.8 ± 5.4	74.5 ± 1.6	73.6 ± 14.4	67.7 ± 9.3	n.d
[3,4,5^{13}C]glu	81.2 ± 4.7	75.3 ± 1.2	98.7 ± 1.3	75.5 ± 12.3	75.8 ± 9.2	16.2
[4,5-^{13}C]glu	96.6 ± 1.2	85.7 ± 2.4	95.6 ± 2.1	77.3 ± 12.8	90.9 ± 14.6	41.0
Lac-C3	96.1 ± 4.7	93.8 ± 3.4	97.8 ± 1.3	85.4 ± 14.9	71.8 ± 11.9	67.8
Ala-C3	137.0 ± 18.7	97.5 ± 9.6	101.7 ± 14.0	63.6 ± 15.2	107.7 ± 17.4	115.3
[U-13C]glc	74.0 ± 9.8	135.0 ± 0.5	98.1 ± 0.5	111.1 ± 9.4	99.3 ± 8.1	216.4

*The cells were incubated for 6h with [U-^{13}C]glucose and the presence of CAIs (compound **2**, compound **3**, compound **4** and compound **5**). The values are mean ± SD. ns=3(for compound **5** (50 µM) ns=1), n.d.: not detectable.*

3.7.4 Effect of CAIs on lactate and alanine synthesis

The fractional ^{13}C-enrichments of intracellular and extracellular lactate in 3T3-L1 cells in the presence of various CAIs are given in Table 3.6. The followers of compound **1** have no significant effect on *de novo* synthesised Ala and Lac from [U-^{13}C]glucose. In the presence of (50 μM) compound **5**, Lac will be reduced to 68% of control.

3.7.5 The effect of the new carbonic anhydrase inhibitors on DNL.

In HEP-G2 cells, 50 μM compound **5** caused a 100% decrease of DNL after 6 hours incubation with [U-^{13}C]glucose while the other CAIs i.e. compound **2**, compound **3**, and compound **4** or 10 μM compound **5**, are less effective to inhibit DNL (figure 3.16). As mentioned above, the compound **2**, compound **3**, and compound **4** are the follower of compound **1** but the result of these studies show that this new CAIs are not as effective as compound **1** (figure 3.17). The specific CAIs are developed to inhibit one or more specific CA isozymes [96]. A very important factor to assess a new CAI is the number of water molecule forming hydrogen bond with the active site of CA and the CAI [97]. Thus it is possible that the follower of compound **1** don't host favourable van der Waals interactions with many amino acid residues lining the active site [97]. The result of inhibitory effect of compound **5** on DNL shows that this CAI might be a suitable candidate to reduce DNL.

Figure 3.16 The ^{13}C-enrichment in F_ω of lipid fractions of HEP-G2 cells.

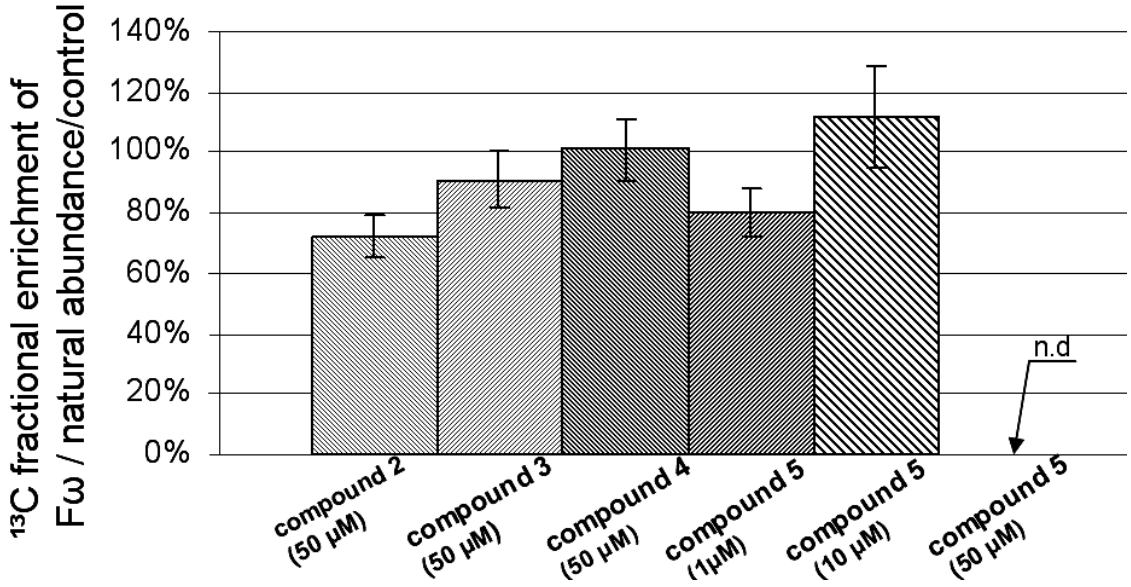

The columns show the ratio of doublet spectra of F_ω (terminal carbon of fatty acid residue) to spectrum of natural abundance after 6 h incubation in the presence of various carbonic anhydrase inhibitors. The columns are obtained by referring the area of doublet spectra of F_ω to the area of natural abundance singlet peak of F_ω.

Figure 3.17 The ^{13}C-NMR segments in F_ω of lipid fractions of HEP-G2 cells

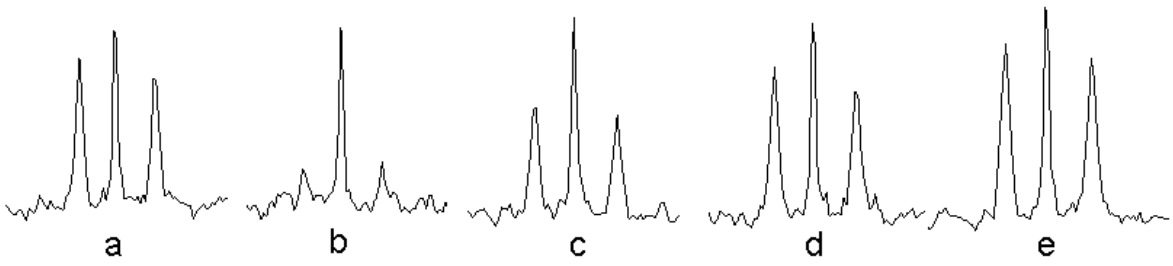

*^{13}C-NMR signals at F_ω of the lipid fractions. The HEP-G2 cells were incubated for 6 hours with 5 mM [U-^{13}C]glucose and 4 mM glutamine and: a) absence of CAI as control; b) 50 µM compound **1**; c) 50 µM compound **2**; d) 50 µM compound **3**; e) 50 µM compound **4**. The last three CAIs are followers of compound **1**. The spectra show that the followers of compound **1** are not as effective as compound **1**.*

3.8 Comparing the inhibitory effect of compound 5 and compound 1

3.8.1 Introduction

At first look it gives the impression that the effect of compound **5** on glucose influx into the TCA cycle via *pc* (see 3.6.3) and on DNL (see 3.6.5) is comparable with the effect of compound **1** but the inhibitory effect of compound **1** and compound **5** in long term experiments, i.e. 24 hours incubation, are different.

3.8.2 Comparing the inhibitory effect of CAIs on glucose metabolism

DNL is inhibited to 100% in the presence of 50 µM compound **5** or 100 µM compound **1**, thus the effects of 50 µM compound **5** on bicarbonate fixation in cultured HEP-G2 cells were compared with the inhibitory effect of 100 µM compound **1**. The HEP-G2 cells were incubated in the presence of CAIs or drug vehicle (DMSO 0.1%) for control with [U-^{13}C]glucose for 6 or 24h. The relative amount of metabolites were obtained from ^{1}H- and ^{13}C- NMR spectra of PCA extracts (see figures 3.18 and 3.19).

After 6h the effect of 50 µM compound **5** and 100 µM compound **1** on the glucose influx into the TCA cycle via *pc* and on *pdh* are similar (figure 3.18). However after 24h in the presence of 50 µM compound **5**, the influx of labelled glucose into the TCA cycle via *pc* ([2,3,4-^{13}C]glutamate) is decreased by only 20% and *pdh* ([4,5-^{13}C]glutamate) activity is not affected (figure 3.19). In fact 100 µM compound **1** produce 3254% lactate and dead of cells after 24h. These results show that the interaction between compound **1** and CA is very strong [97], whereas compound **5** seem to be effective for interaction with many amino acid residues lining for a short time only.

Figure 3.18 Fractional ^{13}C-enrichment per control in individual carbon of glutamate, Lac, and Ala after 6h incubation

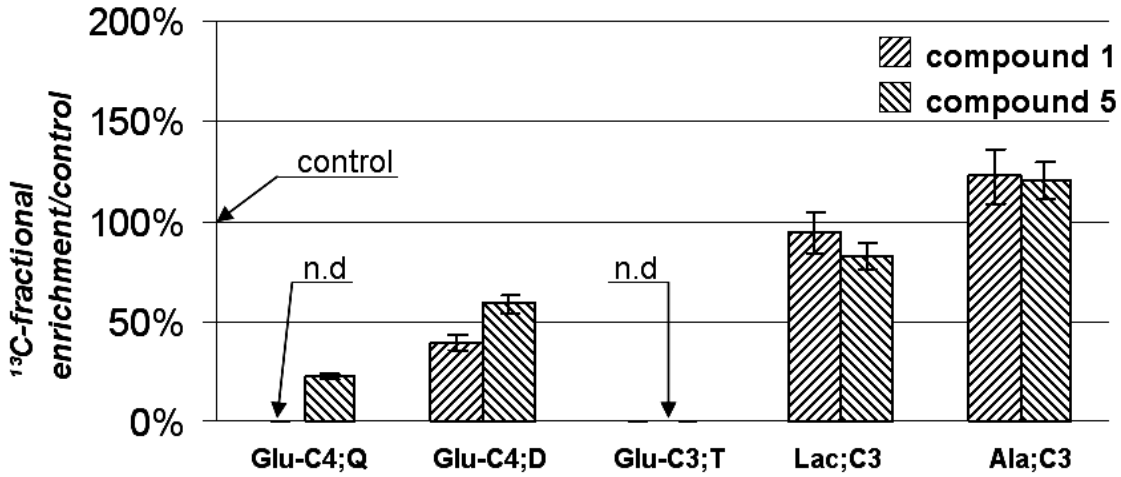

*The relative amount of metabolites from HEP-G2 cells incubated with 5mM [U-^{13}C]glucose in the presence of 100 µM compound **1** and 50 µM compound **5** in cell extracts. The cells were incubated for 6h. The vale are mean± SD. Glu-C4;Q: [3,4,5-^{13}C]glutamate; Glu-C4;D: [4,5-^{13}C]glutamate; Glu-C3;T : [2,3,4-^{13}C]glutamate; Lac:lactate; Ala:alanine; n.d.: not detectable.*

Figure 3.19 Fractional^{13}C-enrichment per control in individual carbon of glutamate, Lac, and Ala after 24h incubation

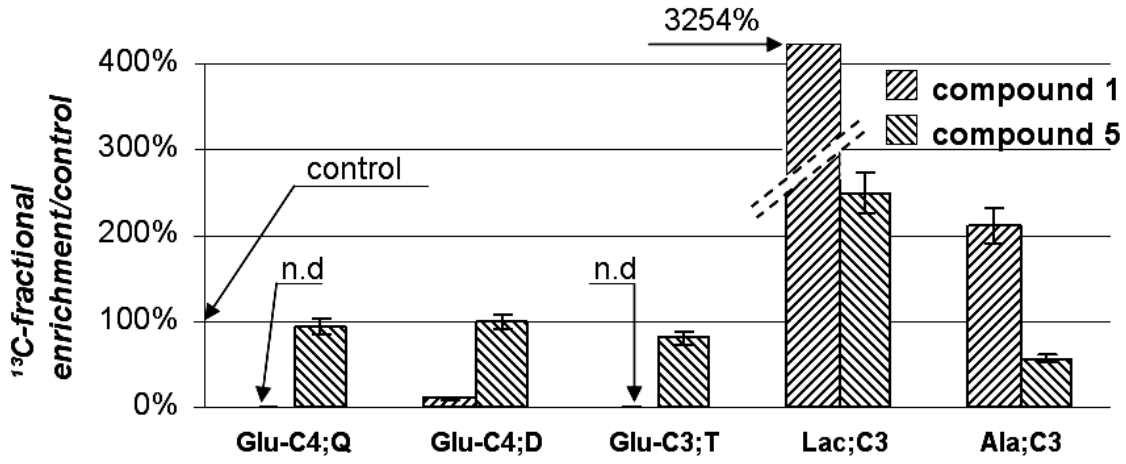

*The relative amount of metabolites incubated with 5mM [U-^{13}C]glucose from HEP-G2 cells in the presence of compound **1** and compound **5** in cell extracts. The cells were incubated for 24h. The value are mean± SD. Glu-C4;Q: [3,4,5-^{13}C]glutamate; Glu-C4;D: [4,5-^{13}C]glutamate; Glu-C3;T : [2,3,4-^{13}C]glutamate; Lac:lactate; Ala:alanine; n.d.: not detectable.*

3.8.3 Comparing the effect of CAIs on acetate metabolism

The HEP-G2 cells were incubated with [2-^{13}C]acetate as tracer in the presence of 50 µM compound **1**, 20 µM compound **5** or drug vehicle (DMSO 0.1%) as control for 6h to compare the effect of CAIs, i.e. compound **5** and compound **1**, on *pdh* activity and ACC in cytosol,. The ^{13}C-fractional enrichment/control of glutamate at C4, C3 and C2 are schematically shown in figure 3.20. The data show that 50 µM compound **1** caused 70-80% increase in cell extract of the entry of [2-^{13}C]acetate into the TCA cycle, whereas 20 µM from compound **5** lead to a 45% decrease in cell extract of entry of [2-^{13}C]acetate into the TCA cycle. The newly synthesised glutamate from labelled glucose via *pdh* activity in the presence of 100 µM compound **1** was reduced to nearly 70-100% of control in HEP-G2 cells (figures 3.6 and 3.19). If these decreases were caused via an inhibitory effect on *pc* only, the increase in the new synthesised glutamate from labelled acetate could not be seen. Thus the increase of newly synthesised glutamate in figure 3.20 is possibly a direct inhibitory effect of compound **1** on *pdh*, while the newly synthesised labelled glutamate via *pdh* in the presence of compound **5** is reduced to 70% of control after 6h (figure 3.18) and the newly synthesised labelled glutamate from [2-^{13}C]acetate is reduced to 70% of control (figure 3.20). The reduction in newly synthesised glutamate from labelled acetate can be interpreted as an effect of compound **5** on *pc* only i.e. compound **5** has no effect on *pdh* activity.

Figure 3.20 Effect of carbonic anhydrases on the pdh pathway

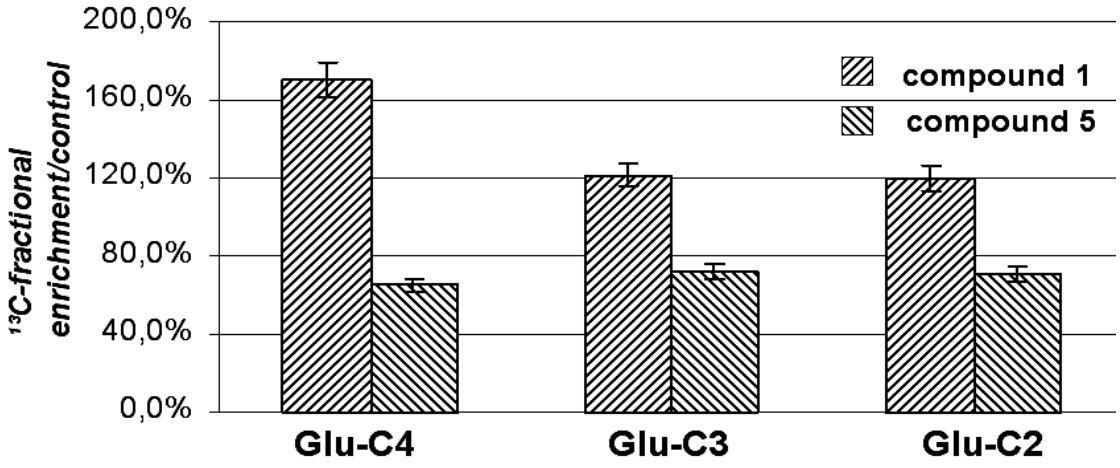

The HEP-G2 cells were incubated for 6h in the presence of CAIs or 0.1 % of DMSO as drug vehicle and 4 mM glutamine and 5 mM glucose and 2.5 mM [2-^{13}C]acetate as tracer.

3.8.4 Comparing the effect of compound 1 and compound 5 on DNL

The role of carbonic anhydrase in *de novo* lipid synthesis was examined by measuring [U-^{13}C]glucose influx into lipid synthesis.

Figure 3.21 shows the ^{13}C-NMR spectra at F_ω (terminal carbon of fatty acid residue) of lipids from HEP-G2 cells after 6 and 24h incubation with [U-^{13}C]glucose as tracer in the presence of 50 µM compound **5**. The results show that 50 µM compound **5** causes a 100% decrease in DNL after 6h whereas compound **5** caused only a 20% decrease in DNL after 24h (figure 3.21 c and d), while the lipid synthesis is 100% inhibited after 6h and 24h in the presence of 100 µM compound **1** (figure 3.7).

Figure 3.21 The ^{13}C-NMR spectra at F_ω of lipids

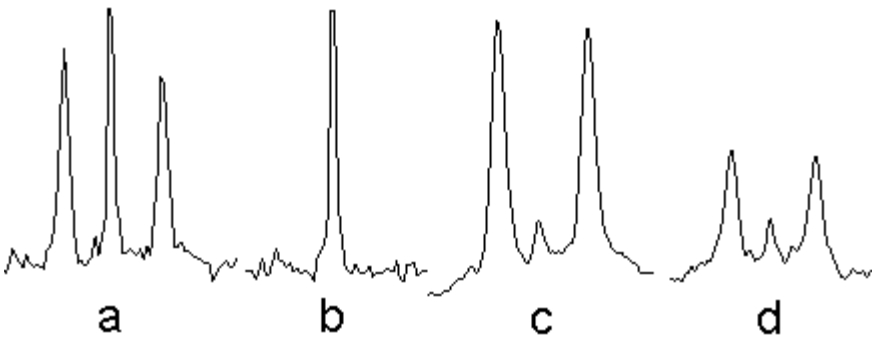

*^{13}C-NMR signals at F_ω of the lipid fractions. The HEP-G2 cells were incubated with [U-^{13}C]glucose in the presence or absence (as control) of 50 µM compound **5** for 6 or 24h. a) control after 6h incubation; b) incubation in the presence of 50 µM compound **5** for 6h ; c) control after 24h; d) incubation in the presence of 50 µM compound **5** for 24h.*

As noted in 3.5.3.2.2, the first hypothesis to inhibit DNL using CAIs, was an interaction between acetyl-CoA carboxylase, a bicarbonate requiring enzyme, and the cytosolic carbonic anhydrases [85, 91]. To examine, whether the effect of compound **5** on DNL is at the stage of CA V and/or CA II or at the acetyl-CoA carboxylase, the newly synthesised lipids originating from [2-^{13}C]acetate were investigated using NMR spectroscopy. The results of experiments with [2-^{13}C]acetate show that in the presence or absence of 50 µM compound **5**

and 50 µM compound **1** DNL is unchanged in the presence of compound **1** and compound **5**, which means that the new CAIs have no effect on acetyl-CoA carboxylase in cytosol (data not shown). If the effect of compound **1** and compound **5** on DNL was at the level of acetyl-CoA carboxylase, a large reduction in DNL would have be seen in the presence of CAIs but no direct effect of the CAIs could be observed on DNL in the presence of labelled acetate.

3.8.5 Effect of compound 1 and compound 5 on the cellular energy status

The exposure of HEP-G2 cells to 50 µM compound **5** for 6 hours decrease PCr to 22% of control and NTP to 75% of control but after 24h PCr was decreased to 73% of control and NTP was unchanged. The results of experiments with compound **1** are given in 3.5.2.3. Since cellular energy production in the cells depends almost exclusively on mitochondrial oxidation of glucose in the TCA-cycle, a reduction of glucose entry into the TCA-cycle (via *pc* and *pdh*) should be reflected by a decreased production of NTP. The results of the present study show that the inhibition of CAs via compound **1** deteriorates the cellular energy state of HEP-G2 cells. A decrease of the energy state of cells could explain the effect on the novo lipid synthesis even after 24h in the presence of compound **1** since the synthesis of fatty acids is ATP requiring [43]. The results of this study indicate also that the decrease in TCA cycle intermediates in the presence of compound **5** is not strong enough to change the high energy state of cells after 24 hours. Thus in the cells may be sufficient ATP for ATP citrate-lyase after compound **5** treatment for 24h.

Chapter 4

Methods

Introduction

Cell cultures of 3T3-L1 (clonal mouse fibroblasts) and HEP-G2 (clonal hepatocytes) are used as cell model to study the effect of carbonic anhydrase inhibitors on bicarbonate fixation and subsequent flux through the anaplerotic enzyme pyruvate carboxylase (*pc*). Furthermore, pathways through the mitochondrial TCA cycle, the synthesis of TCA-cycle related metabolites (in particular glutamate, but also aspartate, malate and others) and the *de novo* lipid synthesis were measured by multinuclear NMR spectroscopy and ^{13}C-NMR isotopomer analysis.

4.1 Cell culture

4.1.1 Definition

3T3-L1 (Mouse embryonic fibroblast - adipose like cell line) are derived from the original line 3T3-Swiss albino developed by Green, Meuth and Kehinde [98, 99]. These cells are widely used to study the biology of adipose tissue. HEP-G2 cells belong to a hepatoblastoma cell line which retains the expression of most liver-specific genes [100]. This cell line is used extensively for toxicological and pharmacological studies in liver type cells.

4.1.2 Preparation of cell cultures

The 3T3-L1 and HEP-G2 ($4x10^6$ cells/ampoule) are stored at – 196 °C (liquid nitrogen) and contain 70% (V/V) DMEM, 20% (V/V) FBS, 10% (V/V) DMSO. To avoid the toxic effects of DMSO, during thawing of the cells, DMSO must be quickly removed. Therefore the cells from an ampoule were quickly thawed and immediately placed into a 50 mL centrifuge tube

containing 30 mL DMEM (10% FBS and 1% penicillin/streptomycin). The cell suspension was centrifuged at 1300 rpm at 4ºC for 3 minutes. The upper phase was removed and the pellet was redissolved in a sufficient amount of DMEM, supplemented with 1% penicillin/streptomycin and 10% heat-inactivated FBS (HEP-G2 cells)/CS (3T3-L1 cells). The cells from one ampoule were plated into two 10 cm petri dishes with each 10 ml DMEM medium. The cultures were kept in an incubator with a humidified atmosphere of 10% (3T3-L1) or 5% (HEP-G2) CO_2 in air at 37°C. Subculture passages of cells were obtained by exposure of the starting passage to 3 ml trypsin/EDTA followed by harvesting the cells with a Pasteur pipette, centrifugation (1300 rpm, 4ºC, 3 min) and resuspension of the cells in fresh culture medium. The cells were plated per 10 cm culture dish. The medium of the cell cultures was replaced every 2-3 days. The cells were cultured at last for 7-10 days.

4.2 Introduction to experimental procedures

Due to the low sensitivity of NMR spectroscopy compared to other analytical methods, for each NMR experiment 10 (8-cm) or 3 (15-cm) dishes of the cell cultures were used after incubation with labelled substances (i.e. glucose, acetate or pyruvate). After incubation of the cells for 6, 12 or 24 h, the cells were extracted with 10% perchloric acid (PCA), as will be discussed later. Figure 4.1 shows a summary of the combined acid and lipid extraction steps of the cells for subsequent NMR measurements.

4.2.1 Incubation procedure

Both the 3T3-L1 cells and HEP-G2 cells metabolism was followed up to investigate the metabolic effects of various carbonic anhydrase inhibitors as well as to determine the IC_{50}-values of these inhibitors. For the incubation of cells, a serum-free medium (DMEM) without glucose, but containing 4 mM glutamine, was used. After removal of the culture medium, the cells were washed twice with 7 ml PBS buffer. Then, the previously prepared incubation medium containing defined concentrations of substrates, e.g. [U-^{13}C]glucose (5 mM), [2-^{13}C]pyruvate (2.5 mM), [3-^{13}C]pyruvate (2.5 mM) or [2-^{13}C]acetate (2,5 mM), in the presence or absence of CAIs, was added to the cells. After a defined incubation period, e.g. 6,

12 or 24 hours, the incubation media were removed and the cells were extracted as described below.

Figure 4.1 Flow for combined PCA/lipid extraction

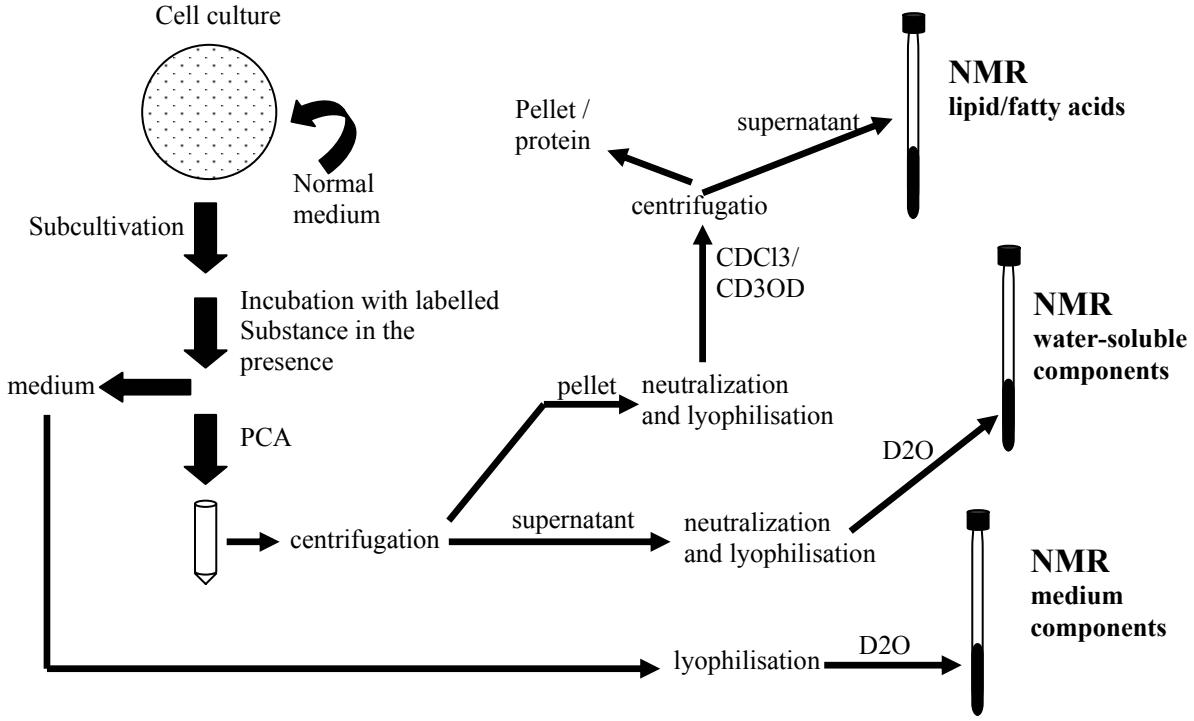

After incubation with ^{13}C-labelled substances and other supplements, the medium was removed from the cells. The cells were immediately extracted with PCA. The suspension was centrifuged, the supernatant collected, neutralized with KOH, again centrifuged and lyophilised. After the first centrifugation, the remaining pellet containing insoluble components including proteins and lipids/fatty acids, was redissolved in 5 ml water, neutralized with KOH and lyophilized. For NMR measurements, the pellet was dissolved in $CDCl_3$/MeOD. The solid residue was dried and used for the quantification of the protein content.

4.2.2 Preparation of perchloric acid and lipid extracts

After experimental incubation of the cells for a defined time interval, the medium was removed and the cells were immediately washed twice with 7 ml ice-cold saline (150 mM NaCl), frozen in liquid nitrogen and suspended with ice-cold 0.9 M perchloric acid (PCA). The suspension was sonicated for 10 min and centrifuged at 4000 rpm at 4ºC for 20 min. The supernatant was collected, neutralised with KOH (10 M/ 1 M/ 0.1 M) to pH=7, again centrifuged and lyophilised. The remaining pellet, after the first centrifugation, containing insoluble components including proteins and lipids/fatty acids, was redissolved in 5 ml water, neutralized with KOH (0.1 M) and lyophilised. The pellet after lyophilisation was dissolved

in 750 µL $CDCl_3$/MeOD (2:1) and centrifuged at 4000 rpm for 20 min at 4°C. The supernatant was transferred into a NMR tube and used for NMR measurements. The solid residue was dried and used for protein determination.

4.2.3 Determination of IC_{50}-values

The IC_{50} measures the effectiveness of a drug. It indicates how much of a particular drug is needed to inhibit 50% of a given biological process. In other words, it is the half maximal (50%) inhibitory concentration (IC) of a compound. For this purpose, the HEP-G2 cells were incubated for 6h with 5 mM [U-^{13}C]glucose in the presence of various carbonic anhydrase inhibitors in different concentrations or with DMSO (0.1 %) as vehicle. After extraction of cells with PCA only the lipid fractions were used to determine the IC_{50} of carbonic anhydrase inhibitors in first group, i.e. TPM, ACT, ETZ, and compound **1**. IC_{50} values for CAIs in second group were determined using cell extract fractions. The concentration of CAIs, which were used for the determination of IC_{50} values are summarized in table 4.1. In each experiment, we have also determined the fractional enrichment of ^{13}C at F_ω of fatty acids and their derivative.

Table 4.1 The CAIs and their concentrations, which were used for determination of IC_{50}

Carboxyanhydrase inhibitor	***The concentrations of CAIs, that were used to determine the IC_{50} values, in µM***
Topiramate	0, 100, 150, 300, 450, 600, 1000
Acetazolamide	0, 150, 200, 300, 450, 600, 1000
Ethoxyzolamide	0, 13, 20, 30, 45, 60, 100
compound **1**	0, 10, 20, 30, 45, 50, 60, 80, 100
compound **2**	0, 60, 70, 80, 100
compound **3**	0, 60, 70, 80, 100
compound **4**	0, 60, 70, 80, 100, 150
compound **5**	0, 1, 5, 10, 15, 20, 30, 50

4.3 Protein determination methods

4.3.1 UV/VIS spectroscopy

Several photometric methods are used to determine the protein concentration in solution. Most methods are based on binding of a chromophore to specific amino acids or bonds in the protein. The resulting colour enhancement can be detected at specific wavelengths of the UV/VIS spectrum. The protein determinations are dependent on the sensitivity of the assay and the relationship between absorbance (A) and protein concentration (Lambert-Beer law). A plot of (A) vs. protein concentration will be linear over a limited range of protein concentration depending on the protein and method used. The standard curve, produced by measuring the absorbance of protein solutions of known concentrations, can be used to estimate the protein concentration of an unknown solution. Standard curves are generated using purified proteins. Bovine serum albumine (BSA) is usually used for this purpose. A linear equation is calculated from the absorbance values of three different concentrations of the protein standard and used to calculate the protein concentration from the absorbance of the unknown solution.

4.3.2 Biuret-method

The principle of the Biuret-method [101] is based on the reaction of Cu^{2+} in an alkaline solution with the carbonyl and amino groups of peptide linkages in proteins forming a violet-coloured copper-protein complex. The adsorption maximum is at 540-560 nm. The sensitivity of this method is 1 – 6 mg protein/ml. The advantage is that the copper reagent reacts with peptide bonds and thus is independent of the amino acid composition. The disadvantage is the low sensitivity.

4.3.3 Lowry-method

The Lowry method [102] is a modified Biuret reaction, in which peptide bonds react with copper II under alkaline conditions followed by the Folin – Ciocalteay phosphomolybdic-phosphotungstic acid reduction to heteropolymolybdenum blue by the copper-catalysed oxidation of aromatic amino acids. The adsorption maximum is at 750 nm. The sensitivity is linear between 0.1 – 1.5 mg protein/ml for BSA. It is more sensitive than the Biuret reaction. The major disadvantage of the Lowry method is the narrow pH range within which it is

accurate (i.e. pH between 10 and 10.5). The other disadvantage of this method is instability of the reagents.

Despite the fact that the protein concentrations of the cell extracts were 3-6 mg protein/ml, the protein content in solution was quantified using a slightly modified Biuret reaction [101]. The VIS absorption was recorded at 540 nm and bovine serum albumin was used as a standard. The intensity of the colour produced is proportional to the protein concentration measured by an UV-VIS spectrometer at 540 nm.

Implementation: The protein pellet was suspended in 3-4 ml 0.1 M NaOH, 0.1% SDS. From each sample, 5, 10 and 50 µL were transformed in 96 multiwells and diluted to 100 µL with bidistilled water. 100 µL 6% NaOH and than 100 µL Biuret-reagent were added to each sample. A violet complex of copper (II) and protein was formed within 45 minutes. Its VIS-absorption at λ = 540 nm is measured with a multiplate reader. In order to determine the protein content, a standard curve using BSA (bovine serum albumine) was determined (0-2000 µg).

Composition of the Biuret-reagent: 9.85 g sodium citrate x 2 H_2O and 13.5 g sodium carbonate x 10 H_2O were dissolved in 25 ml H_2O. 135 mg copper (II) sulfate x 5 H_2O were dissolved in 5 ml H_2O. Both solutions were combined and filled up to 50 ml with bidistilled water.

4.4 NMR spectroscopy

Introduction

The most commonly nuclei in biological NMR experiments are ^{1}H (the most sensitive isotope at natural abundance), ^{13}C, ^{31}P, ^{19}F and ^{23}Na.

NMR was first described and measured in molecular beams by Isidor Rabi in 1938 [103]. Eight years later, in 1946, nuclear magnetic resonances in bulk condensed phase were reported for first time by Bloch et al. [104] and by Purcell et al. [105].

The highest sensitivity in NMR spectroscopy belongs to ^{1}H nuclei. After ^{1}H, the most significant nucleus is ^{13}C because carbon is the building block of all organic molecules. The ^{13}C gyromagnetic ratio, γ_C, is about one fourth of that of ^{1}H ($\gamma_C/\gamma_H \approx 1/4$), leading to a sensitivity (γ^3) of 1/64 of that of ^{1}H. Considering the fact that a ^{13}C nucleus has only about 1.1% natural abundance (of carbon atoms), the general sensitivity of ^{13}C is about

(1/64x0.011) = $1.72x10^{-4}$ relative to that of ^{1}H. To get the same ^{13}C signal-to-noise ratio as a single-scan proton signal it would require 33,850,000 more scans because S/N is proportional to the square root of the number of scans. On the other hand, the use of ^{13}C-enriched substrates, such as amino acids and glucose, has enabled also to record ^{13}C-NMR spectra of cells and tissues with short time and good spectra resolution.

4.4.1 Theory of NMR spectroscopy

NMR is concerned with the interaction between an oscillating magnetic field (the radio frequency field) and the net magnetisation of nuclear isotopes. The nuclei that are NMR active must possess an angular momentum called spin, I. If a nucleus with a spin is placed in a static magnetic field of strength B_o, the nuclear magnetic moment will interact with the applied field, B_0. The nuclear spin has an energy which varies with its orientation with respect to B_0.

Figure 4.2 The basic explanation of spectroscopy in expression of energy levels.

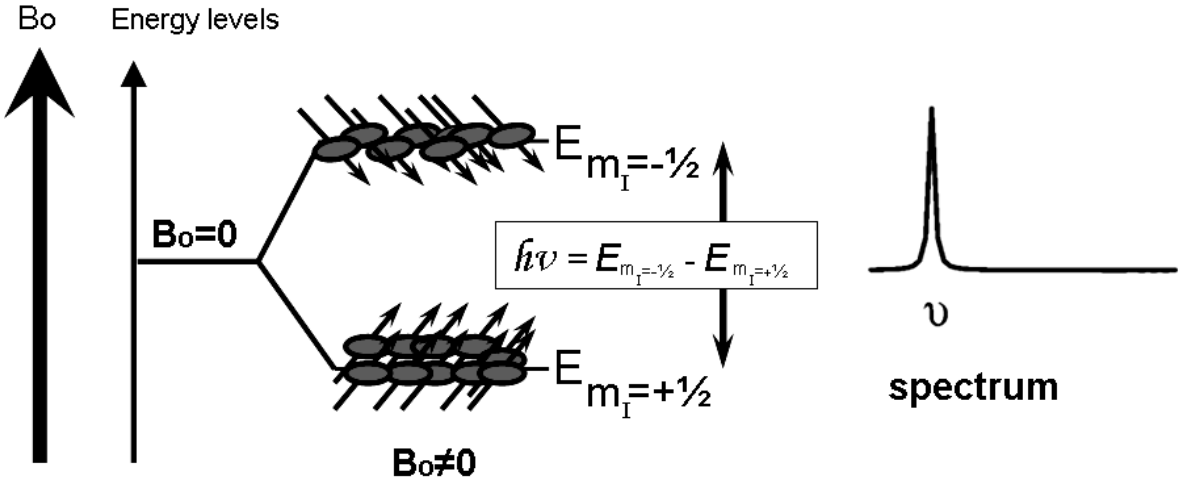

A photon may be absorbed, if its energy equals the energy difference between two energy levels, here $E_{mI=-½}$ - $E_{mI=+½}$. The result is an absorption line in the spectrum at frequency v.

The possible energies of a nucleus with I=½ are quantitised and can be related the magnetic quantum number m (±½), which represent the projection of the magnetic moment onto the

orientation of the magnetic field. According to Boltzmann distribution, the populations of two energy states can be predicted. At equilibrium, these populations can be written as [106]:

$$n_{\alpha,eq} = \tfrac{1}{2}N\exp(-E_\alpha/K_BT) \qquad n_{\beta,eq}=\tfrac{1}{2}N\exp(-E_\beta/K_BT)$$

Where E_α and E_β are the energies of two levels ($m_I=\pm\frac{1}{2}$), K_B is Boltzmann's constant, T is the temperature and N is the total number of spins in magnetic field. If gyromagnetic ratio, $\gamma>0$ than the α state has the lower energy. In this situation, when the spins are at equilibrium (no B_1), the Boltzmann distribution predict that $n_{\alpha,eq}>n_{\beta,eq}$, and it means, that the sample will have a bulk z-magnetization. If the nuclei in the lower energy state (α) absorbs photons, whose energy match the difference in energy between two energy levels (α and β states), i.e. $h\nu=\Delta E$, nuclei will be transferred from α-level to β-level. The result is an absorption line in the spectrum, at frequency ν (figure 4.2).

The photon is irradiated using a radiofrequency (RF) pulse orthogonal to B_o. The pulse represents an oscillating magnetic field (B_1). When the nuclei in the higher energy state makes a transition to the lower energy state, the nuclei emits energy in form of photons. This photon will be detected by a receiver as an induced voltage called free induction decay (FID) signal. The FID that is a time-domain signal can be converted by Fourier transformation (FT) into the frequency-domain function that represents the NMR spectrum (figure 4.3). The integral of each signal can be quantified corresponding to the number of nuclei contributing to particular resonance in a ^{1}H-NMR spectrum. Another important parameter of NMR signal is the fine structure of signals due to spin-spin-coupling with the neighbouring nuclei.

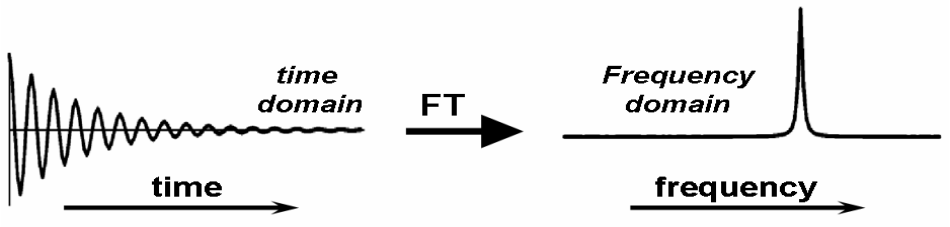

Figure 4.3 The fourier transform, FT, is a mathematical method to translate a time-domain signal, the FID, into a frequency-domain signal, the spectrum.

In a molecule the magnetic moment of each nucleus is susceptible to affect the local magnetic field around neighbouring nuclei, which changes the energy states of the observed nuclei and changes the resonance frequency. This causes a line splitting of the resonance line depending upon number and type of neighbouring nuclei.

4.4.2 Multinuclear high-resolution NMR spectroscopy

4.4.2.1 Preparation of samples

The lyophilised cell extracts and medium samples were redissolved in 800 and 1000 µl D_2O respectively, centrifuged and transferred into a 5-mm NMR tube. In order to prevent glutamine carbamate formation [107] the solutions were adjusted to a pH value of 7 with deuterium chloride (DCl) and deuterium sodium hydroxide (NaOD). The remaining pellet (lipid and protein) was redissolved in 750 µl of $CDCl_3/CD_3OD$ (2:1) and centrifuged. The supernatant solution (lipid fraction) was transfered into a 5-mm NMR tube to NMR analysis (figure 4.1).

4.4.2.2 Acquisition- and processing parameter of NMR spectra

4.4.2.2.1 ^{1}H-NMR spectroscopy

^{1}H-NMR spectra were recorded on a Bruker DRX 600 MHz spectrometer, operating at a frequency of 600.2 MHz using a 5 mm H,C,N inverse triple resonance probe (5-mm HX probe). The acquisition- and processing parameters are shown in table 4-1. Chemical shifts were referenced to lactate methyl at 1.33 ppm, corresponding to tetramethylsilane at 0 ppm. The concentrations of metabolites were determined from fully relaxed ^{1}H-NMR spectra (repetition time of 19 sec) using (trimethylsilyl) propionic-2,2,3,3d_4-acid (TSP) as an external standard. The concentrations were calculated with respect to the corresponding protein content.

4.4.2.2.2 ^{13}C-NMR spectroscopy

^{13}C-NMR spectra were recorded on a Bruker 600 MHz spectrometer, operating at a frequency of 150.9 MHz using a 5-mm ^{1}H/^{13}C dual probe. The acquisition- and processing parameters are shown in table 4-2. Chemical shift were referenced to the C-3 signal of lactate at 21.3 ppm. In addition to PCA- and lipid extracts, also lyophilised incubation media were recorded by ^{13}C-NMR.

Table 4.1 Parameter for recording of ^{1}H-NMR spectra

	DRX 600 MHz
NMR probe	HCN-5mm inverse probe x,y,z-gradients
Number of scans	256-512
Flip angle	40
Repetition time	19 sec
Spectral width	7,200 Hz
Data size*	16,384 byte
Apodisation	EM
*Zero filing to 32768 byte GM: Gaussian Multiplication For ^{1}H-NMR measurements the H_2O signal was suppressed.	

4.4.3 Identification of metabolites from ^{1}H- and ^{13}C-NMR spectra

The lactate resonance at 1.33 ppm in ^{1}H- spectra and 21.3 ppm in ^{13}C-NMR spectra was used as internal reference for detection of chemical shift of other metabolites. The concentration of lactate was determined from fully relaxed ^{1}H-NMR spectra of cell extracts and media using (trimethylsilyl)propionic-2,2,3,3,d_4-acid (TSP) as an external standard. The pool size of other metabolites has been determined using ^{13}C-NMR spectra. Assignments of the other signals in ^{13}C-NMR spectra were confirmed by two dimensional (2D) heteronuclear single quantum coherence (HSQC) spectroscopy. The 2D-HSQC spectra were acquired on a DRX 600 MHz

spectrometer using a 5-mm H, C, N inverse triple resonance probe with shielded gradients. Gradients were shaped by a waveform generator and amplified by a Bruker Acustar II amplifier. Sinusoidal z gradients of 1 ms duration and a recovery time of 100 µs were used for the echo/antiecho gradient selection.

Table 4.2 Parameter for recording of ^{13}C-NMR spectra

	DRX 600 MHz	
	Lipid	***PCA***
NMR probe	CH-5mm dual probe z-Gradient	
Number of scans	61,440-10,2400	20,480
Flip angle	27º	90º
Repetition time	0.3 sec	3 sec
Spectral width	30,180 Hz	33,000 Hz
Data size*	16,384 byte	16,384 byte
Apodisation	EM	EM
* zero filing to 32768 byte EM: exponential multiplication (1-2 Hz) Composite pulse decoupling with WALTZ-16		

A gradient fine-tuning (4:1.008) was performed to get optimum intensity. Low-power adiabatic composite pulse decoupling with WURST [108] was used for hetronuclear decoupling. One thousand twenty-four t_1 increments with 24 scans per increment were acquired. For the assignment of metabolites by two dimensional NMR techniques see [109].

4.4.3.1 Analysis of ^{13}C isotopomer from ^{13}C-NMR spectra of cell extracts

After incubation of cells with ^{13}C-labelled substances, e.g. glucose, the metabolites of glycolysis and the TCA cycle are labelled with ^{13}C in different carbon positions depending on the relative contribution of the enzymatic pathways.

Metabolic fate of [U-^{13}C]glucose

[U-^{13}C]glucose is a often used labelled substance for ^{13}C-NMR spectroscopy to study the cellular biological reactions in mitochondria and/or cytosol of cells. The metabolic pathways transforming [U-^{13}C]glucose into various metabolites are presented schematically in figure 4.4. Glycolysis transforms [U-^{13}C]glucose into [U-^{13}C] pyruvate as the end product of glycolysis and subsequently to [U-^{13}C]alanine via alanine aminotransferase (ALAT; EC 2.6.1.2) and to lactate via lactate dehydrogenase (LDH; EC 1.1.2.3).

[U-^{13}C]pyruvate may enter the tricarboxylic (TCA) cycle via the anaplerotic pathway (pyruvate carboxylase; *pc*; EC 6.4.1.1 or malic enzyme; *me*; EC 1.1.1.40) or via the oxidative pathway (pyruvate dehydrogenase, *pdh*; EC 1.2.4.1). In the anaplerotic pathway, the ^{13}C-labelled positions of pyruvate become the C1, C2 and C3 positions in oxaloacetate. Condensation of [1,2,3-^{13}C]oxaloacetate with labelled acetyl-CoA leads to [2,3,4,5-^{13}C]glutamate or [1,2,3,4,5-^{13}C]glutamate (upon equilibration of oxaloacetate with fumarate). If pyruvate enters the TCA cycle as [1, 2-^{13}C]acetyl-CoA via *pdh* in the oxidative pathway, glutamate will be doubly labelled at C-4 and C-5 after the first TCA cycle turn. The ratio of the C-4 signal intensity of [4,5-^{13}C]glutamate to that of [1,2,3,4,5-^{13}C]glutamate was used to determine the relative contributions of *pdh* and *pc*.

Metabolic fate of [2-^{13}C]pyruvate

[2-^{13}C]pyruvate may enter the TCA cycle via the anaplerotic pathway (pyruvate carboxylase; *pc*; EC 6.4.1.1 or malic enzyme; *me*; EC 1.1.1.40) or the oxidative pathway (pyruvate dehydrogenase, *pdh*; EC 1.2.4.1). In the anaplerotic pathway the 2-^{13}C-labelled position of pyruvate becomes the C2 or C3 position in oxaloacetate (the later after equilibration with fumarate). Condensation of [2(3)-^{13}C]oxaloacetate with acetyl-CoA leads to [3(2),-^{13}C]2-oxoglutarate. After the first TCA cycle turn, [3(2)-^{13}C]glutamate will appear. If [2(3)-^{13}C]oxaloacetate remains in the TCA cycle, monolabelled glutamate C-2 or C-3 appear. If pyruvate enters the TCA cycle as [1-^{13}C]acetyl-CoA via *pdh* in the oxidative pathway, glutamate will be labelled at C-5 after the first turn and at C-1 after the second turn. The signal intensity at C-2 and C-3 of monolabelled glutamate was used to determine the contribution of the *pc* pathway.

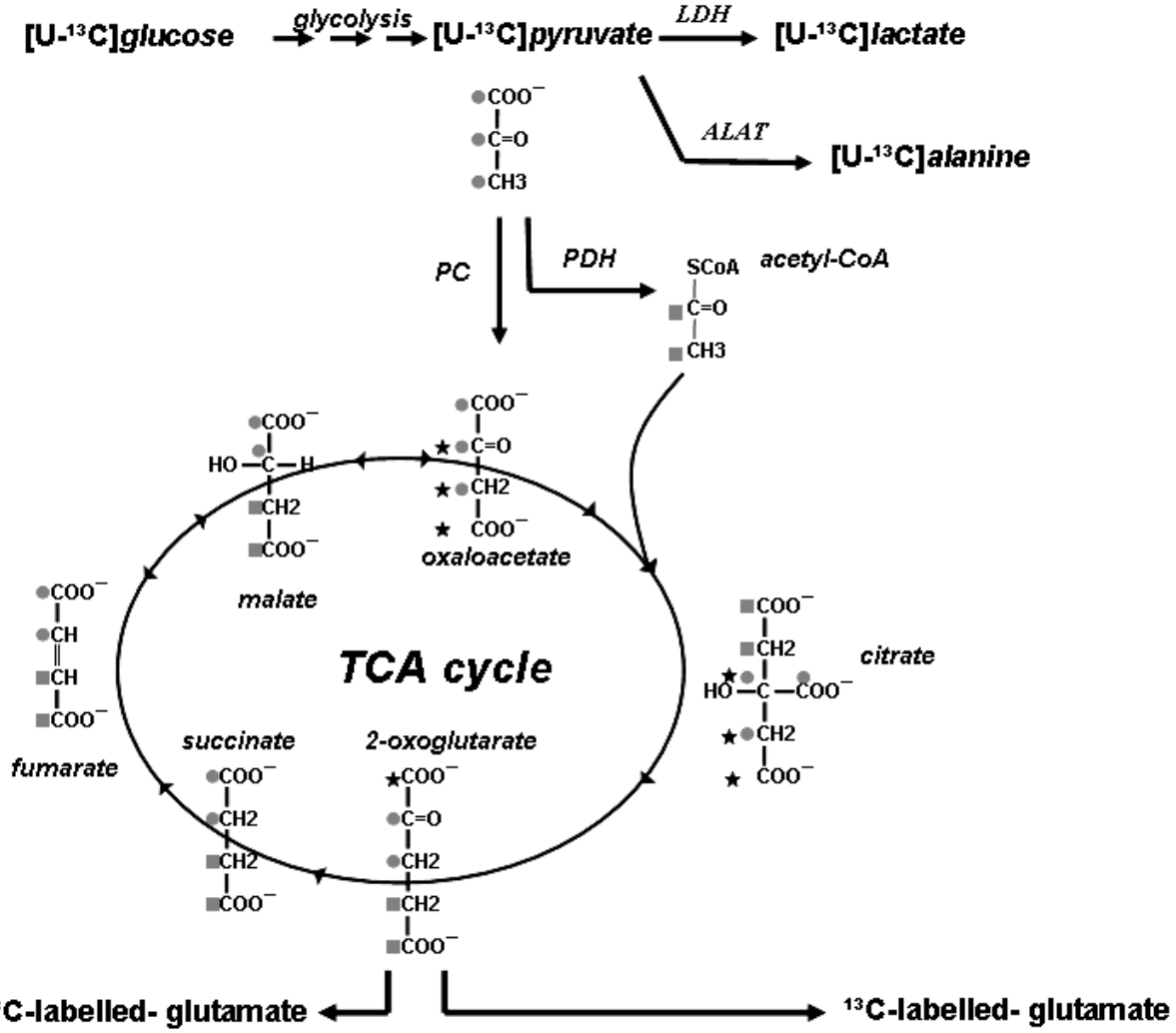

pc, 1st turn	*pdh*, 1st turn	*pc*, 2nd turn	*pdh*, 2nd turn
[2,3-^{13}C]glu	**[4, 5-^{13}C]glu**	**[2,3-^{13}C]glu**	**[3-^{13}C]glu**
[1,2,3-^{13}C]glu		**[1,2,3-^{13}C]glu**	**[1,2-^{13}C]glu**
[2,3,4,5-^{13}C]glu		**[2,3,4,5-^{13}C]glu**	**[3,4,5-^{13}C]glu**
[U-^{13}C]glu		**[U-^{13}C]glu**	**[1,2,4,5-^{13}C]glu**

Figure 4.4 Metabolic fate of [U-^{13}C]glucose

Metabolic fate of [3-^{13}C]pyruvate

Similar [2-13C], in the anaplerotic pathway the 3- ^{13}C-labelled position of pyruvate becomes the C2 or C3 position in oxaloacetate (the later after equilibration with fumarate) but Condensation of [2(3)-^{13}C]oxaloacetate with [2-^{13}C]acetyl-CoA leads to [3,4-^{13}C]-, [2,4-^{13}C]2-

oxoglutarate. After the first TCA cycle turn, [3,4-^{13}C]- and [2,4-^{13}C]glutamate will appear. If labelled [3,4-^{13}C]2-oxoglutarate remains in the TCA cycle, only [2,3-^{13}C]oxaloacetate will be appeared and after condensation of this oxaloacetate with [2-^{13}C]acetyl-CoA, after second TCA cycle turn [2,3,4-^{13}C]glutamate will be appeared. If [3-^{13}C]pyruvate enters the TCA cycle as [2-^{13}C]acetyl-CoA via *pdh* in the oxidative pathway, glutamate will be labelled at C-4 after the first turn and at C-2, C-4 or at C-3, C-4 after the second turn. The intensity of triplet signal of glutamate at C-3 was used to determine the contribution of the *pc* pathway.

Metabolic fate of [2-^{13}C]acetate

[2-^{13}C]acetate was used as tracer to study the effect of CAIs on the flux through *pdh* and through enzymes related to cytosolic fatty acid synthesis. The metabolic pathway of acetate in the TCA cycle is shown in Figure 4.5. Acetate is a short-chain fatty acid that cells use in many of their metabolic processes. Prokaryotic cells convert acetate into acetyl-CoA via acetyl-CoA synthetase. Acetyl-CoA cannot pass through the mitochondrial membrane. Therefore cells use mitochondrial carnitine acetyltransferase (Cat) for the transport of acetyl units into mitochondria as shown in figure 4.6. Thus, [2-^{13}C]acetate can enter the TCA cycle only as [2-^{13}C]acetyl-CoA, which can condensate with oxaloacetate. Condensation of [2-^{13}C]acetyl-CoA with unlabelled oxaloacetate leads to [4-^{13}C]glutamate after the first turn and to [2(3)-^{13}C]glutamate after the second TCA cycle turn (after equilibration of oxaloacetate with fumarate). [2-^{13}C]acetate was used for two purposes. First, to study the effect of CAIs on *pdh* flux, and second, to study the effect of CAIs on acetyl-CoA carboxylase (ACC), an enzyme that catalyses the irreversible carboxylation of acetyl-CoA in the cytosol to produce malonyl-CoA.

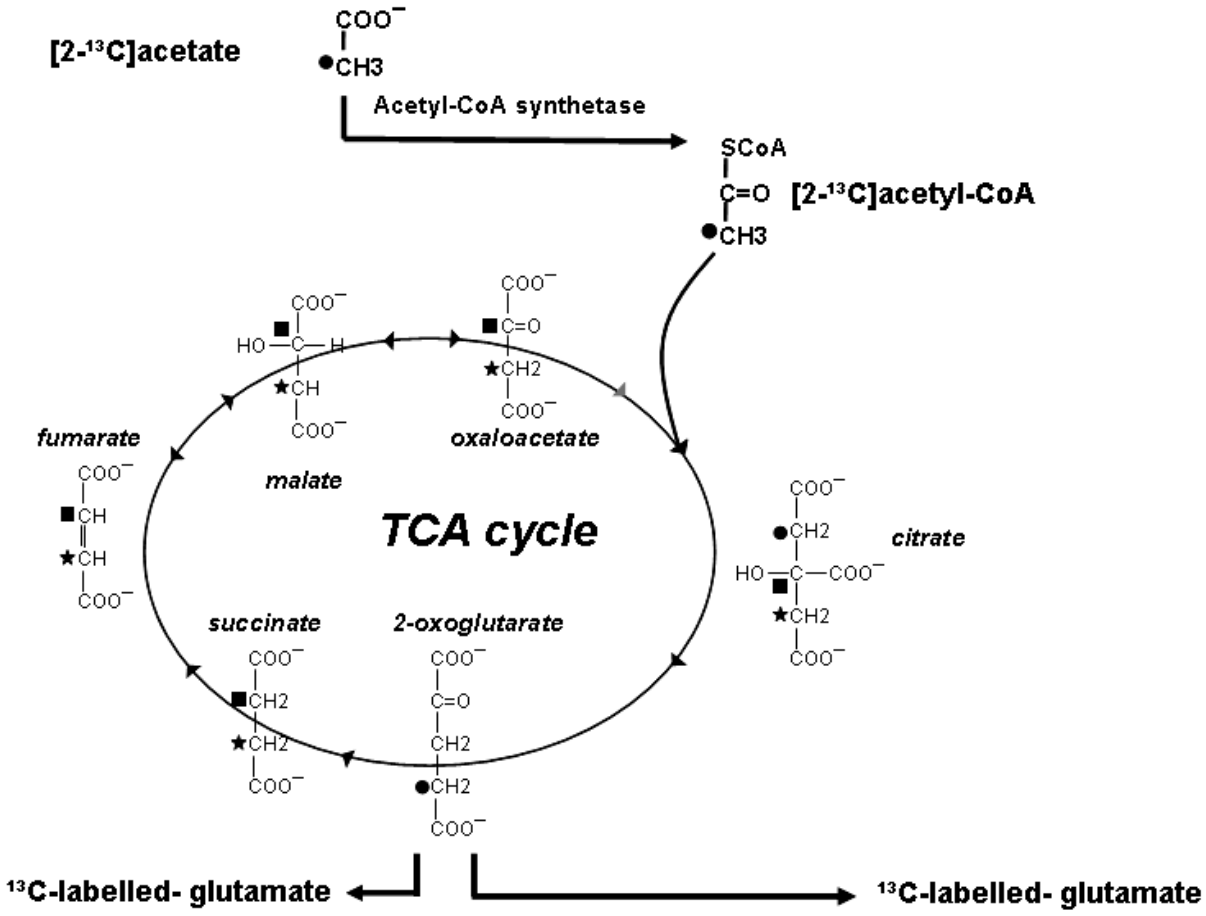

pdh, 1st turn	*pdh*, 2nd turn
[4-13C]glutamate	[2-13C]glutamate [3-13C]glutamate

Figure 4.5. The metabolic pathway of acetate into the TCA cycle. After the first turn, glutamate will be labelled at C4. After second turn glutamate is labelled at C3 or C2.

4.4.3.2 Quantitative analysis of ^{13}C-NMR spectra

In the present study, analysis of ^{1}H- NMR spectra allows to determine the *de novo* synthesised lactate from ^{13}C-labelled substrates (i.e. glucose). The synthesis and percentage enrichments in TCA-cycle related amino acids, such as glutamate, was determined from ^{13}C-NMR spectra. The incorporation of ^{13}C label from substrates into different metabolites reflects the dynamics of cellular metabolism. The percentage of newly synthesised lactate was calculated using the fully relaxed ^{1}H-NMR spectra of extracts and media by equation (1).

$$^{13}C\text{-enrichment in lactate (\% of control)} = \frac{[TSP]_S \times \left(\int lac\text{-}C3\right)_S \times V_S \times [Protein]_C}{[TSP]_C \times \left(\int lac\text{-}C3\right)_C \times V_C \times [Protein]_S} \times 100 \quad (1)$$

Where

$[TSP]_S$; Concentration of trimethylsilylpropionic-2,2,3,3,-d_4-acid in CAI experiment

$[TSP]_c$; Concentration of trimethylsilylpropionic-2,2,3,3,-d_4-acid in control experiments

$(\int lac\text{-}C3)_s$; Integral of lactate C-3 in ^{1}H-spectra from the experiment with CAI.

$(\int lac\text{-}C3)_c$; Integral of lactate C-3 in ^{1}H-spectra from the experiment without CAI (control).

V_S; Volume of sample dissolved in D_2O (µl) from the experiment with CAI.

V_C; Volume of sample dissolved in D_2O (µl) from the experiment without CAI (control).

$[Protein]_S$; Protein amount (mg) from the experiment with CAI.

$[Protein]_C$; Protein concentration (mg) from the experiment without CAI (control).

4.4.3.3 ^{13}C isotopomer analysis of ^{13}C-NMR spectra of lipid extracts

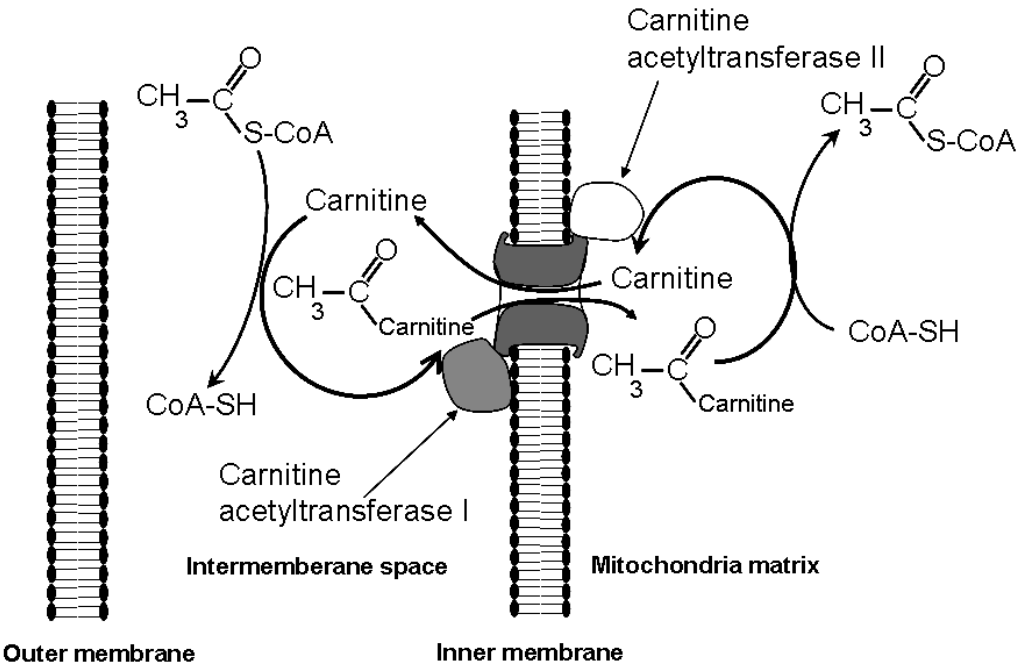

Figure 4.6 Mechanism of the transport of acetyl units across mitochondria membranes. Formation of acetyl-carnitine is necessary to allow this transport.

Synthesis of fatty acids from [U-^{13}C]glucose: The nomenclature for fatty acid carbons is shown in figure 4.7. The metabolism of [U-^{13}C]glucose via [1,2-^{13}C]acetyl-CoA labels all carbons of fatty acids i.e. F_{ω}, $F_{\omega-1}$, $F_{\omega-2}$, F_{α}, and F_{β} (F_{ω} is the terminal carbon of the fatty acid chain).

Figure 4.7 Nomenclature of carbons of the fatty acids

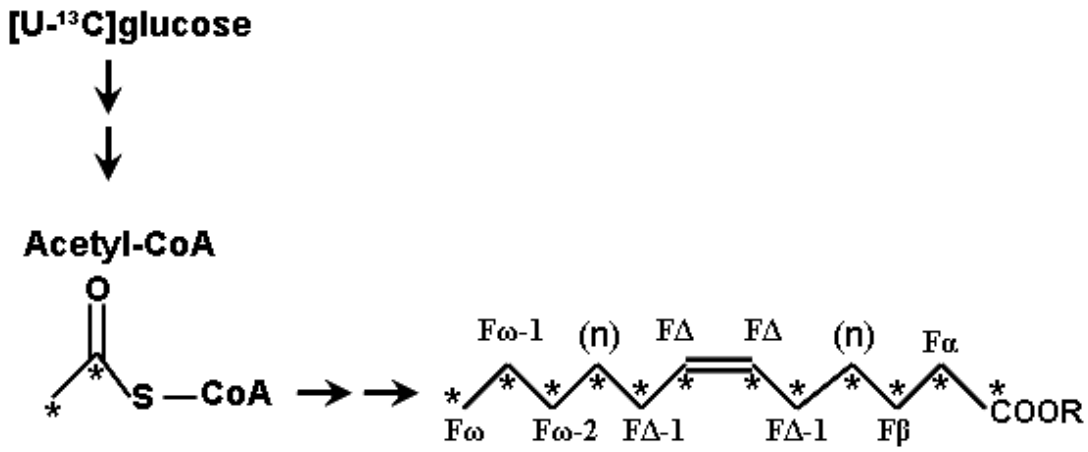

[U-^{13}C]glucose will label all carbons or at least pairwise odd/even numbered carbons in the de novo fatty acid synthesis; the terminal carbon F_{ω} will show a doublet or a singlet (natural abundance).

From ^{13}C-NMR spectra the relative part of newly synthesised fatty acids from [U-^{13}C]glucose was determined as ratio of an doubled signal of the terminal carbon of the fatty acid chain (F_{ω}), which arises from coupling to the $F_{\omega-1}$ carbon, to the resonance of the unlabelled (natural abundance) fatty acid carbon F_{ω} (equation 2).

$$^{13}\text{C-enrichment (\%)} = \left(\frac{F\omega}{F\omega\ (n.a)} \right) * 100 \qquad (2)$$

Synthesis of fatty acids from [2-^{13}C]acetate: [2-^{13}C]acetate is converted into [2-^{13}C]acetyl-CoA in the cytosol. Thus, the cells can directly use these units for fatty acid synthesis. In the synthesis of fatty acids, [2-^{13}C]acetyl-CoA labels the even-numbered carbons (F_{ω}, $F_{\omega-2}$ and F_{α}). The relative part of newly synthesised fatty acids was determined as ratio of a ^{13}C enriched signal to the resonance of the unlabelled fatty acid carbon $F_{\omega-1}$ (equation 3). The

ratio of $F_{\omega}/ F_{\omega-1}$ was corrected for natural abundance ^{13}C (F_{ω} n.a.) using control experiments with unlabeled acetate.

$$^{13}\text{C-enrichment (\%)} = \left(\frac{F\omega}{F\omega\text{-}1} - \frac{F\omega\ (n.a)}{F\omega\text{-}1} \right) * 100 \qquad (3)$$

4.4.3.4 Determination of relative amount of metabolites using ^{13}C-NMR spectra

The pool size of other metabolites, e.g. glutamate, has been determined using ^{13}C-NMR spectra. The percentage of newly synthesised metabolites was calculated using the ^{13}C-NMR spectra of extracts and media by equation 4.

$$^{13}C\text{-enrichment in Metabolite (\% of control)} = \frac{\left(\int_{metabolite\ from\ ^{13}C\text{-}spectra}\right)_S}{\left(\int_{metabolite\ from\ ^{13}C\text{-}spectra}\right)_C} \times {}^{13}C\text{-enrichment in Lactate (\% of control) (Eq. 1)} \qquad (4)$$

Where

$(\int \text{metabolite from } ^{13}C)_S$; ^{13}C-Integral of metabolite in 13C-spectra from the experiment with CAI.

$(\int \text{metabolite from } ^{13}C)_C$; ^{13}C-Integral of metabolite from the experiment without CAI (control).

^{13}C-enrichmenit in lactate was determined media equation 1.

Chapter 5

5 References

1: World Health Organization. Obesity and overweight. WHO Fact. Available at http://www.who.int/dietphysicalactivity/publications/facts/obesity/en/

2: Anderson, J.W., Konz, E.C., Frederich, R.C. and Wood, C.L. () Long-term weight-loss maintenance: a meta-analysis of US studies. Am J Clin Nutr 2001, **74**, 579–584.

3: Astrup, A. and Rossner, S. Lessons from obesity management programmes: greater initial weight loss improves long-term maintenance. ObesRev 2000, **1**, 17–19.

4: Wadden, T.A. Treatment of obesity by moderate and severe caloric restriction. Results of clinical research trials. Ann Intern Med, 1993, **119**, 688–693.

5: Lau, D.C., Douketis, J.D., Morrison, K.M., Hramiak, I.M., Sharma, A.M. and Ur, E. 2006 Canadian Clinical Practice Guidelines on the Management and Prevention of Obesity in Adults and Children. CMAJ., 2007, **176**, S1–S13.

6: Tong, P.C., Lee, Z.S., Sea, M.M., Chow, C.C., Ko, G.T., Chan, W.B. et al. The effect of orlistat-induced weight loss, without concomitant hypocaloric diet, on cardiovascular risk factors and insulin sensitivity in young obese chinese subjects with or without type 2 diabetes. Arch Intern Med, 2002, **162**, 2428–2435.

7: Wadden, T.A., Berkowitz, R.I., Sarwer, D.B., Prus-Wisniewski, R. and Steinberg, C. Benefits of lifestyle modification in the pharmacologic treatment of obesity: a randomized trial. Arch Intern Med 2001, **161**, 218–227.

8: NIH, Practical Guide to the Identification, Evaluation, and Treatment of Overweight and Obesity in Adults. National Institutes of Health. National Heart, Lung, and Blood Institute. NIH Publication No. 00-4084, October 2000. Available at:<5http://www.nhlbi.nih.gov/guidelines/obesity/prctgd_c.pdf4>, accessed on 11 June 2008.

9: La Noue, K. F. and Scholwerth, A.C. Metabolic transport in mitochondria. Annu. Rev. Biochem. 1979, **48**, 871–922.

10: Wallace J. C., Jitrapakdee S. and Chapman-Smith A. Pyruvate carboxylase. Int. J. Biochem. Cell Biol. 1998, **30**, 1–5.

11: Jitrapakdee S. and Wallace J. C. Structure, function and regulation of pyruvate carboxylase. Biochem. J. 1999, **340**, 1–16.

12: W. Richard Chegwidden and Nicholas D. Carter. Introduction to the carbonic anhydrases. The Carbonic Anhydrases -New Horizons. Basel: Birkhauser Verlag: 2000. pp 13-28.

13: Itada, N., & Forster, R. E. Carbonic anhydrase activity in intact red blood cells measured with 18O exchange. Journal of Biological Chemistry, 1977, **252**, 3881–3890.

14: Eigen, M., & DeMaeyer, L. Relaxation methods. In S. L. Friess, E. S. Lewis, A. Weissberger (Eds.), Investigation of rates and mechanisms of reactions. 1963 (p. 1034). New York: Interscience.

15: Joachim w. Deitmer and Christing R. Rose. pH regulation and proton signalling by glial cells. Progress in Neurobiology. 1996, **48**, 73-103.

16: Susanna J. Dodgson and R. E. Forster. Inhibition of CA V decrease glucose synthesis from pyruvate. Arch Biochem Biophys. 1986, **251**, 198-204.

17: Dodgson, S. J., R. E. Forster II, and B. T. Storey. The role of carbonic anhydrase in hepatocytes metabolism. Ann. NY Acad Sci. 1984, **429**, 516-524.

18: Susanna J. Dodgson. Inhibition of mitochondrial carbonic anhydrase and ureagenesis: a discrepancy examined. 1987, **63**, 2134-2141.

19: Hewett-Emmett D. Evolution and distribution of the carbonic anhydrase gene families. In: Chegwidden WR, Edwards Y, Carter N, editors. The carbonic anhydrases—New horizons. Basel: Birkhauser Verlag; 2000. pp 29–78.

20: Hewett-Emmett, D. and Tashian, R.E., Structure and evolution of the carbonic anhydrase multigene family. In S.J. Dodgson, R.E. Tashian, G. Gros and N.D. Carter_Eds.., The Carbonic Anhydrases: Cellular Physiology and Molecular Genetics, Plenum Press, New York, 1991, pp. 15–32.

21: Shah GN, Emmett DH, Grubb JH, Migas MC, Fleming RE, Waheed A, Sly WS. Mitochondrial carbonic anhydrase CA VB: differences in tissue distribution and pattern of evolution from those of CA VA suggest distinct physiological roles. Proc Natl Acad Sci USA, 2000, **97**, 1677–1682.

22: Claudiu T. Supuran: Carbonic anhydrases, catalytic and inhibition mechanisms, distribution and physiological roles carbonic anhydrase. Its inhibitors and activators. CRC Press, London, 2004, pp 1–23.

23: Sukhamay Lahiri and Robert E. Forster, II. CO2/H+ sensing: peripheral and central chemoreception. The international Journal of Biochemistry & Cell Biology. 2003, **35**, 1413-1435.

24: Tashian, R.E., and Carter, N. D., Biochemical genetics of carbonic anhydrase. Adv. Hum. Genet. 1976, **7**, 1-56.

25: lindskog, S., Advan. Inorg. Biochem. 1982, **4**, 115-170.

26: Kim G, Selengut J, Levine RL. Carbonic anhydrase III: The phosphatase activity is extrinsic. Arch Biochem Biophys 2000, **377**, 334–340.

27: Briganti F, Mangani S, Orioli P, ScozzafavaA,Vernaglione G, Supuran CT. Carbonic anhydrase activators: X-ray crystallographic and spectroscopic investigations for the interaction of isozymes I and II with histamine. Biochemistry 1997, **36**, 10384–10392.

28: Lindskog S, SilvermanDW. The catalytic mechanism of mammalian carbonic anhydrases. In: Chegwidden WR, Edwards Y, Carter N, editors. The carbonic anhydrases—New horizons; Basel: Birkha¨user Verlag; 2000, pp 175–196.

29: Briganti F, ScozzafavaA, Supuran CT. Carbonic anhydrase activators: Part 19 Spectroscopic and Kinetic Investigations for the Interaction of Isozymes I and II With Primary Amines. Met Based Drugs 1997, **4**, 221-227.

30: C. Temperini, A. Cecchi, A. Scozzafava and C. T. Supuran. Carbonic Anhydrase Inhibitors. Comparison of Chlorthalidone and Indapamide X-ray Crystal Structures in Adducts with Isozyme II: When Three Water Molecules and the Keto−Enol Tautomerism Make the Difference. J. Med. Chem., 2009, **52 (2)**, 322–328.

31: Claudiu T. Supuran, Andrea Scozzafava, Angela Casini. Carbonic anhydrase inhibitors. Medicinal Research Reviews. 2003, **23**, 146-189.

32: Supuran CT, Scozzafava A. Carbonic anhydrase inhibitors and their therapeutic potential. Exp Opin Ther Patents. 2000, **10**, 575–600.

33: Bertini I, Luchinat C, Scozzafava A. Carbonic anhydrase: An insight into the zinc binding site and into the active cavity through metal substitution. Struct Bonding. 1982,**48**,45–92.

34: Briganti F, Pierattelli A, Scozzafava A, Supuran CT. Carbonic anhydrase inhibitors. Part 37. Novel classes of carbonic anhydrase inhibitors and their interaction with the native and

cobalt-substituted enzyme: Kinetic and spectroscopic investigations. Eur J Med Chem. 1996, **31**, 1001–1010.

35: Mann T, Keilin D. Sulphanilamide as a specific carbonic anhydrase inhibitor. Nature 1940, **146**, 164–165.

36: Maren TH. Carbonic anhydrase: Chemistry, physiology and inhibition. Physiol Rev 1967, **47**, 595–781.

37: Maren TH. Relations between structure and biological activity of sulfonamides. Annu Rev Pharmacol Toxicol 1976, **16**, 309–327.

38: Drew J. Drug discovery: A historical perspective. Science 2000, **287**, 1960–1964.

39: Owa T, Nagasu T. Novel sulphonamide derivatives for the treatment of cancer. Exp Opin Ther Patents 2000, **10**, 1725–1740.

40: Shank RJ, Gardocki JF, Streeter AJ, Maryanoff BE. An overview of the preclinical aspects of topiramate: pharmacology, pharmacokinetics and mechanism of action. Epilepsia 2000, **41**, S3 – S9.

41: Vullo, D.; Franchi, M.; Gallori, E.; Antel, J.; Scozzafava, A.; Supuran, C. T. Carbonic anhydrase inhibitors. Inhibition of mitochondrial isozyme V with aromatic and heterocyclic sulfonamides. J. Med. Chem. 2004, **47**, 1272–1279.

42: Innocenti, A.; Antel, J.; Wurl, M.; Scozzafava, A.; Supuran, C. T. Bioorg. Med. Chem. Lett. 2004, **14**, 5703–5707.

43: Cheristopher J. Lynch, Heather Fox, Stacy A. Hazen, Bruce A. Stanley and Susanna Dodgson. Role of hepatic carbonic anhydrase in *de novo* lipogenesis. Biochem. J. 1995. **310**, 197-202.

44: Stacy A. Hazen, Abdul Waheed, William s. Sly, Kathryn F. Lanoue, and Cheristopher J. Lynch. Differentiation-dependent expression of CA V and the role of carbonic anhydrase isozymes in pyruvate carboxylation in adipocytes. FASEB, 1996, **10**, 481- 490.

45: James O Hill, et al. Orlistat, a lipase inhibitor, for weight maintenance after conventional dieting: a 1-y study. Am J Clin Nutr 1999, **69**, 1108–1116.

46: Susanna j. Dodgson Richard P. Shank and Bruce E. Maryanoff. Topiramate as an inhibitor of carbonic anhydrase isoenzymes. Epilepsia, 2000, **41 (Suppl.)**, S35-S39.

47: Schneiderhan ME and Maryn R. Is acetazolamide similar to topiramate for reversal of antipsychotic-induced weight gain? Am. J. Thr. 2007, **14(6)**, 581-584.

48: G. De Simone et. al. Carbonic anhydrase inhibitors: The X-ray crystal structure of ethoxzolamide complexed to human isoform II reveals the importance of thr200 and gln92 for obtaining tight-binding inhibitors. Bioorg. Med. Chem. Lett. 2008, **18**, 2669-2674.

49 : Nishimori, I.; Minakuchi, T.; Onishi, S.; Vullo, D.; Cecchi, A.; Scozzafava, A.; Supuran, C. T. Carbonic anhydrase inhibitors: cloning, characterization, and inhibition studies of the cytosolic isozyme III with sulfonamides. Bioorg. Med. Chem. 2007, **15**, 7229-7236.

50: Nishimori I, Vullo D, Innocenti A, Scozzafava A, Mastrolorenzo A, Supuran CT. Carbonic anhydrase inhibitors. The mitochondrial isozyme VB as a new target for sulfonamide and sulfamate inhibitors. J Med Chem 2005, **48**, 7860-7866.

51: Ghandour MS, Parkkila AK, Parkkila S, Waheed A, Sly WS. Mitochondrial carbonic anhydrase in the nervous system: expression in neuronal and glial cells. J Neurochem. 2000, **75(5)**, 2212-2220.

52: Jitrapakdee S, St Maurice M, Rayment I, Cleland WW, Wallace JC, Attwood PV. Structure, mechanism and regulation of pyruvate carboxylase. Biochem J. 2008, **413(3)**, 369-387.

53: William C. G. et. al. Role of Pyruvate Carboxylase in Facilitation of Synthesis of Glutamate and Glutamine in Cultured Astrocytes. J. Neurochem. 1997, **69**, 2312-2325.

54: Millichip JG, Acetazolamide therapy (Letter, comment). Neurology 1991, **41**, 764.

55: Woodgury DM (ed), Antiepileptic Drug, Carbonic anhydrase inhibitors. New York, Raven Press, 1980.

56: Woodbury DM, Engstrom FL, white HS, Chen CF, Kemp JW, Chow SY. Ionic and acid-base regulation of neurons and glial during seizures. Ann Neurol. 1984, **16**, S135-S144.

57: Kinsman SL, Vining EP, Queskey SA, Mellits D, freeman JM. Efficacy of the ketogenic diet for intractable seizure disorders. Review of 58 cases. Epilepsia 1992, **33**, 1132-1136.

58: Hoffmann GF, Meier-Augenstein W, Stockler S, Surtees R, Rating D, Nyhan WL. Physiology and pathophysiology of organic acids in cerebrospinal fluid (review). J Inherit Metab Dis 1993, **16**, 648-669.

59: Westergaard N, Sonnewald U, Unsgard G, Peng L, Hertz L, Schousboe A. Uptake, release, and metabolism of citrate in neurons and astrocytes in primary cultures. J neurochem 1994, **62**, 1727-1733.

60: fukahori m, Itoh M. Effects of dietary zinc status on seizure susceptibility and hippocampal zinc content in the EI (epilepsy) mause. Brain res 1990, **529(1-2)**, 16-22.

61: Sonnewald U, Westergaard N, Kran J, Unsgrad G, Petersen SB, Schousboe A. First direct determination of preferential release of citrate from astrocytes using [^{13}C]NMR spectroscopy of cultured neurons and astrocytes. Neurosci Lett 1991, **128**, 235-239.

62: Lerman-Sagie T, Statter M, Szabo G, Lerman P. Effect of Valporic acid therapy on zinc metabolism in children with ptimary epilepsy. Clin Neuropharmacol 1987, **10**, 80-86.

63: Hazen SA, Waheed A, Sly WS, LaNoue KE, Lynch CJ. Effect of carbonic anhydrase inhibition and acetoacetate on anaplerotic pyruvate carboxylase activity in cultured rate astrocytes. Dev Neurosci 1997, **19**, 162-171.

64: Shank RP, Bennett GS, Freytag SO. and Campbell GL. Pyruvat carboxylase: an astrocyte-specific enzyme implicated in the replenishment of amino acid nurotransmitter pools. Brain Res. 1985, **329**, 364-367.

65: Marrif H. and Juurlink BH. Astrocytes respond to hypoxia by increasing glycolytic capacity. J. Neurosci. Res. 1999, **57**, 255-260.

66: Tricarico D, Lovaglio S, Mele A, Rotondo G, Mancinelli E, Meola G, Camerino DC. Acetazolamide prevents vacuolar myopathy in skeletal muscle of K(+) -depleted rats. Br J Pharmacol. 2008, **154(1)**, 183-190.

67: Holger M. Becker, Daniela Hirnet, Claudia Fecher-Trost, Dieter Sültemeyer, and Joachim W. Deitmer. Transport Activity of MCT1 Expressed in Xenopus Oocytes Is Increased by Interaction with Carbonic Anhydrase. J Biol Chem 2005, **280(48)**, 39882-39889.

68: Cooper AJ, Mora SN, Cruz NF. and Gelbard AS. Cerebral ammonia metablism in hyperammonemic rats. J. Neurochem. 1985, **44**, 1716-1723.

69: Butterworth RF, Girard G. and Giguere JF. Regional differences in the capacity for ammonia removal by brain following protocaval anastomosis. J. Neurochem. 1988, **51**, 486-490.

70: Marc K. Hellerstein. Regulation of hepatic *de novo* lipogenesis in humans. Annu Rev. Nurr. 1996, **16**, 523-557.

71: Norman B. Javitt. Hep G2 cells as a resource for metabolic studies: lipoprotein, cholesterol, and bile acids. FASEB, 1990, **4**, 161-168.

72: Dodgson SJ, Forster II, R. E, Storey B. T. and mela L. Mitochondrial carbonic anhydrase. Proc. Nati. Acad. Sci. USA. 1980, **77**, 5562-5566.

73: Dodgson SJ, and Forster II, R. E, Carbonic anhydrase: inhibition results in decreased urea production by hepatocytes. J. Appl. Physiol. 1986, **60**, 646-652.

74: Dodgson SJ, Why are there carbonic anhydrases in the liver? Biochem. Cell Biol. 1991, **69**, 761-763.

75: J. Lynch, W. A. Brennan Jr, T. C. Vary, N. Carter and S. J. Dodgson S. J. Carbonic anhydrase III in obese Zucker rats. Am. J. Physiol. 1993, **264**, E621-E630.

76: Charter N, Jeffery S, and Shiels A. Immunoassay of carbonic anhydrase III in rate tissues. FEBS Lett. 1982, **139**, 265-266.

77: Jeffery S., Carter N. D., and Wilson C. Carbonic anhydrase II isoenzyme in rat liver is under hormonal control. Biochem. J. 1984, **221**, 927-929.

78: Sokoloff L. Relation between physiological function and energy metabolism in the central nervous system. J. Neurochem. 1977, **29**, 13-26.

79: Sokoloff L. The brain as a chemical machine. Prog. Brain Res. 1992, **94**, 19-33

80: Gjedde A. and Marrett S. Glycolysis in neurons, not astrocytes, delays oxidative metabolism of human visual cortex during sustained checkerboard stimulation in vivo. J. Cereb. Blood Flow Metab. 2001, **21**, 1384-1392

81: Gjedde A, Marrett S. and Vafaee M. Oxidative and nonoxidative metabolism of excited neurons and astrocytes. J. Cereb. Blood Flow Metab. 2002, **22**, 1-14.

82: Dodgson S. Liver mitochondrial carbonic anhydrase (CA V), gluconeogenesis, and ureagenesis in the hepatocytes; (Dodgson SJ, Tashian RE, Gros G, Garter ND., eds.): in the carbonic anhydrases. Cellular Physiology and Molecular Genetics. New York, Plenum Press, 1991, pp 297-308.

83: Coulson RA, Herbert JD. A role for carbonic anhydrase in intermediary metabolism. Ann NY Acad Sci 1984, **429**, 505-515.

84: Rubio V. Enzymatic HCO_3^- fixation: a common mechanism for all enzymes involved? Biosci Rep 1986, **6**, 335-347.

85: Herbert, J. D. and Coulson, R. A. A role of carbonic anhydrase in *de novo* fatty acid synthesis in liver.Ann. N. Y. Acad Sci. 1984, **429**, 525-527.

86: Bray, g. A. Lipogenesis in Human Adipose Tissue: Some Effects of Nibbling and Gorging. J. clin. Invest. 1972, **51**, 537-548.

87: Haussinger, D., Kaiser, S., Stehle, T. and Gerok, W. Liver carbonic anhydrase and urea synthesis. The effect of diuretics. Biochem. Pharmacol. 1986, **35**, 3317-3322.

88: Bode, A. M., Foster, J. D. and Nordlie, R. C. Glycogenesis from glucose and ureagenesis in isolated perfused rat livers. Influence of ammonium ion, norvaline, and ethoxyzolamide. J. Biol. Chem. 1994, **269**, 7879-7886.

89: Robert A. Waniewski and David L. Martin. Preferential utilization of acetate by astrocytes is attributable to transport. J. Neurosci.1998, **18(14)**, 5225–5233.

90: Taguci Y, Ono Y, Lin L, Storey BT, Dodgson SJ, Forster RE. Mechanism of the acceleration of CO_2 production from pyruvate in liver mitochondria by HCO_3^-. Am J Pysiolo. 1997, **273**, C92-100.

91: Cao, T. P. and Rous, S. Inhibitory effect of acetazolamide on the activity of acetyl CoA carboxylase of mouse liver. Life Sci. 1978, **22**, 2067-2072.

92: Dodgson S. In the carbonic anhydrases, (Dodgson SJ, Tashian RE, Gros G, Garter ND., eds.), Cellular Physiology and Molecular Genetics. New York, Plenum Press, 1991, pp 3-14.

93: Lowenstein, J. M. The pyruvate dehydrogenase complex and the citric acid cycle. In Comprehensive Biochemistry: Pyruvate and fatty acid metabolism (M. Florkin, and E. H. Stolz, ed), 1971, pp. 31-48, Elsevier Publishing Company, New York.

94: Longmuir, I. S., Forster, R. E., II, and Woo, C. Y. Diffusion of carbon dioxide through thin layers of solution. Nature (London), 1966, **209**, 393-394

95: Claudia Temperini, Alessandro Cecchi, Andrea Scozzafava and Claudiu T. Supuran. Carbonic anhydrase inhibitors. Sulfonamide diuretics revisited—old leads for new applications? Org. Biomol. Chem., 2008, **6**, 2499–2506.

96: De Simone G, Di Fiore A, Menchise V, Pedone C, Antel J, Casini A, Scozzafava A, Wurl M, Supuran CT. Carbonic anhydrase inhibitors. Zonisamide is an effective inhibitor of the cytosolic isozyme II and mitochondrial isozyme V: solution and X-ray crystallographic studies. Bioorg Med Chem Lett. 2005, **15 (9)**, 2315-2320.

97: Claudia Temperini, Alessandro Cecchi, Andrea Scozzafava, Claudiu T. Supuran. Carbonic anhydrase inhibitors. Comparison of chlorthalidone, indapamide, trichloromethiazide, and furosemide X-ray crystal structures in adducts with isozyme II, when several water molecules make the difference. Bioorg Med Chem. 2009, **17**, 1214–1221.

98: H. Green and M. Meuth, An established pre-adipose cell line and its differentiation in culture, Cell 3, 1974, pp. 127–133.

99: H. Green and O. Kehinde, An established preadipose cell line and its differentiation in culture. II. Factors affecting the adipose conversion, Cell 5, 1975, pp. 19–27.

100: D.P. Aden, A. Fogel, S. Plotkin, I. Damjanov, B.B. Knowles, Controlled synthesis of HBsAg in a differentiated human liver carcinoma-derived cell line, Nature, 1979, **282**, 615-616.

101: Goa J. A micro biuret method for protein determination; determination of total protein in cerebrospinal fluid. Scand. J. Clin. Lab. Invest. 1953, **5**, 218-222.

102: Lowry OH, Rosebrough NJ, Farr AL. and Randall RJ. Protein measurement with the Folin-Phenol reagents. J. Biol. Chem. 1951, **193**, 265-275.

103: Martin, G.E; Zekter, A.S., ‘’Two-Dimensional NMR Methods for Establishing Molecular Connectivity’’; VCH Publishers, Inc: New York, 1988 (p.59).

104: Bloch F, Hansen WW. and Packard ME. *Nuclear induction. Phys. Rev. 1946,* **69**, 27.

105: Purcell EM, Torrey HC. and Pound RV. Resonance absorption by nuclear magnetic moments in a solid. Phys. Rev. 1946, **69**, 37-38.

106: Keeler J. Understanding NMR Spectroscopy. Wiley Publisher, 2005 (p.119).

107: Martin M, Portais JC, Labousse J et al. [1-^{13}C]glucose metabolism in rat cerebellar granule cells and astrocytes in primary culture. Evaluation of flux parameters by ^{13}C- and ^{1}H-NMR pectroscopy. Eur J Biochem. 1993, **217**, 617–625.

108: Kupće E, Freeman R. Stretched adiabatic pulses for broadband spin inversion. J Magn Reson A, 1995, **117**, 246–256.

109: Willker W, Engelmann J, Brand A et al. Metabolite identification in cell extracts and culture media by proton-detected 2D-H, C-NMR spectroscopy. J Magn Reson Anal. 1996, **2**, 21–32.

Chapter 6

Appendixes

The studies of glial metabolism of Isoleucine and valine were a cooperation of Professor B. Hamprecht, the Interfaculty Institute for Biochemistry, University of Tuebingen, Tuebingen, Germany and Professor D. Leibfritz, Institute for Organic Chemistry, University of Bremen, Bremen, Germany.

The NMR spectroscopic analyses in these studies were carried out in the laboratory of Instrumental Analysis at the University of Bremen under supervision of Professor Dr. Dieter Leibfritz.

Neurochem Res (2009) 34:194–204
DOI 10.1007/s11064-008-9840-4

ORIGINAL PAPER

Glial Metabolism of Isoleucine

Radovan Murín · Ghasem Mohammadi · Dieter Leibfritz · Bernd Hamprecht

Accepted: 19 August 2008 / Published online: 12 September 2008

Abstract Isoleucine, together with leucine and valine, constitutes the group of branched-chain amino acids (BCAAs). BCAAs are transported from the blood into the brain parenchyma, where they can serve several distinct functions. Since brain tissue is known to oxidatively metabolize BCAAs to CO_2, they are considered as fuel material in brain energy metabolism. Also, in the case of leucine, cultured astrocytes have been reported to be able to completely oxidize BCAA. While the metabolism of leucine by astroglia-rich primary culture (APC) has already been studied in detail, the metabolic fates of isoleucine and valine in these cells remained to be identified. Therefore, in the present study an NMR analysis was performed of ^{13}C-labelled metabolites generated in the catabolism of [U-^{13}C]Ile by astrocytes and released by them into the incubation medium. APC potently removed isoleucine from the medium and metabolized it. The major isoleucine metabolites released from APC are 2-oxo-3-methylvalerate, 2-methylbutyrate, 3-hydroxy-2-methylbutyrate and propionate. To a lesser extent, APC generate and release also [2,3-^{13}C]glutamine, [4,5-^{13}C]glutamine and ^{13}C-labelled isotopomers of lactate and citrate. These results show that APC can release into the extracellular milieu catabolites and several TCA cycle dependent metabolites resulting from the degradation of isoleucine.

Keywords Astroglia · Energy metabolism · Isoleucine · NMR · Branched-chain amino acid · Branched-chain 2-oxo acid

Special issue article in honor of Dr. George DeVries.

R. Murín (✉) · B. Hamprecht
Interfaculty Institute for Biochemistry, University of Tuebingen, Hoppe-Seyler-Str. 4, 72076 Tuebingen, Germany
e-mail: radovan.murin@uni-tuebingen.de

G. Mohammadi · D. Leibfritz
Institute for Organic Chemistry, University of Bremen, Bremen, Germany

Introduction

Three essential amino acids, valine, leucine and isoleucine constitute the group of branched-chain amino acids (BCAAs). Besides other common functions they share features of their metabolism. BCAAs are easily transported through the blood-brain barrier into the brain parenchyma [1], where they fulfill several distinct tasks [2, 3]: (1) As proteinogenic amino acids they are indispensable in protein synthesis; (2) together with their cognate branched-chain 2-oxo acids, BCAAs serve in maintaining the nitrogen balance in the glutamate/glutamine cycle [4, 5]; (3) since, even in the presence of glucose, the BCAAs are rapidly degraded by brain slices [6], neuron-rich [7, 8] and astroglia-rich primary cultures [7, 9], they are considered as valuable fuel molecules in brain energy metabolism. Furthermore, degradation of BCAAs, especially leucine, provides carbon residues which enter the general metabolism of neural cells and thus are incorporated, e.g., into lipids [10, 11] and amino acids [12, 13]. The importance of BCAAs for brain metabolism is also stressed by the fact that disorders in their metabolism are associated with pathobiochemical conditions leading to metabolic diseases that are frequently coupled with neurological symptoms [14].

Textbooks usually indicate that the catabolism of isoleucine yields acetyl-CoA and propionyl-CoA (Fig. 1). The

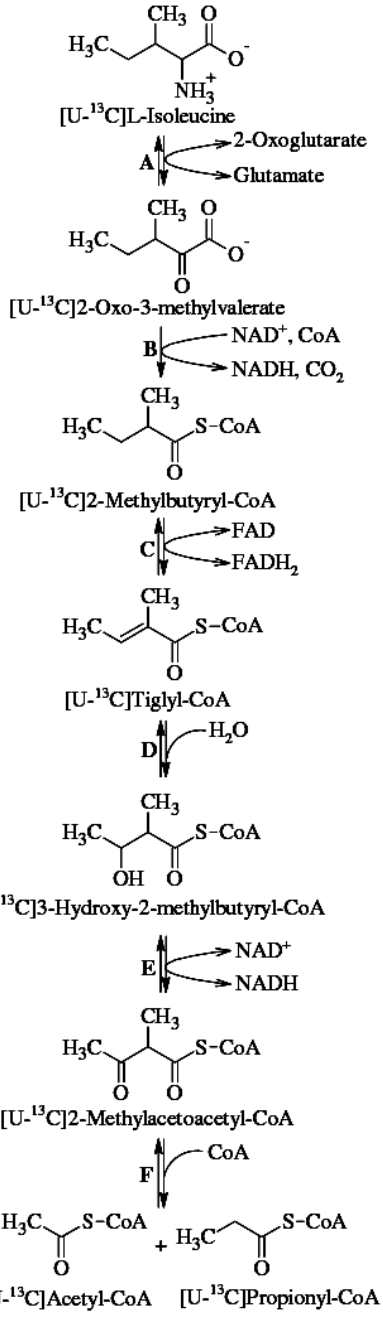

Fig. 1 Scheme of the pathway of L-isoleucine catabolism (modified version of the pathway presented by Sweetman and Williams [14]). The first two enzymes of the pathway, branched-chain amino acid transaminase (**a**) and branched-chain α-keto acid dehydrogenase (**b**), are common for all three BCAAs and their cognate branched-chain α-keto acids, respectively. 2-Methylbutyryl-CoA is subsequently converted to the products of isoleucine degradation, acetyl-CoA and propionyl-CoA, in a sequence of four enzymatic reactions catalyzed by 2-methylacyl-CoA dehydrogenase (**c**), enoyl-CoA hydratase (**d**) 3-hydroxyacyl-CoA dehydrogenase (**e**) and acetyl-CoA C-acyltransferase (**f**). These enzymes are identical with the enzymes occurring in the 3-methyl branched-chain fatty acid β-oxidation pathway

acetyl residue of the former compound enters tricarboxylic acid (TCA) cycle by reaction with oxaloacetate, thus being incorporated into citrate (Fig. 2a). The latter compound is carboxylated to generate methylmalonyl-CoA, which is racemized and then isomerized to form succinyl-CoA, a member of the TCA cycle (Fig. 2b). As in the case of the two other BCAAs, the catabolism of isoleucine is initiated by reversible transamination to its cognate 2-oxo branched-chain acid, 2-oxo-3-methylvaleric acid, that subsequently is oxidatively decarboxylated to the corresponding acyl-CoA derivative, 2-methylbutyryl-CoA (Fig. 1). In brain, the first enzymatic step of BCAA metabolism is facilitated by either one of two branched-chain amino acid transaminase (BCAT; EC 2.6.1.42) isozymes. These isozymes are located in different cellular compartments, either the mitochondria [15] or the cytosol [16], and they are distributed in a cell-type specific manner [5, 17]. In cultured neural cells, the mitochondrial isoform of BCAT predominates in astrocytes and microglia, while cytosolic BCAT is present in high concentrations in neurons and oligodendrocytes, and to a variable extent also in astrocytes [5, 17]. In an immunocytochemical examination of rat brain, the cytosolic isoform of BCAT was assigned to neurons [18]. The second enzymatic step in the catabolic pathways of all three BCAAs is catalyzed by the branched-chain α-keto acid dehydrogenase complex (BCKDH; EC 1.2.4.4, EC 1.8.1.4 and EC 2.3.1.168) [19], which initiates the practically irreversible conversion of branched-chain 2-oxo acids to the corresponding acyl-CoA derivates. BCKDH is ubiquitously expressed in cultured neural cells [17]. Enzymatically active BCKDH is present in brain [20]. However the distribution of this enzyme among neural cell types remains to be established. The enzymatic conversion of 2-methylbutyryl-CoA to acetyl-CoA and propionyl-CoA is analogous to a reaction in the β-oxidation pathway of fatty acids. While the expression of these enzymes among neural cells has not yet been studied in detail, their presence could be deduced from the results of experiments in which carbon atoms from ^{13}C- or ^{14}C-labelled isoleucine were incorporated into amino acids [21, 22].

Astrocytes are considered to serve as "fuel processing plants" for neurons [23] and are likely to provide other cells of the brain parenchyma with certain nutrients. Cultured astrocytes remove BCAAs from their incubation medium [9]. Leucine was shown to be metabolized by astrocytes to a certain extent and some of the leucine metabolites released into the extracellular milieu have been identified [9, 24]. The isoleucine metabolites, which may be also released by astrocytes, are still unknown.

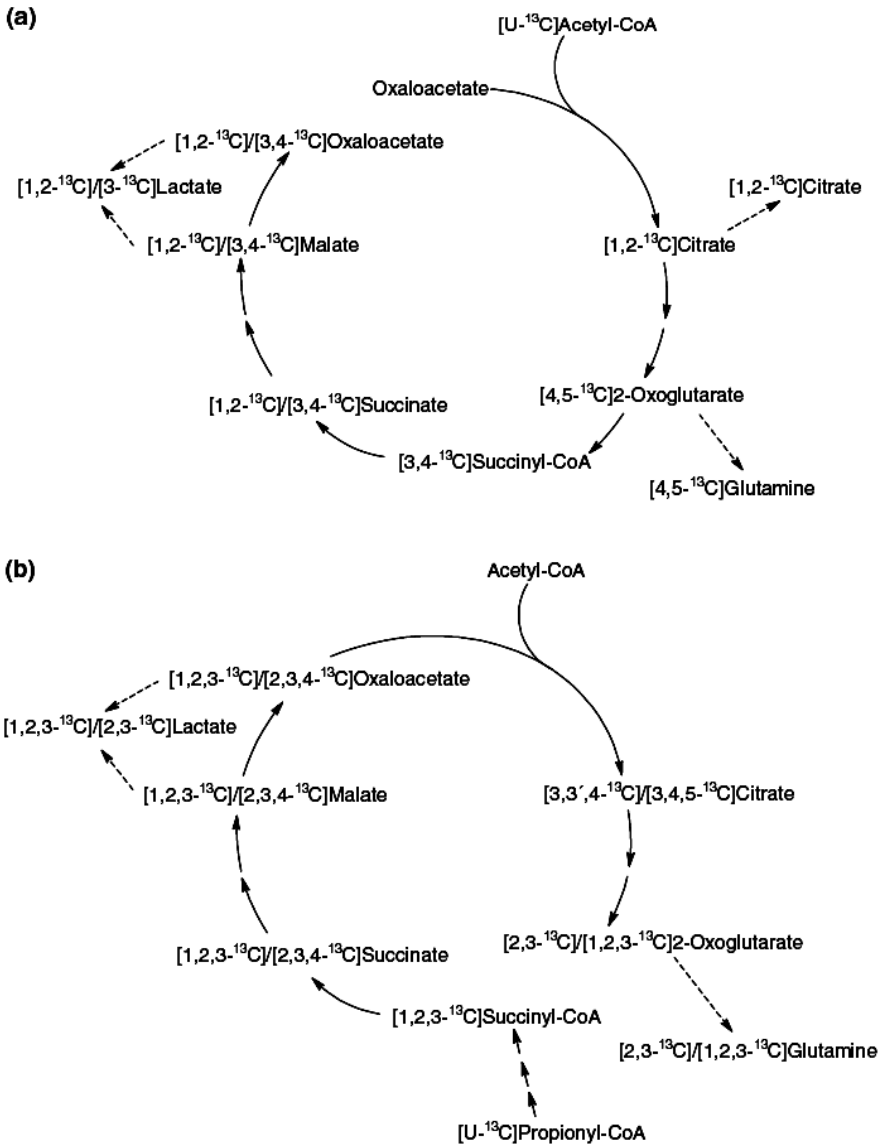

Fig. 2 Schemes of processing of the products of [U-^{13}C]Ile catabolism, [U-^{13}C]acetyl-CoA (**a**) and [U-^{13}C]propionyl-CoA (**b**), in the TCA cycle and of enzymatic conversion of TCA cycle members to isotopomers of glutamine and lactate. (**a**) [U-^{13}C]Acetyl-CoA enters the TCA cycle directly as one of the substrates of citrate synthase, giving rise to [1,2-^{13}C]citrate. This is converted to [4,5-^{13}C]2-oxoglutarate. Subsequently [3,4-^{13}C]succinyl-CoA is formed, which in turn gives rise to the succinate isotopomers [1,2-^{13}C]succinate and [3,4-^{13}C]succinate. In the two following steps of the TCA cycle, succinate is transformed to the two malate isotopomers [1,2-^{13}C]malate and [3,4-^{13}C]malate. Subsequently these isotopomers are oxidized to [1,2-^{13}C] and [3,4-^{13}C]oxaloacetate, respectively, which in a second round of the TCA cycle, can serve as substrate for citrate synthase. The scheme also depicts the compounds [1,2-^{13}C]citrate, [4,5-^{13}C]glutamine and [1,2-^{13}C]/[3-^{13}C]lactate, which are either TCA cycle intermediates or derivatives thereof that can be withdrawn from the cycle by release from the cells (broken line arrows). (**b**) For entry into the TCA cycle the propionyl-carbon atoms of [U-^{13}C]propionyl-CoA have to become part of [1,2,3-^{13}C]succinyl-CoA in a series of reactions catalyzed by propionyl-CoA carboxylase, methylmalonyl-CoA racemase and methylmalonyl-CoA mutase (since these enzymes constitute the pathway of propionyl-CoA metabolism, they are not depicted in the scheme). In the first round of the TCA cycle, [1,2,3-^{13}C]succinyl-CoA is successively converted to [1,2,3-^{13}C]/[2,3,4-^{13}C]succinate, [1,2,3-^{13}C]/[2,3,4-^{13}C]malate, [1,2,3-^{13}C]/[2,3,4-^{13}C]oxaloacetate, [3,3′,4-^{13}C]/[3,4,5-^{13}C]citrate and [1,2,3-^{13}C]/[2,3-^{13}C]2-oxoglutarate. The isotopomers [2,3-^{13}C]/[1,2,3-^{13}C]glutamine and [1,2,3-^{13}C]/[2,3-^{13}C] lactate (broken line arrows) are the potential metabolites that can appear in the incubation medium after being generated by processing of the pertinent members of the TCA cycle

Therefore, the aim of the present investigation was to fill this gap in our knowledge.

Materials and Methods

Materials

[U-^{13}C, ^{15}N]L-Isoleucine was purchased from Cambridge Isotope Laboratories (Andover, USA); this labeled isoleucine was purchased despite the commercial availability of [U-^{13}C]isoleucine, since it was considerably cheaper and the presence of ^{15}N did not interfere with the analysis of ^{13}C-labeled metabolites. For convenience's sake [U-^{13}C, ^{15}N]L-isoleucine is henceforth called [U-^{13}C]Ile. Dulbecco's Modified Eagle's Medium (DMEM) was from Gibco-Invitrogen (Karlsruhe, Germany). Bovine serum albumin (BSA) was purchased from Roche Diagnostics (Mannheim, Germany). Fetal calf serum (FCS) was from Biochrom (Berlin, Germany). Penicillin G and streptomycin sulfate were from Serva (Heidelberg, Germany). Aqueous-based mounting medium "Immu-mount" was from Thermo Shandon (Pittsburgh, USA). Deuterium oxide (D_2O), deuterium chloride (DCl), deuterium sodium hydroxide (NaOD) were obtained from E. Merck (Darmstadt, Germany) and (trimethylsilyl)propionic-2,2,3,3-D_4 acid (TSP) as well as NMR tubes from Aldrich (Steinheim, Germany). Sterile plastic material and culture dishes for cell culture were from Nunc (Wiesbaden, Germany) and Greiner (Frickenhausen, Germany).

Cell Culture

Astroglia-rich primary cultures were derived from the brains of new-born rats and maintained as described [25]. The cells were seeded in plastic culture dishes (9 cm in diameter) at a plating density of 5×10^6 viable cells per dish and incubated in culture medium [DMEM supplemented with 10% (v/v) fetal calf serum, 20 units/ml penicillin G, and 20 µg/ml streptomycin sulfate]. The culture medium was renewed after 7 days and 24 h before each experiment. The present studies were carried out with 15-day-old cultures.

Incubation of APC with [U-^{13}C]Isoleucine

After removal of the culture medium, the cells were washed twice with 5 ml of a minimal medium (MM; 110 mM NaCl, 5.4 mM KCl, 1.8 mM $CaCl_2$, 0.8 mM $MgSO_4$, 44 mM $NaHCO_3$, 0.9 mM NaH_2PO_4, 7 mM glucose; osmolarity 320 mOsmol/l) and incubated with 5 ml of MM supplemented with 0.8 mM [U-^{13}C]Ile (MM-Ile) in a Heraeus cell incubator containing a humidified atmosphere of 10% CO_2/90% air for 12, 24 and 48 h. Thereafter, the media of 10 culture dishes were combined, clarified by centrifugation (10,000 *g*, 4°C, 10 min) and lyophilized. The data presented here were obtained with four independent cultures, 10 cultured dishes each.

Cell Viability Test

Cell viability was assessed by determining the appearance of lactate dehydrogenase (LDH) in the medium by the modification of a described method [26]. Briefly, 25 µl aliquots of medium were added to 475 µl of reaction buffer (80 mM Tris/HCl buffer pH 7.2, 200 mM NaCl) and the reaction was started by entering 500 µl of substrate mixture (3.2 mM pyruvate and 0.4 mM NADH in reaction buffer). The decrease in the absorbance at 340 nm was recorded and used for the calculation of LDH activity. The LDH activity in the medium was compared to that obtained by the complete lysis of cells in lysis buffer [0.1% (w/v) Triton X-100, 50 mM Tris/HCl, pH 7.5]. By definition, 0% viability corresponds to 100% LDH activity in the medium [27].

Protein Determination

Protein content was determined according to the method of Bradford [28] using bovine serum albumin as a standard.

NMR Analysis

Each lyophilizate was dissolved in 1 ml deuterium oxide (D_2O). The solutions were centrifuged, and the supernatants were transferred to NMR tubes. In order to prevent glutamine carbamate formation [29] the solutions were adjusted to a pH value of 7 with deuterium chloride (DCl) and deuterium sodium hydroxide (NaOD). All ^{1}H-NMR and ^{13}C-NMR spectra of media were recorded on a Bruker DRX 600-MHz spectrometer, operating at a frequency of 600 MHz for ^{1}H and 150.9 MHz for ^{13}C measurement. Signals were assigned in a two-dimensional (2D) NMR experiment using heteronuclear single quantum coherence (HSQC) spectroscopy. The 2D-HSQC spectra were acquired on a DRX 600-MHz spectrometer using a 5-mm H, C, N inverse triple resonance probe with shielded gradients. Gradients were shaped by a waveform generator and amplified by a Bruker Acustar II amplifier. Sinusoidal z gradients of 1 ms duration and a recovery time of 100 µs were used for the echo/antiecho gradient selection. A gradient fine tuning (40:10.08) was performed to achieve optimum intensity. Low-power adiabatic composite pulse decoupling with WURST [30] was used for heteronuclear decoupling. One thousand twenty-four t1 increments with

24 scans per increment were acquired. The assignment of metabolites by two-dimensional NMR techniques was performed as described previously [31].

No NMR studies of nitrogen metabolism were carried out to follow up the fate of the ^{15}N isotope.

^{1}H-NMR Spectra

For ^{1}H-NMR spectra 128 scans were accumulated with a flip angle of 90° and a repetition time of 20 s. The scans were accumulated using a 5-mm H,C,N inverse triple resonance probe. Spectral width 7,200 Hz, data size 16 K, zero filling to 32 K. All ^{1}H-NMR spectra were calibrated on the methyl signal of lactate at 1.33 ppm.

^{13}C-NMR Spectra

^{13}C-NMR spectra were recorded with a 5-mm ^{1}H/^{13}C dual probe: 20,000 accumulations, (repetition time 3 s; flip angle 90°), composite pulse decoupling with WALTZ-16, spectral width 33.198 Hz, data size 32 K, zero filling to 64 K. Chemical shifts were referenced to the C-3 signal of lactate at 21.3 ppm.

Absolute Quantification

The concentration of lactate was determined from fully relaxed ^{1}H-NMR spectra of media using (trimethylsilyl)propionic-2,2,3,3-D_4 acid (TSP) as an external standard. The pool size of other metabolites was determined using ^{13}C-NMR spectra. The ^{13}C signal integrals of various metabolites were corrected for partial saturation nuclear Overhauser enhancement (NOE) effect by comparison with a standard mixture of amino acids.

Results

For assessing the capability of astrocytes to metabolize isoleucine, APC were used as a model system. These cultures also contain cell types other than astrocytes [32, 33]. Therefore, the ratio between the number of astrocytes and the total number of cells was determined. The astrocytes from 15-day-old APC were immunocytochemically labelled with rabbit antiserum against the astrocyte-marker glutamine synthetase [34, 35]. Glutamine synthetase positive cells represent the great majority (70–80%) of the cells present in APC.

The lack of fetal calf serum, essential amino acids and vitamins in the incubation medium may affect protein content and viability of the cells. Therefore, the amount of protein in APCs and the release of LDH into the incubation medium were determined. Indeed, the protein content of APC had decreased significantly from 1.9 ± 0.2 mg/culture dish at the beginning of the incubation to 1.5 ± 0.2, 1.5 ± 0.1 and 1.3 ± 0.2 mg/culture dish after 12, 24 and 48 h incubation with MM-Ile, respectively. The total activity of LDH in a cell homogenate at the beginning of the incubation period ($t = 0$ h) was 4.0 ± 0.4 U/culture dish. The incubation of APC in MM-Ile resulted in a release of 12 ± 3%, 13 ± 4% and 17 ± 4% of total LDH activity detected in the culture media after 12, 24 and 48 h, respectively.

Catabolism of [U-^{13}C]Ile

The intracellular amounts of metabolites in the cultured cells were too low to be amenable to analysis by the instrumentation available. Therefore, only the metabolite content of the medium was analyzed. The assignments of ^{13}C-labelled individual carbon positions within a molecule were performed by conventional two-dimensional NMR techniques such as HSQC, heteronuclear multiple bond correlation (HMBC) and homonuclear correlation spectroscopy (COSY) [31]. ^{13}C chemical shifts and carbon–carbon spin coupling constants of the metabolites found in the medium are presented in Table 1. Starting from an isoleucine concentration of 0.8 mM in the incubation medium, several metabolites appeared in concentrations at which they were detectable by ^{13}C-NMR spectroscopy (Table 2). Figure 3 shows the section of the ^{13}C-NMR spectrum with the protonated carbon signals from an APC medium 48 h after the start of incubation with 0.8 mM [U-^{13}C]Ile. Figure 4 displays the blow-ups of sections of the ^{13}C spectrum (Fig. 3) representing the spectrum of carbon C2 of lactate (Fig. 4a) and the spectrum of carbon C2 of propionate. The latter partially overlaps with the spectrum of carbon C4 of glutamine (Fig. 4b). Line splitting with a coupling constant around 50 Hz reflects an adjacent sp^2 hybridized carbon, while a coupling constant below 40 Hz indicates a neighboring sp^3 hybridized carbon. Therefore, the signal pattern around C2 of lactate reflects the presence of [1,2-^{13}C]lactate (doublet with a coupling constant of 56 Hz), of [1,2,3-^{13}C]lactate (doublet of doublets with coupling constants of 36.6 and 56 Hz) and of [2,3-^{13}C]lactate (doublet with a coupling constant of 36.6 Hz). In addition the intense singlet of natural abundance [2-^{13}C]lactate is seen (Fig. 4a). Similarly, the spectrum of C2 of propionate consists of a doublet of doublets with coupling constants of 34.6 and 51.4 Hz ([1,2,3-^{13}C]propionate; Fig. 4b), and a doublet with a coupling constant 36.6 Hz ([2,3-^{13}C]propionate; Fig. 4b). To the left of these signals are located those for [4,5-^{13}C]glutamine (Fig. 4b).

Table 1 ^{13}C-Coupling constants for ^{13}C-labeled isoleucine and for the isoleucine metabolites found released into the incubation medium of astroglial-rich primary cultures after 48 h of incubation

Compound	C_x-atom	Chemical shift (ppm)	Coupling constant (Hz)	Compound	C_x-atom	Chemical shift (ppm)	Coupling constant (Hz)
[U-^{13}C]Ile	1	174.80	$J_{C1C2} = 53.4$	[U-^{13}C]2-Oxo-3-methylvalerate	1	171.94	$J_{C1C2} = 61.0$
	2	60.25	$J_{C2C3} = 34.6$		2	212.13	$J_{C2C3} = 38.1$
	3	36.29	$J_{C3C4} = 34.6$		3	43.99	$J_{C1C3} = 11.7$
	4	25.15	$J_{C4C5} = 34.6$		4	25.10	$J_{C3C4} = 34.6$
	5	12.14	$J_{C4C5} = 34.6$		5	11.18	$J_{C4C5} = 34.6$
	6	15.71	$J_{C3C6} = 34.6$		6	14.74	$J_{C3C6} = 34.6$
[U-^{13}C]2-Methylbutyrate	1	187.96	$J_{C1C2} = 51.4$	[U-^{13}C]3-Hydroxy-2-methylbutyrate	1	185.20	$J_{C1C2} = 51.4$
	2	45.05	$J_{C2C3} = 34.1$		2	50.44	$J_{C2C3} = 38.1$
	3	27.95	$J_{C3C4} = 34.6$		3	70.65	$J_{C3C4} = 38.1$
	4	12.41	$J_{C3C4} = 34.6$		4	20.43	$J_{C3C4} = 38.1$
	5	18.23	$J_{C2C5} = 34.1$		5	14.55	$J_{C2C5} = 33.6$
[U-^{13}C]Propionate	1	179.80	$J_{C1C2} = 51.4$	[1,2-^{13}C]Lactate	1	183.26	$J_{C1C2} = 56.0$
	2	31.35	$J_{C2C3} = 34.6$		2	69.15	$J_{C1C2} = 56.0$
	3	11.60	$J_{C2C3} = 34.6$	[2,3-^{13}C]Lactate	2	69.15	$J_{C2C3} = 36.6$
[1,2,3-^{13}C]Lactate	1	183.26	$J_{C1C2} = 56.0$		3	21.33	$J_{C2C3} = 36.6$
	2	69.15	$J_{C2C3} = 36.6$	[2,3-^{13}C]Glutamine	2	54.96	$J_{C2C3} = 35.4$
	3	21.33	$J_{C2C3} = 36.6$		3	26.85	$J_{C2C3} = 35.4$
[1,2-^{13}C]Citrate	1	46.44	$J_{C1C2} = 50.3$	[4,5-^{13}C]Glutamine	4	31.80	$J_{C4C5} = 48.8$
	2	181.85	$J_{C1C2} = 50.3$		5	178.22	$J_{C4C5} = 48.8$

The numbers following the symbol *J* for the coupling constants indicate the numbers of the carbon atoms the nuclear spin coupling of which is considered. The carbon atoms of the various compounds are numbered according to IUPAC rules

Table 2 Quantification of [U-^{13}C]Ile metabolites in the incubation media as a function of the time of incubation of the labeled isoleucine with APCs

Metabolite	Amount of metabolite per culture dish (nmol)			Concentration of metabolite (% of isoleucine consumed)		
	Time of incubation			Time of incubation		
	12 h	24 h	48 h	12 h	24 h	48 h
[U-^{13}C]2-Oxo-3-methylvalerate	161	188	402	18	10	13
[U-^{13}C]2-Methylbutyrate	237	333	658	26	18	21
[U-^{13}C]3-Hydroxy-2-methylbutyrate	349	453	387	39	25	12
[U-^{13}C]Propionate	349	399	361	39	22	11
[1,2-^{13}C]Citrate	66	116	173	7	6	5
[1,2,3-^{13}C]Lactate	n.d.	51	78	n.d	3	2
[1,2-^{13}C]Lactate	n.d.	73	133	n.d	4	4
[2,3-^{13}C]Lactate	33	58	77	4	3	2
[4,5-^{13}C]Glutamine	75	70	111	8	4	3

Presented are (i) the amounts per culture dish of ^{13}C-labeled metabolites contained in the incubation media, and (ii) the ratios of the concentrations of the ^{13}C-labeled metabolites generated and the [U-^{13}C]Ile consumed by the cultures. The concentration of [U-^{13}C]Ile in the medium at the onset of incubation ($t = 0$ h) was 0.8 mM. n.d., not detectable

APCs took up and metabolized [U-^{13}C]Ile (isoleucine disappeared from the medium with a half-life of about 30 h; Fig. 5a) and released ^{13}C-labelled metabolites into the culture medium (Fig. 5b; Table 2). The following catabolites of isoleucine were identified and quantified: 2-oxo-3-methylvalerate, 2-methylbutyrate, 3-hydroxy-2-methylbutyrate and propionate (Fig. 5b; Table 2). The highest concentration in the medium was reached by

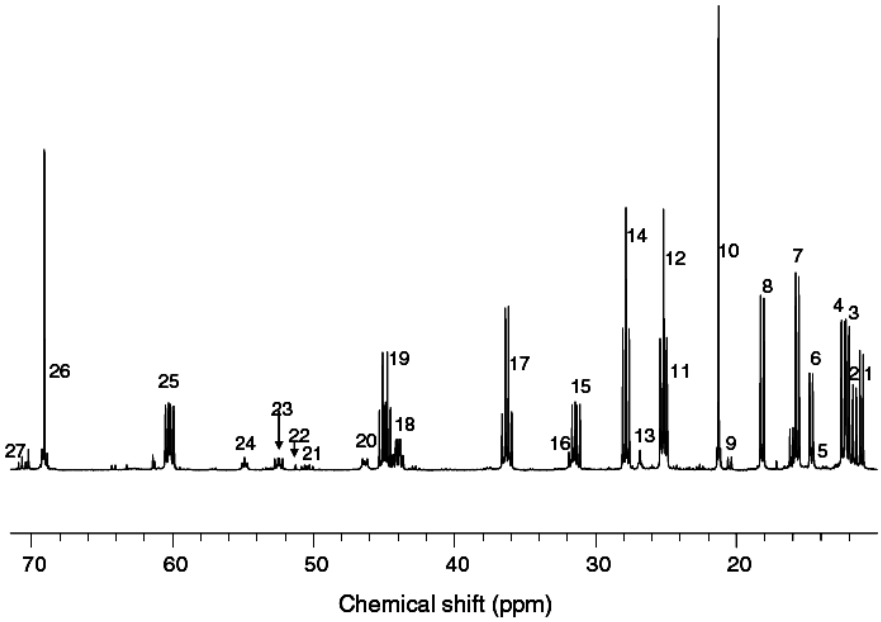

Fig. 3 ^{13}C-NMR spectra of a medium from primary astrocytes incubated with 0.8 mM [U-^{13}C]Ile and 5 mM glucose for 48 h. (1) 2-oxo-3-methylvalerate C5; (2) propionate C3; (3) Ile C5; (4) 2-methylbutyrate C4; (5) 3-hydroxy-2-methylbutyrate CH_3 at C2; (6) 2-oxo-3-methylvalerate CH_3 at C3; (7) Ile CH_3 at C3; (8) 2-methylbutyrate CH_3 at C2; (9) 3-hydroxy-2-methylbutyrate C4; (10) Lac C3; (11) 2-oxo-3-methylvalerate C4; (12) Ile C4; (13) Gln C3; (14) 2-methylbutyrate C3; (15) propionate C2; (16) Gln C4; (17) Ile C3; (18) 2-oxo-3-methylvalerate C4; (19) 2-methylbutyrate C2; (20) citrate; (21) 3-hydroxy-2-methylbutyrate C2; (22) Ala C2; (24) Gln C2; (25) Ile C2; (26), Lac C2; (27) 3-hydroxy-2-methylbutyrate C3. Ala, alanine; Ile, isoleucine, Lac, lactate; Gln, glutamine

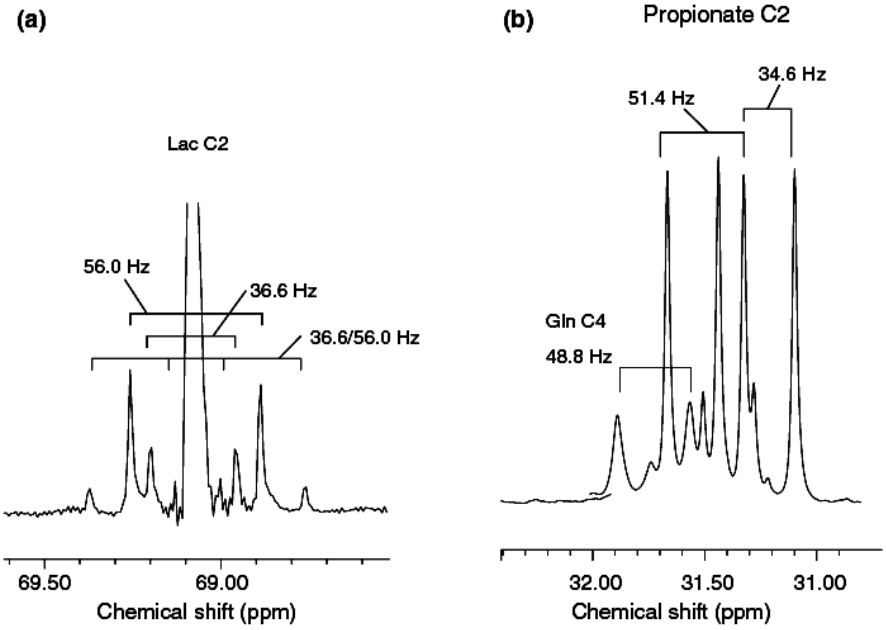

Fig. 4 Sections taken from the ^{13}C spectrum (Fig. 3) of a medium from primary astrocytes that were incubated with [U-^{13}C]Ile (0.8 mM) und glucose (5 mM) for 48 h. These sections show the multiplet structure at lactate C2 (a; see Fig. 3, peak 26), the doublet structure of glutamine C4 and the doublet of doublet structure at propionate C2 (b; see Fig. 3, peak 16 and 15, respectively)

2-methylbutyrate, while the concentration of the other three compounds were considerably lower and practically identical to each other.

Upon carboxylation of propionyl-CoA the ^{13}C atoms will appear in succinyl-CoA, a member of the TCA cycle. The second product of isoleucine catabolism,

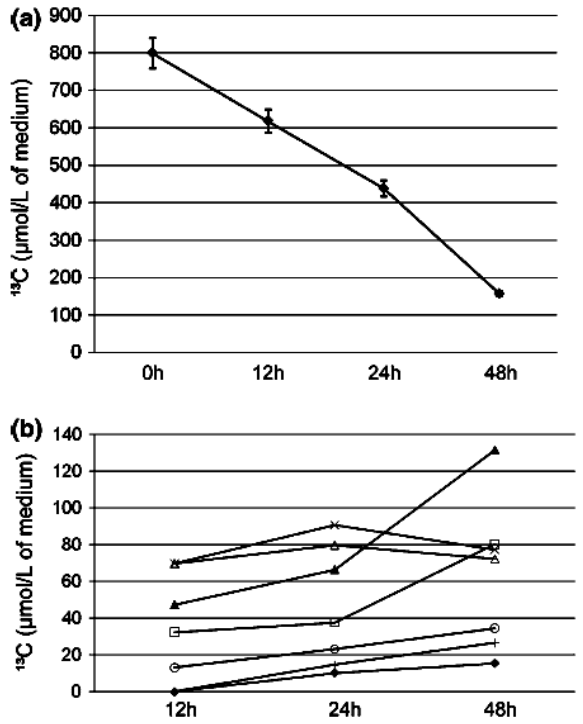

Fig. 5 Time-dependent changes in the concentrations of [U-^{13}C]Ile (**a**) and of the ^{13}C-labelled metabolites (**b**) released into the incubation medium of APC. The APCs (15 days old) were incubated in minimal medium (see Materials and methods) supplemented with 0.8 mM [U-^{13}C]Ile. The concentrations of [U-^{13}C]Ile (**a**) in the medium were determined after 0, 12, 24 and 48 h. In (**b**) are shown the levels of ^{13}C-labelled compounds derived from labelled isoleucine and released by APCs into the incubation medium: [1,2,3-^{13}C]lactate (◆), [1,2-^{13}C]lactate (+), [1,2-^{13}C]citrate (◯), 2-oxo-3-methylvalerate (□), 2-methylbutyrate (▲), propionate (△) and 3-hydroxy-2-methylbutyrate (x). Mean values ± SD were calculated from data obtained in four independent experiments ($n = 4$). The SD values (95% confidence internal) are given as error bars in (**a**); in (**b**) the error bars were omitted since they were smaller than the symbols for the data points. Due to the small size of the SD values no analysis of statistically significant differences of values was carried out

[U-^{13}C]acetyl-CoA, can enter the cycle through the reaction catalyzed by citrate synthase (Fig. 2a). On continuation of the cycle ^{13}C atoms can either be metabolized further by enzymes of the TCA cycle or leave the cycle at the stages of malate, oxaloacetate or citrate and appear in the ensuing pyruvate and especially in the lactate formed from the latter in the cytosol (Fig. 2a). ^{13}C of pyruvate may re-enter the cycle by successive actions of the pyruvate dehydrogenase complex and citrate synthase. Indeed, labelled spin-offs from the TCA cycle were identified as [1,2-^{13}C]lactate, [1,2,3-^{13}C]lactate, [2,3-^{13}C]lactate, [3-^{13}C]lactate, [1,2-^{13}C]citrate, [2,3-^{13}C]Gln and [4,5-^{13}C]Gln (Fig. 5b; Table 2). The signal intensities of [3-^{13}C]lactate and [2,3-^{13}C]Gln released into the incubation media were to low for a quantification. However, from theoretical considerations (see Fig. 2) the formation of these compounds would be expected since they have to appear in stoichiometrically equal amounts to [1,2-^{13}C]lactate and [1,2,3-^{13}C]glutamine, respectively.

Discussion

During the maximum exposure (48 h) of the cultured cells to the simple incubation medium containing only salts, glucose and isoleucine, the protein content dropped by one third. This indicates that protein degradation was no longer matched by protein synthesis. This does not come as a surprise since the cells are capable of degrading amino acids, essential ones such as isoleucine (the object of the present study), valine [36] and leucine [9] as well as non-essential ones [27, 37–40]. Degradation of these amino acids can serve as a source of nitrogen for synthetic purposes, as has been shown in the case of serine [41].

Despite the fact that, as an essential amino acid, isoleucine is indispensable, APC rapidly dispose of it by metabolism ([9, 42], present results). The rate of isoleucine disappearance was calculated from the difference in the concentrations of isoleucine in the medium at the onset of the incubation and at a certain experimental time point. The average value for the rate of isoleucine disappearance is approximately 0.83 nmol/mg protein/min. This is in good agreement with the value of 0.81 nmol/mg protein/min reported by Yudkoff et al. [42] and similar to the rate by which APC dispose of leucine from their medium [9, 42].

Disappearance of isoleucine from the medium was associated with the release of several intermediates—and their derivatives—of the isoleucine degradative pathway (Fig. 1). The amount of 2-oxo-3-methylvalerate released into the medium amounted to 10–20% of the isoleucine taken up from the medium, indicating that the majority of the isoleucine taken up by the cells was irreversibly metabolized by BCKDH. Similar to the complementary branched-chain 2-oxo-acid of leucine, α-ketoisocaproate, 2-oxo-3-methylvalerate can cross the plasma membrane of astroglial cells by facilitated transport via monocarboxylate transporter 1 [43]. 2-Oxo-3-methylvalerate present in the extracellular milieu can be taken up either into neurons, where in a reaction accompanying the glutamate/glutamine cycle it could serve as an acceptor of NH_2 groups [2, 5], or into neurons and/or glial cells for further metabolism. Indeed, CNS neurons express a monocarboxylate transporter [44], the cytosolic isoform of BCAT [17, 18], and BCKDH, an enzyme complex ubiquitous in various types of neural cells in culture [17].

In addition to 2-oxo-3-methylvalerate, astrocytes release also 2-methylbutyrate, 3-hydroxy-2-methylbutyrate and propionate the CoA derivatives of which are intermediates

in the isoleucine degradative pathway. These CoA esters are located in the mitochondria. Since there is no mechanism known for the transport of CoA esters through the inner mitochondrial membrane, the presence of the unesterified compounds in the medium may indicate the hydrolysis of the CoA esters prior to their exit from the mitochondria. Alternatively, the acyl residues may be transported out of the mitochondria linked to a compound other than CoA and this acylated compound would subsequently be hydrolyzed in the cytosol or in another organelle, e.g. lysosomes. This situation resembles that encountered in many inherited metabolic disorders such as propionic aciduria or methylmalonic aciduria [45]. The levels of 2-methylbutyrate and propionate in the media were high in respect to concentrations of the other compounds released. In view of the fact that the incubation media used for the experiment were lacking essential amino acids and vitamins, the release of the two catabolites may be a consequence of insufficient expression and/or activity of enzymes of the downstream part of the isoleucine catabolic pathway. For example, the activity of propionyl-CoA carboxylase would be negatively affected by the absence of biotin from the culture medium [46]. Moreover, the mitochondrial carboxylases are highly susceptible to proteolytic cleavage [47]. Insufficient enzymatic activity of acetoacetyl-CoA thiolase is associated with increased release of 3-hydroxy-2-methylbutyrate into the extracellular space [48].

Besides the compounds derived from intermediates of the isoleucine degradative pathway and their metabolites, ^{13}C-labelled citrate, glutamine and lactate were detected in the incubation media. This indicates that APC are capable of degrading isoleucine all the way to acetyl-CoA and propionyl-CoA. [1,2-^{13}C]acetyl-CoA entering the TCA cycle by citrate synthase gives rise to [4,5-^{13}C]glutamine via [4,5-^{13}C]2-oxoglutarate. If the latter remains in the cycle its carbon chain will be converted to the symmetrical molecules succinate and fumarate and subsequently will give rise to [1,2-^{13}C]malate and [3,4-^{13}C]malate as well as the corresponding isotopomers of oxaloacetate. These ^{13}C-labelled isotopomers of malate and oxaloacetate can be transformed under the influence of malic enzyme or phosphoenolpyruvate carboxykinase to [1,2-^{13}C]pyruvate or [3-^{13}C]pyruvate, thereby leaving the cycle and serving as precursors of the corresponding lactate isotopomers (Fig. 2a).

Propionyl-CoA can undergo conversion to the TCA cycle member succinyl-CoA by passing through the steps catalyzed by the enzymes propionyl-CoA carboxylase, methylmalonyl-CoA racemase and methylmalonyl-CoA mutase. However, under the experimental condition of a biotin-deficient culture medium used for the 48 h incubation, it is likely, that only limited amounts of labelled propionyl-CoA can be carboxylated and subsequently enter the TCA cycle at the position of succinyl-CoA. Consequently, propionyl-CoA becomes subject to hydrolysis and thus gives rise to propionate. Indeed, only low amounts of [1,2,3-^{13}C]lactate were detected. [1,2,3-^{13}C]Lactate can be formed in two ways: (i) the reaction in which citrate synthase catalyzes the condensation of [1,2-^{13}C]oxaloacetate with [1,2-^{13}C]acetyl-CoA, followed by reactions of the TCA cycle up to the formation of [1,2,3-^{13}C]malate; this can be oxidatively decarboxylated to [1,2,3-^{13}C]pyruvate by malic enzyme, which, in turn, is reduced to [1,2,3-^{13}C]lactate; or (ii) by entering [1,2,3-^{13}C]propionyl-CoA into the TCA cycle as [1,2,3-^{13}C]succinyl-CoA that is subsequently converted to [1,2,3-^{13}C]malate. This, in turn, is withdrawn from the TCA cycle by enzymatic conversions resulting in the formation of [1,2,3-^{13}C]lactate. The first way is unlikely, since acetyl-CoA is strongly diluted by unlabelled acetyl-CoA [21]. Thus, the presence of [1,2,3-^{13}C]lactate in the extracellular milieu confirms the capability of astrocytes to metabolize isoleucine to propionyl-CoA, the conversion of which to succinyl-CoA, a member of the TCA cycle, channels the propionyl carbon atoms into the cycle, thereby serving an anaplerotic role [21].

Recently, also the ability of APC to generate and release 3-hydroxyisobutyrate, an intermediate of valine catabolism, has been documented [36]. Therefore it can be stated that astrocytes can metabolize BCAAs and release monocarboxylates, which are genuine intermediates or are derived from intermediates that are CoA esters. These compounds may be utilized as fuel substances by adjacent neural cells. Like the energy metabolism of neurons [49] also that of oligodendrocytes may depend to a certain degree on the uptake of astrocyte-born substances. Oligodendrocytes express hexokinase only at low level and they are supposed to utilize in their energy metabolism substrates other than glucose [50, 51]. Therefore, oligodendrocytes may well utilize BCAAs and substances derived from them for their energy metabolism. This view is supported by observations that branched-chain organic acidurias are generally associated with cell damage in white matter [14]. Furthermore, cultured oligodendroglial cells express the cytosolic isoform of BCAT [5], β-methylcrotonyl-CoA carboxylase [52] and 3-hydroxyisobutyrate dehydrogenase [36], enzymes indicating the ability of these cells to include BCAAs into their metabolism.

The astrocytic release of intermediates of BCAAs catabolism ([9, 24, 36], present work) is in agreement with the known consumption of amino acids, including BCAAs, by brain tissue for the generation of energy [6, 53]. It also is compatible with the hypotheses that one of the functions of these cells is to serve as "fuel processing plants" in brain [23] and that BCAAs can serve in brain energy

metabolism to an extent of 10% in respect to glucose [6] as additional or alternative fuel molecules.

Acknowledgment The authors should like to acknowledge some preliminary experiments carried out by Krešimir Mikić.

References

1. Smith QR, Momma S, Aoyagi M et al (1987) Kinetics of neutral amino acid transport across the blood-brain barrier. J Neurochem 49:1651–1658. doi:10.1111/j.1471-4159.1987.tb01039.x
2. Yudkoff M (1997) Brain metabolism of branched-chain amino acids. Glia 21:92–98. doi:10.1002/(SICI)1098-1136(199709)21:1<92::AID-GLIA10>3.0.CO;2-W
3. Murín R, Hamprecht B (2008) Metabolic and regulatory roles of leucine in neural cells. Neurochem Res 33:279–284. doi:10.1007/s11064-007-9444-4
4. Yudkoff M, Daikhin Y, Nelson D et al (1996) Neuronal metabolism of branched-chain amino acids: flux through the aminotransferase pathway in synaptosomes. J Neurochem 66:2136–2145
5. Bixel MG, Hutson SM, Hamprecht B (1997) Cellular distribution of branched-chain amino acid aminotransferase isoenzymes among rat brain glial cells in culture. J Histochem Cytochem 45:685–694
6. Swaiman KF, Milstein JM (1965) Oxidation of leucine, isoleucine and related ketoacids in developing rabbit brain. J Neurochem 12:981–986. doi:10.1111/j.1471-4159.1965.tb10257.x
7. Murthy CR, Hertz L (1987) Acute effect of ammonia on branched-chain amino acid oxidation and incorporation into proteins in astrocytes and in neurons in primary cultures. J Neurochem 49:735–741. doi:10.1111/j.1471-4159.1987.tb00955.x
8. Honegger P, Braissant O, Henry H et al (2002) Alteration of amino acid metabolism in neuronal aggregate cultures exposed to hypoglycaemic conditions. J Neurochem 81:1141–1151. doi:10.1046/j.1471-4159.2002.00888.x
9. Bixel MG, Hamprecht B (1995) Generation of ketone bodies from leucine by cultured astroglial cells. J Neurochem 65:2450–2461
10. Kabara JJ, Okita GT (1961) Brain cholesterol: biosynthesis with selected precursors in vivo. J Neurochem 7:298–304. doi:10.1111/j.1471-4159.1961.tb13516.x
11. Patel MS, Owen OE (1978) The metabolism of leucine by developing rat brain: effect of leucine and 2-oxo-4-methylvalerate on lipid synthesis from glucose and ketone bodies. J Neurochem 30:775–782. doi:10.1111/j.1471-4159.1978.tb10784.x
12. Roberts S, Morelos BS (1965) Regulation of cerebral metabolism of amino acids. IV. Influence of amino acid levels on leucine uptake, utilization and incorporation into protein in vivo. J Neurochem 12:373–387. doi:10.1111/j.1471-4159.1965.tb04238.x
13. Berl S, Frigyesi TL (1968) Metabolism of [14C]leucine and [14C]acetate in sensorimotor cortex, thalamus, caudate nucleus and cerebellum of the cat. J Neurochem 15:965–970. doi:10.1111/j.1471-4159.1968.tb11639.x
14. Sweetman L, Williams JC (2001) Branched chain organic aciduria. In: Scriver C, Beaudet A, Sly W (eds) The metabolic and molecular basis of inherited disease. McGraw-Hill, Philadelphia, pp 2125–2163
15. Wallin R, Hall TR, Hutson SM (1990) Purification of branched chain aminotransferase from rat heart mitochondria. J Biol Chem 265:6019–6024
16. Hall TR, Wallin R, Reinhart GD et al (1993) Branched chain aminotransferase isoenzymes. Purification and characterization of the rat brain isoenzyme. J Biol Chem 268:3092–3098
17. Bixel M, Shimomura Y, Hutson S et al (2001) Distribution of key enzymes of branched-chain amino acid metabolism in glial and neuronal cells in culture. J Histochem Cytochem 49:407–418
18. Garcia-Espinosa MA, Wallin R, Hutson SM et al (2007) Widespread neuronal expression of branched-chain aminotransferase in the CNS: implications for leucine/glutamate metabolism and for signaling by amino acids. J Neurochem 100:1458–1468. doi:10.1111/j.1471-4159.2006.04244.x
19. Pettit FH, Yeaman SJ, Reed LJ (1978) Purification and characterization of branched chain alpha-keto acid dehydrogenase complex of bovine kidney. Proc Natl Acad Sci USA 75:4881–4885. doi:10.1073/pnas.75.10.4881
20. Suryawan A, Hawes JW, Harris RA et al (1998) A molecular model of human branched-chain amino acid metabolism. Am J Clin Nutr 68:72–81
21. Johansen ML, Bak LK, Schousboe A et al (2007) The metabolic role of isoleucine in detoxification of ammonia in cultured mouse neurons and astrocytes. Neurochem Int 50:1042–1051. doi:10.1016/j.neuint.2007.01.009
22. Nguyen NHT, Morland C, Gonzalez SV et al (2007) Propionate increases neuronal histone acetylation, but is metabolized oxidatively by glia. Relevance for propionic acidemia. J Neurochem 101:806–814. doi:10.1111/j.1471-4159.2006.04397.x
23. Hamprecht B, Dringen R (1995) Energy metabolism. In: Kettenmann H, Ranson B (eds) Neuroglia. Oxford University Press, New York, pp 473–487
24. Bixel MG, Engelmann J, Willker W et al (2004) Metabolism of [U-(13)C]leucine in cultured astroglial cells. Neurochem Res 29:2057–2067. doi:10.1007/s11064-004-6879-8
25. Hamprecht B, Löffler F (1985) Primary glial cultures as a model for studying hormone action. Methods Enzymol 109:341–345. doi:10.1016/0076-6879(85)09097-8
26. Vassault A (1983) Lactate dehydrogenase: UV-method with pyruvate and NADH. In: Bergmeyer HU (ed) Methods of enzymatic analysis, vol 3. Verlag Chemie, Weinheim, pp 118–126
27. Dringen R, Hamprecht B (1996) Glutathione content as an indicator for the presence of metabolic pathways of amino acids in astroglial cultures. J Neurochem 67:1375–1382
28. Bradford MM (1976) A rapid and sensitive method for the quantitation of microgram quantities of protein utilizing the principle of protein-dye binding. Anal Biochem 72:248–254. doi:10.1016/0003-2697(76)90527-3
29. Martin M, Portais JC, Labousse J et al (1993) [1-^{13}C]glucose metabolism in rat cerebellar granule cells and astrocytes in primary culture. Evaluation of flux parameters by ^{13}C- and ^{1}H-NMR spectroscopy. Eur J Biochem 217:617–625. doi:10.1111/j.1432-1033.1993.tb18284.x
30. Kupće E, Freeman R (1995) Stretched adiabatic pulses for broadband SPMn inversion. J Magn Reson A117:246–256
31. Willker W, Engelmann J, Brand A et al (1996) Metabolite identification in cell extracts and culture media by proton-detected 2D-H, C-NMR spectroscopy. J Magn Reson A 2:21–32
32. Hansson E, Sellstroem A, Perlsson LI et al (1980) Brain primary culture A characterization. Brain Res 188:233–246. doi:10.1016/0006-8993(80)90570-3
33. Reinhart PH, Pfeiffer B, Spengler S et al (1990) Purification of glycogen phosphorylase from bovine brain and immunocytochemical examination of rat glial primary cultures using monoclonal antibodies raised against this enzyme. J Neurochem 54:1474–1483. doi:10.1111/j.1471-4159.1990.tb01194.x
34. Martinez-Hernandez KP, Bell KP, Norenberg ND (1977) Glutamine synthetase. Glial localization in brain. Science 195:1356–1358. doi:10.1126/science.14400
35. Hallermayer K, Hamprecht B (1984) Cellular heterogeneity in primary cultures of brain cells revealed by immunocytochemical

localization of glutamine synthetase. Brain Res 295:1–11. doi:10.1016/0006-8993(84)90810-2
36. Murín R, Schaer A, Kowtharapu BS et al (2008) Expression of 3-hydroxyisobutyrate dehydrogenase in cultured neural cells. J Neurochem 105:1176–1186. doi:10.1111/j.1471-4159.2008.05298.x
37. Brand A, Leibfritz D, Hamprecht B et al (1998) Metabolism of cysteine in astroglial cells: synthesis of hypotaurine and taurine. J Neurochem 71:827–832
38. Verleysdonk S, Martin H, Willker W et al (1999) Rapid uptake and degradation of glycine by astroglial cells in culture: synthesis and release of serine and lactate. Glia 27:239–248. doi:10.1002/(SICI)1098-1136(199909)27:3<239::AID-GLIA5>3.0.CO;2-K
39. Zwingmann C, Leibfritz D (2003) Regulation of glial metabolism studied by ^{13}C NMR. NMR Biomed 16:370–399. doi:10.1002/nbm.850
40. Zwingmann C, Leibfritz D (2007) Glial-neuronal shuttle systems. In: Gibson GE, Dienel G (eds) Handbook of neurochemistry and molecular neurobiology. Brain energetics: integration of molecular and cellular processes. Springer, New York, pp 197–238
41. Verleysdonk S, Hamprecht B (2000) Synthesis and release of L-serine by rat astroglia-rich primary cultures. Glia 30:19–26. doi:10.1002/(SICI)1098-1136(200003)30:1<19::AID-GLIA3>3.0.CO;2-3
42. Yudkoff M, Daikhin Y, Lin ZP et al (1994) Interrelationships of leucine and glutamate metabolism in cultured astrocytes. J Neurochem 62:1192–1202
43. Bröer S, Rahman B, Pellegri G et al (1997) Comparison of lactate transport in astroglial cells and monocarboxylate transporter 1 (MCT 1) expressing Xenopus laevis oocytes. Expression of two different monocarboxylate transporters in astroglial cells and neurons. J Biol Chem 272:30096–30102. doi:10.1074/jbc.272.48.30096
44. Pierre K, Pellerin L (2005) Monocarboxylate transporters in the central nervous system: distribution, regulation and function. J Neurochem 94:1–14. doi:10.1111/j.1471-4159.2005.03168.x
45. Deodato F, Boenzi S, Santorelli FM et al (2006) Methylmalonic and propionic aciduria. Am J Med Genet C Semin Med Genet 142C:104–112. doi:10.1002/ajmg.c.30090
46. Rodríguez-Pombo P, Sweetman L, Ugarte M (1992) Primary cultures of astrocytes from rat as a model for biotin deficiency in nervous tissue. Mol Chem Neuropathol 16:33–44
47. Chandler CS, Ballard FJ (1985) Distribution and degradation of biotin-containing carboxylases in human cell lines. Biochem J 232:385–393
48. Daum RS, Scriver CR, Mamer OA et al (1973) An inherited disorder of isoleucine catabolism causing accumulation of alpha-methylacetoacetate and alpha-methyl-beta-hydroxybutyrate, and intermittent metabolic acidosis. Pediatr Res 7:149–160. doi:10.1203/00006450-197303000-00007
49. Pellerin L, Magistretti PJ (1994) Glutamate uptake into astrocytes stimulates aerobic glycolysis: a mechanism coupling neuronal activity to glucose utilization. Proc Natl Acad Sci USA 91:10625–10629. doi:10.1073/pnas.91.22.10625
50. Kao-Jen J, Wilson JE (1980) Localization of hexokinase in neural tissue: electron microscopic studies of rat cerebellar cortex. J Neurochem 35:667–678. doi:10.1111/j.1471-4159.1980.tb03706.x
51. Snyder CD, Wilson JE (1983) Relative levels of hexokinase in isolated neuronal, astrocytic, and oligodendroglial fractions from rat brain. J Neurochem 40:1178–1181. doi:10.1111/j.1471-4159.1983.tb08111.x
52. Murín R, Verleysdonk S, Rapp M et al (2006) Immunocytochemical localization of 3-methylcrotonyl-CoA carboxylase in cultured ependymal, microglial and oligodendroglial cells. J Neurochem 97:1393–1402. doi:10.1111/j.1471-4159.2006.03819.x
53. Abood LG, Geiger A (1955) Breakdown of proteins and lipids during glucose-free perfusion of the cat's brain. Am J Physiol 182:557–560

Neurochem Res
DOI 10.1007/s11064-008-9895-2

ORIGINAL PAPER

Glial Metabolism of Valine

Radovan Murín · Ghasem Mohammadi · Dieter Leibfritz · Bernd Hamprecht

Accepted: 11 December 2008

Abstract The three essential amino acids, valine, leucine and isoleucine, constitute the group of branched-chain amino acids (BCAAs). BCAAs are rapidly taken up into the brain parenchyma, where they serve several distinct functions including that as fuel material in brain energy metabolism. As one function of astrocytes is considered the production of fuel molecules that support the energy metabolism of adjacent neural cells in brain. Astroglia-rich primary cultures (APC) were shown to rapidly dispose of the BCAAs, including valine, contained in the culture medium. While the metabolisms of leucine and isoleucine by APC have already been studied in detail, some aspects of valine metabolism remained to be determined. Therefore, in the present study an NMR analysis was performed to identify the ^{13}C-labelled metabolites that are generated by APC during catabolism of [U-^{13}C]valine and that are subsequently released into the incubation medium. The results presented show that APC (1) are potently disposing of the valine contained in the incubation medium; (2) are capable of degrading valine to the tricarboxylic acid (TCA) cycle member succinyl-CoA; and (3) release into the extracellular milieu valine catabolites and compounds generated from them such as [U-^{13}C]2-oxoisovalerate, [U-^{13}C]3-hydroxyisobutyrate, [U-^{13}C]2-methylmalonate, [U-^{13}C]isobutyrate, and [U-^{13}C]propionate as well as several TCA cycle-dependent metabolites including lactate.

Keywords Astroglia · Energy metabolism · Valine · Branched-chain amino acid · Branched-chain 2-oxoacid · 2-Oxoisovalerate · 3-Hydroxyisobutyrate

This article is dedicated to Dr. George DeVries.

R. Murín · B. Hamprecht (✉)
Interfaculty Institute for Biochemistry, University of Tuebingen, Hoppe-Seyler-Str. 4, 72076 Tuebingen, Germany
e-mail: bernd.hamprecht@uni-tuebingen.de

G. Mohammadi · D. Leibfritz
Institute for Organic Chemistry, University of Bremen, Bremen, Germany

Introduction

Glucose is considered the major fuel molecule for sustaining brain energy metabolism. However, also other compounds imported into the brain can be oxidized and serve as "minor" substrates in brain energy metabolism. Valine together with isoleucine and leucine constitutes the group of branched-chain amino acids (BCAAs). These are transported through the blood-brain barrier into the brain parenchyma [1–4]. Although in brain BCAAs appear to be predominantly metabolized [5, 6], they also fulfill other distinct tasks [7–9]. The most prominent among them are the roles as vehicle molecules for nitrogen import into the brain parenchyma and as shuttle molecules for the exchange of nitrogen in the glutamate/glutamine cycle [10, 11]. BCAAs are recognized as a significant source of nitrogen for the synthesis of non-essential amino acids in brain, especially glutamate and glutamine [7]. Catabolic disposal of BCAA-carbon skeletons has an impact on the maintenance of the physiological functions of neural tissue. This is made obvious by the fact that disorders in utilization of BCAAs result in metabolic diseases usually characterized by neuropathological symptoms [12].

In contrast to the metabolism of leucine by neural cells and tissue, that of valine remained to be investigated in detail. The cells of the brain parenchyma readily metabolize leucine [6]. The capacity of brain tissue to metabolize

Published online: 06 January 2009

also valine can be deduced from experiments with brain slices, which showed that brain cells oxidize the cognate 2-oxo acid of valine, 2-oxoisovaleric acid (Fig. 1 [13]).

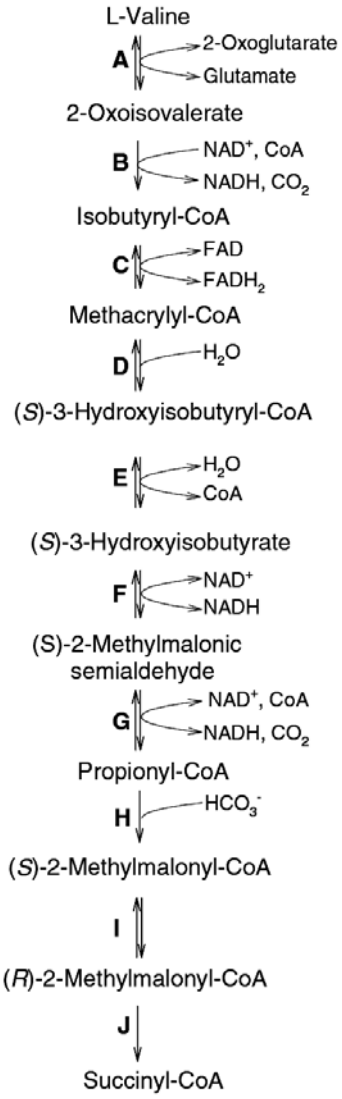

Fig. 1 Scheme of the pathway of L-valine catabolism (modified version of the pathway presented by Sweetman and Williams [12] and Murín et al. [18]). The first two enzymes of the pathway, branched-chain amino acid aminotransferase (*A*) and branched-chain 2-oxo acid dehydrogenase (*B*), are common for all three BCAAs and their cognate branched-chain 2-oxo acids, respectively. The isobutyryl-CoA thus generated is subsequently converted into propionyl-CoA in a sequence of five enzymatic reactions catalyzed by 2-methylacyl-CoA dehydrogenase (*C*), enoyl-CoA hydratase (*D*), 3-hydroxyisobutyryl-CoA deacylase (*E*), 3-hydroxyisobutyrate dehydrogenase (*F*), and methylmalonic semialdehyde dehydrogenase (*G*). Propionyl-CoA is transformed to the member of the citrate cycle, succinyl-CoA, by the series of enzymatic reactions catalyzed by propionyl-CoA carboxylase (*H*), methylmalonyl-CoA racemase (*I*), and methylmalonyl-CoA mutase (*J*)

Investigation of the ability to metabolize BCAAs by different types of cultured neural cells revealed the high capacity of neural cells to dispose of valine and the other two BCAAs from their culture medium either in the presence of glucose [14–16] or under hypoglycemic conditions [16]. Especially the metabolism of valine seems to be important in the process of glutamate translocation between astrocytes and neurons during glutamatergic signaling [17]. Recently, cultured astroglial cells have been shown to release in their medium 3-hydroxyisobutyrate, a metabolite of valine [18].

The catabolic pathway of valine consists of several enzymatic steps and results in the formation of succinyl-CoA (Fig. 1), a member of the tricarboxylic acid (TCA) cycle. Astrocytes which are considered to serve as "fuel processing plants" for neurons and possibly other neural cells [19–21] are likely to provide other cells of the brain parenchyma with certain nutrients [22]. The expression of a few enzymes required [11, 23] or specific [24] for valine catabolism has been investigated in astrocytes. Cultured astrocytes remove BCAAs from their incubation medium and metabolize them [15]. Although the catabolites of leucine [15, 24] and isoleucine [25] are known, the compounds derived from valine that astrocytes generate and release into their extracellular milieu remain to be determined. Therefore, the aim of the present investigation was to fill this gap in our knowledge and (1) study the ability of astroglial cells to metabolize valine, (2) identify the valine-metabolites released by cultured astroglial cells and consider them as potential fuel molecules for other brain cells, and (3) examine the possibility that the carbon skeleton of valine appears in the TCA cycle as succinyl-CoA, thereby contributing to the anaplerotic function of the astroglial cells.

Materials and Methods

Materials

[U-^{13}C, ^{15}N]L-Valine was purchased from Cambridge Isotope Laboratories (Andover, USA); this labelled valine was purchased despite the commercial availability of [U-^{13}C]valine, since it was considerably cheaper and the presence of ^{15}N did not interfere with the analysis of ^{13}C-labelled metabolites. For convenience's sake [U-^{13}C, ^{15}N]L-valine is henceforth called [U-^{13}C]Val. Dulbecco's modified Eagle's medium (DMEM) was from Gibco-Invitrogen (Karlsruhe, Germany). Bovine serum albumin (BSA) was purchased from Roche Diagnostics (Mannheim, Germany). Fetal calf serum (FCS) was from Biochrom (Berlin, Germany). Penicillin G and streptomycin sulfate were from Serva (Heidelberg, Germany). Deuterium oxide

(D_2O), deuterium chloride (DCl), sodium deuterium oxide (NaOD) were obtained from E. Merck (Darmstadt, Germany) and (trimethylsilyl)propionic-2,2,3,3-D_4 acid (TSP) as well as NMR tubes from Aldrich (Steinheim, Germany). Sterile plastic material and culture dishes for cell culture were from Nunc (Wiesbaden, Germany) and Greiner (Frickenhausen, Germany).

Cell Culture

Astroglia-rich primary cultures were derived from whole brains of newborn rats and maintained as described [26]. The cells were seeded in plastic culture dishes (9 cm in diameter) at a plating density of 5×10^6 viable cells per dish and incubated in culture medium [90% (v/v) DMEM, 10% (v/v) FCS, 20 units/ml penicillin G, and 20 µg/ml streptomycin sulfate; the initial concentration of glucose in DMEM was 25 mM, that in the serum was not determined]. The culture medium was renewed after 7 days and 24 h before each experiment. The present studies were carried out with 15-day-old cultures.

Incubation of APC with [U-^{13}C]valine

After removal of the culture medium, the cells were washed twice with 5 ml of a minimal medium (109.5 mM NaCl, 5.4 mM KCl, 1.8 mM $CaCl_2$, 0.8 mM $MgSO_4$, 44 mM $NaHCO_3$, 0.9 mM NaH_2PO_4, 7 mM glucose; osmolarity 320 mOsmol/l) and incubated with 5 ml of minimal medium supplemented with 0.8 mM [U-^{13}C]Val in a Heraeus cell incubator containing a humidified atmosphere of 10% CO_2/90% air for 12, 24 and 36 h. Thereafter, the media of ten culture dishes (50 ml) were combined, clarified by centrifugation (10 000 g, 4 °C, 10 min) and lyophilized.

Cell Viability Test

Cell viability was assessed by determining the appearance of lactate dehydrogenase in the medium using the modification [25] of a described method [27]. By definition, 0% viability corresponds to 100% activity of lactate dehydrogenase in the medium [28].

Protein Determination

Protein content was determined according to Bradford [29] using bovine serum albumin as a standard.

NMR Analysis

The lyophilizate of 50 ml incubation media was dissolved in 1,000 µl of D_2O. The solutions were centrifuged and the supernatants were transferred to NMR tubes. In order to prevent glutamine carbamate formation [30] the solutions were adjusted to a pH value of 7 with DCl and NaOD. All ^{1}H-NMR and ^{13}C-NMR spectra of media were recorded on a Bruker DRX 600-MHz spectrometer, operating at a frequency of 600 MHz for ^{1}H and 150.9 MHz for ^{13}C measurements. Signal assignments were confirmed by two-dimensional (2D) NMR experiments using heteronuclear single quantum coherence (HSQC) spectroscopy and heteronuclear single quantum coherence combined with homonuclear total coherence transfer (HSQC-TOCSY) spectroscopy. The 2D-HSQC and 2D-HSQC-TOCSY spectra were acquired on a Bruker DRX 600-MHz spectrometer using a 5-mm H, C, N inverse triple resonance probe with shielded gradients. An acquisition time of 256 ms was used for HSQC and HSQC-TOCSY. Gradients were shaped by a waveform generator and amplified by a Bruker Acustar II amplifier. Sinusoidal z gradients of 1 ms duration and a recovery time of 100 µs were used for the echo/antiecho gradient selection. A gradient finetuning (40:10.08) was performed to obtain optimal signal intensity. Low-power adiabatic composite pulse decoupling with WURST [31] was used for heteronuclear decoupling. Acquisitions consisted of 1024 t1 increments with 24 scans per increment. The assignment of metabolites by two-dimensional NMR techniques was performed as described previously [32].

As already in the analogous studies of leucine [24] and isoleucine [25] metabolism, the limited number of cultured cells available prevented a corresponding NMR analysis of intracellularly located metabolites derived from ^{13}C-labelled valine. ^{15}N NMR studies aiming at the elucidation of the metabolism of the amino nitrogen of valine were not pursued.

^{1}H-NMR Spectra

For ^{1}H-NMR spectra 128 scans were accumulated with a flip angle of 90° and a repetition time of 20 s. The scans were accumulated using a 5-mm H,C,N inverse triple resonance probe, (spectral width 7200 Hz, data size 16 K, zero filling to 32 K). All ^{1}H NMR spectra were calibrated on the methyl signal of lactate at 1.33 ppm.

^{13}C-NMR Spectra

^{13}C-NMR spectra were recorded with a 5-mm ^{1}H/^{13}C dual probe: 20,000 accumulations (repetition time 3 s; flip angle 90°), composite pulse decoupling with WALTZ-16, spectral width 33.198 Hz, data size 32 K, zero filling to 64 K. Chemical shifts were referenced to the C-3 signal of lactate at 21.3 ppm.

Absolute Quantification

The concentration of lactate was determined from fully relaxed ^{1}H-NMR spectra of media using TSP as an external standard. The pool size of other metabolites was determined using ^{13}C-NMR spectra. The ^{13}C signal integrals of various metabolites were corrected for partial saturation nuclear Overhauser enhancement (NOE) effect by comparison with a standard mixture of amino acids.

Results

The lack of FCS, essential amino acids and vitamins in minimal medium may affect the viability and properties of the cultured cells. Therefore, the amount of protein in APCs and the release of lactate dehydrogenase into the incubation medium were determined. Indeed, the protein content of APC decreased from 1.8 ± 0.2 mg/culture dish at the beginning of the incubation with minimal medium supplemented with 0.8 mM [U-^{13}C]Val to 1.6 ± 0.1, 1.5 ± 0.1 and 1.4 ± 0.1 mg/culture dish after 12, 24 and 48 h of incubation, respectively. The total activity of lactate dehydrogenase in a cell homogenate at the beginning of the incubation period (t = 0 h) amounted to 2.2 ± 0.2 U/mg protein. Incubation of APC in minimal medium supplemented with 0.8 mM [U-^{13}C]Val resulted in the appearance of up to 8% of total lactate dehydrogenase activity in the culture media during all incubation times indicating a cellular viability of greater 90%.

Catabolism of [U-^{13}C]valine by APC

To analyze their ability to metabolize valine, cultured astroglial cells were incubated in the presence of [U-^{13}C]Val. APCs rapidly disposed of the [U-^{13}C]Val contained in the incubation media (Fig. 2a) and subsequently released several ^{13}C-labelled metabolites (Figs. 2b, c, 3; Table 1) as determined by ^{13}C-NMR-analysis of lyophilized culture media. The following compounds, which are either intermediates of the valine catabolic pathway or their derivatives, were present in the incubation media: 2-oxoisovalerate, 3-hydroxyisobutyrate, 2-methylmalonate, isobutyrate, and propionate. Of all detected valine catabolites the concentration of 2-oxoisovalerate was the highest. The concentration of this compound was maximal after 12–24 h of incubation and declined thereafter (Fig. 2b). The concentration of 3-hydroxyisobutyrate, the second most abundant catabolite of valine in the medium after 24 and 48 h of incubation, was still increasing at 48 h of incubation time, when its concentration in the medium exceeded even that of 2-oxoisovalerate

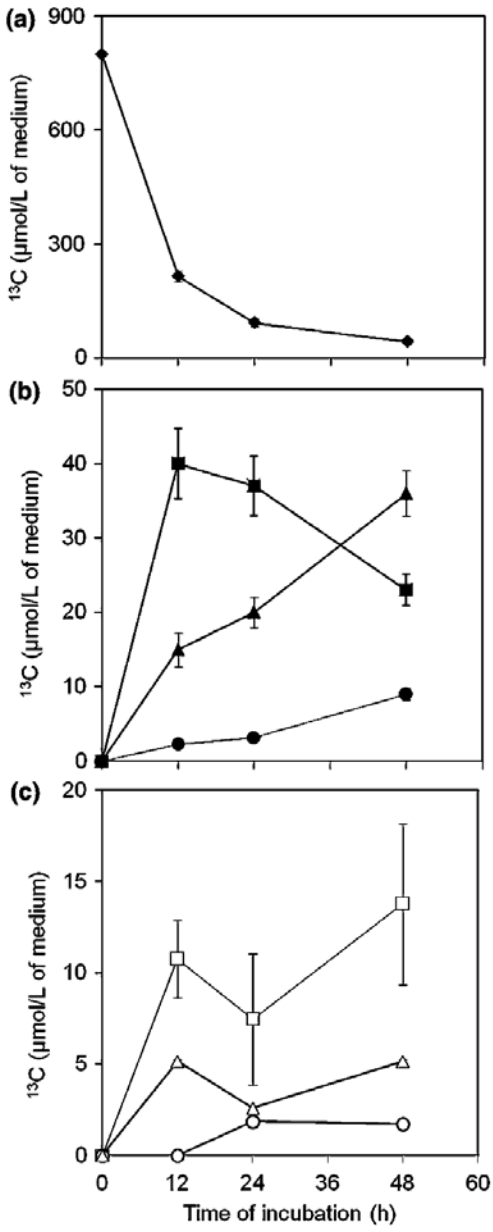

Fig. 2 Changes with incubation time in the concentrations of [U-^{13}C]valine (**a**) and of its ^{13}C-labelled metabolites released into the incubation medium of APC (**b**,**c**). The APCs (15 days old) were incubated in minimal medium (see "Materials and methods") supplemented with 0.8 mM [U-^{13}C]valine. The concentration of [U-^{13}C]valine (**a**) was determined after 0, 12, 24 and 48 h. In **b**,**c** are shown the levels of ^{13}C-labelled compounds derived from [U-^{13}C]valine and released by APCs into the incubation medium: 2-oxoisovalerate (■), 3-hydroxyisobutyrate (▲), propionate (●), isobutyrate (□), 2-methylmalonate (○), and the sum of lactate-isotopomers (△). The data are presented as mean ± SD from four independent experiments. The error bars have been omitted if they were smaller than the symbols depicting the mean values

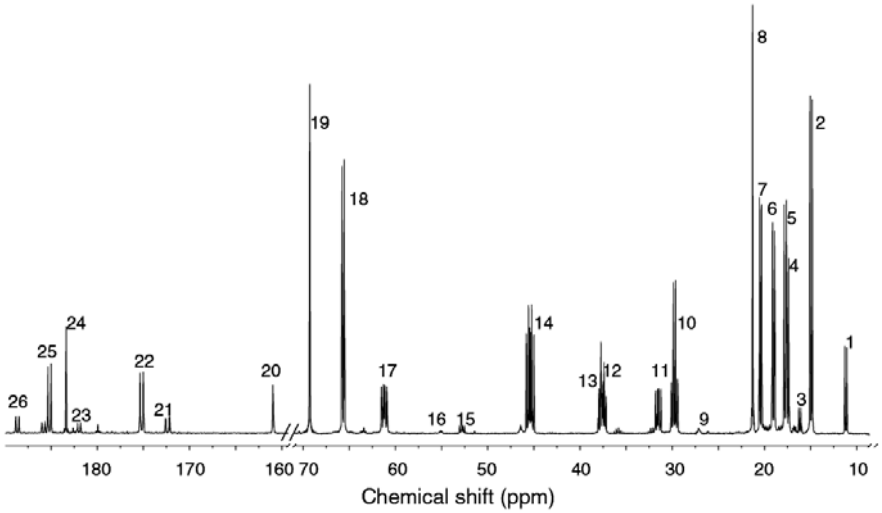

Fig. 3 ^{13}C-NMR spectrum of medium from astrocytes incubated with [U-^{13}C]valine (0.8 mM) and glucose (7 mM) for 48 h. (*1*) Propionate C3, (*2*) 3-hydroxyisobutyrate C4. (*3*) 2-methylmalonate C4, (*4*) 2-oxoisovalerate C4,4′, (*5*) valine C4′, (*6*) valine C4, (*7*) isobutyrate C3,3′, (*8*) lactate C3, (*9*) glutamine C3, (*10*) valine C3, (*11*) propionate C2, (*12*) isobutyrate C2, (*13*) 2-oxoisovalerate C3, (*14*) 3-hydroxyisobutyrate C2, (*15*) 2-methylmalonate C2, (*16*) glutamine C2, (*17*) valine C2, (*18*) 3-hydroxyisobutyrate C3, (*19*) lactate C2, (*20*) bicarbonate, (*21*) 2-oxoisovalerate C1, (*22*) valine C1, (*23*) 2-methylmalonate C1, (*24*) lactate C1, (*25*) 3-hydroxyisobutyrate C1, (*26*) isobutyrate C1

(Fig. 2b). Also the concentrations of three other ^{13}C-labelled valine catabolites detected in media, propionate (Fig. 2b), 2-methylmalonate (Fig. 2b), and isobutyrate (Fig. 2c), varied with the time of incubation. The uniformly labelled isotopomers of the catabolic pathway have been identified by their ^{13}C, ^{13}C-coupling pattern as shown for 3-hydroxyisobutyrate (Fig. 4a), 2-methylmalonate (Fig. 4b). Note that the coupling constants between sp^3–sp^3 carbons are around 35 Hz while those for sp^2–sp^3 carbon bonds are around 50 Hz.

After its formation from propionyl-CoA, succinyl-CoA (Fig. 1) can be further metabolized within the TCA cycle. Some of the ^{13}C-labelled members of the TCA cycle are the obvious precursors of ^{13}C-labelled compounds found in the incubation medium after incubation of astroglial cells with the labelled valine, i.e., glutamine, pyroglutamate and lactate (Fig. 3; Table 1). Starting from propionyl-CoA with a uniformly labelled propionyl residue [1,2,3-^{13}C]succinyl-CoA is formed, which gives rise to the equally populated isotopomers [1,2,3-^{13}C]succinate and [2,3,4-^{13}C]succinate. From the subsequent TCA cycle members further TCA cycle derivatives are formed, i.e., [1,2,3-^{13}C]malate/[2,3,4-^{13}C]malate is transformed into pyruvate via malic enzyme and subsequently into [1,2,3-^{13}C]lactate/[2,3-^{13}C]lactate (Fig. 4c); [2,3-^{13}C]2-oxoglutarate/[2,3,4-^{13}C]2-oxoglutarate is transaminated into [2,3-^{13}C]glutamate/[2,3,4-^{13}C]glutamate, which are further transformed into [2,3-^{13}C]glutamine/[2,3,4-^{13}C]glutamine. The signal intensities of the triple labelled isotopomers of glutamine were too low for quantification.

Discussion

The influx of valine into the brain [1–4] raises the question of the metabolic fate of this amino acid. Since astrocytes play an important role in energy metabolism [19], the astrocytic catabolism of valine was investigated by offering [U-^{13}C]Val to APC and analyzing the incubation media for the presence of ^{13}C-labelled compounds derived from labelled valine. The results of the analysis confirm the ability of astroglial cells to dispose of the valine contained in their culture medium [15]. They also demonstrate that astroglial cells release into their milieu several metabolites generated in the catabolic pathway of valine. Furthermore, the results show that these cells have the capability of funneling the valine-carbon skeleton into the TCA cycle.

The extent of appearance of lactate dehydrogenase in the incubation medium was used as a measure for the extent of cell death. Cell death was quite limited, since only 8% of the total activity of this enzyme appeared in the medium. Thus, of the metabolites contained in the cultured cells only a small, practically negligible amount would become part of the large extracellular pool by cell death rather than by transport processes. The constancy of lactate dehydrogenase activity in the culture media over the entire period of incubation is taken as an indication for the occurrence of cell death and concomitant indiscriminate shedding of metabolites only at the onset of the experimental incubations.

Table 1 ^{13}C-Coupling constants for valine and for its metabolites found released into the incubation medium of astroglia-rich primary cultures after 48 h of incubation

Compound	C_x-atom	Chemical shift (ppm)	Coupling constant (Hz)
[U-^{13}C]Valine	1	175.23	$J_{C1C2} = 54.1$
	2	61.20	$J_{C2C3} = 34.2$
	3	29.85	$J_{C3C4,4'} = 34.2$
	4	19.08	
	4′	17.80	
[U-^{13}C]Isobutyrate	1	185.80	$J_{C1C2} = 51.3$
	2	37.60	$J_{C2C3} = 34.2$
	3,3′	20.48	
[U-^{13}C]Propionate	1	179.80	$J_{C1C2} = 51.4$
	2	31.35	$J_{C2C3} = 34.6$
	3	11.60	
[1,2,3-^{13}C]Lactate	1	183.26	$J_{C1C2} = 56.0$
	2	69.15	$J_{C2C3} = 36.6$
	3	21.33	
[1,2-^{13}C]Lactate	1	183.26	$J_{C1C2} = 56.0$
	2	69.15	
[2,3-^{13}C]Lactate	2	69.15	$J_{C2C3} = 36.6$
	3	21.33	
[U-^{13}C]2-Oxoisovalerate	1	171.94	$J_{C1C2} = 61.0$
	2	212.13	$J_{C2C3} = 38.1$
	3	37.70	$J_{C1C3} = 11.7$
	4,4′	17.63	$J_{C3C4,4'} = 34.6$
[U-^{13}C]3-Hydroxyisobutyrate	1	185.15	$J_{C1C2} = 51.3$
	2	45.44	$J_{C2C3} = 37.1$
	3	65.71	
	4	15.09	$J_{C2C4} = 33.8$
[1,2,4-^{13}C]2-Methylmalonate	1,3	181.98	$J_{C1C2} = 50.4$
	2	52.75	$J_{C2C4} = 34.2$
	4	16.23	
[2,3-^{13}C]Citrate	2	46.44	$J_{C2C3} = 37.9$
	3	76.31	
[2,3-^{13}C]Glutamine	2	55.11	$J_{C2C3} = 35.4$
	3	27.19	
[2,3-^{13}C]Pyroglutamate	2	59.11	$J_{C2C3} = 35.1$
	3	26.32	

The subscript of *J*, the spin–spin coupling constant, defines the coupled carbon atoms. The carbon atoms of the various compounds are numbered according to IUPAC rules. The concentration of labelled citrate in the incubation medium was too low for quantification

The catabolism of valine, similar to that of the other two BCAAs, starts with a reversible transamination catalyzed by BCAA aminotransferase, resulting in the formation of the cognate branched-chain 2-oxo acid, 2-oxoisovalerate (Fig. 1). 2-Oxoglutarate, which serves as the acceptor of the amino group of valine in this process, is transformed to glutamate. The import of valine and the other BCAAs into the brain and their subsequent transamination play major roles in brain nitrogen metabolism. Thus, BCAAs are considered to be vehicles for the import into the brain parenchyma of the nitrogen needed for the biosynthesis of amino acids of intermediary metabolism/neurotransmission such as glutamate and glutamine [7]. Furthermore, together with their cognate branched-chain 2-oxo acids, they can participate in maintaining the glutamate–glutamine cycle between astrocytes and neurons [9–11, 20, 21]. Indeed, cultured astrocytes were shown to release also 2-oxoisocaproate [24] and 2-oxo-3-methylbutyrate [25]. It is very likely that—similar to 2-oxoisocaproate—2-oxoisovalerate crosses the plasma membrane of astroglial cells by facilitated transport mediated by monocarboxylate transporter 1 [33]. 2-Oxoisovalerate present in the interstitial fluid in brain can be taken up into neurons, where in a reaction accompanying the glutamate/glutamine cycle it could serve as an acceptor of an NH_2 group [8, 11]. Although among BCAAs leucine is considered to play a major role as an amino group donor in glutamate and glutamine synthesis [7], valine may also take a significant part in glutamate-glutamine cycling during synaptic activity [17]. Indeed, CNS neurons express both a monocarboxylate transporter [34] and the cytosolic isoform of BCAT [23]. Another role of 2-oxoisovalerate in brain is its contribution to energy metabolism as a "minor" substrate [13] when entering irreversible degradation initiated by BCKDH. This multienzyme complex is expressed in brain [23, 35], while its cell-type specific expression in brain is still unknown. However, in various types of cultured neural cells, BCKDH is ubiquitously expressed [23].

Another valine metabolite released into the culture medium of APC is 3-hydroxyisobutyrate ([18], present study). This monocarboxylate may be crossing the membranes of neural cells by monocarboxylate transporters [33, 34] and subsequently re-enter the valine catabolic pathway in being processed by 3-hydroxyisobutyrate dehydrogenase (Fig. 1). This enzyme is ubiquitously expressed in cultured neural cell types and is detectable among brain proteins by Western blotting [18].

Besides 2-oxoisovalerate and 3-hydroxyisobutyrate, the metabolites isobutyrate, 2-methylmalonate and propionate are detectable in valine-containing media of cultured astroglial cells. The CoA esters of these three compounds are intermediates in the valine degradative pathway and are located in the mitochondria. Since there is no mechanism known for the transport of CoA esters through the inner mitochondrial membrane, the presence of the unesterified compounds in the medium indicates the hydrolysis of the CoA esters prior to their exit from mitochondria. The levels of isobutyrate and propionate in the media were high with

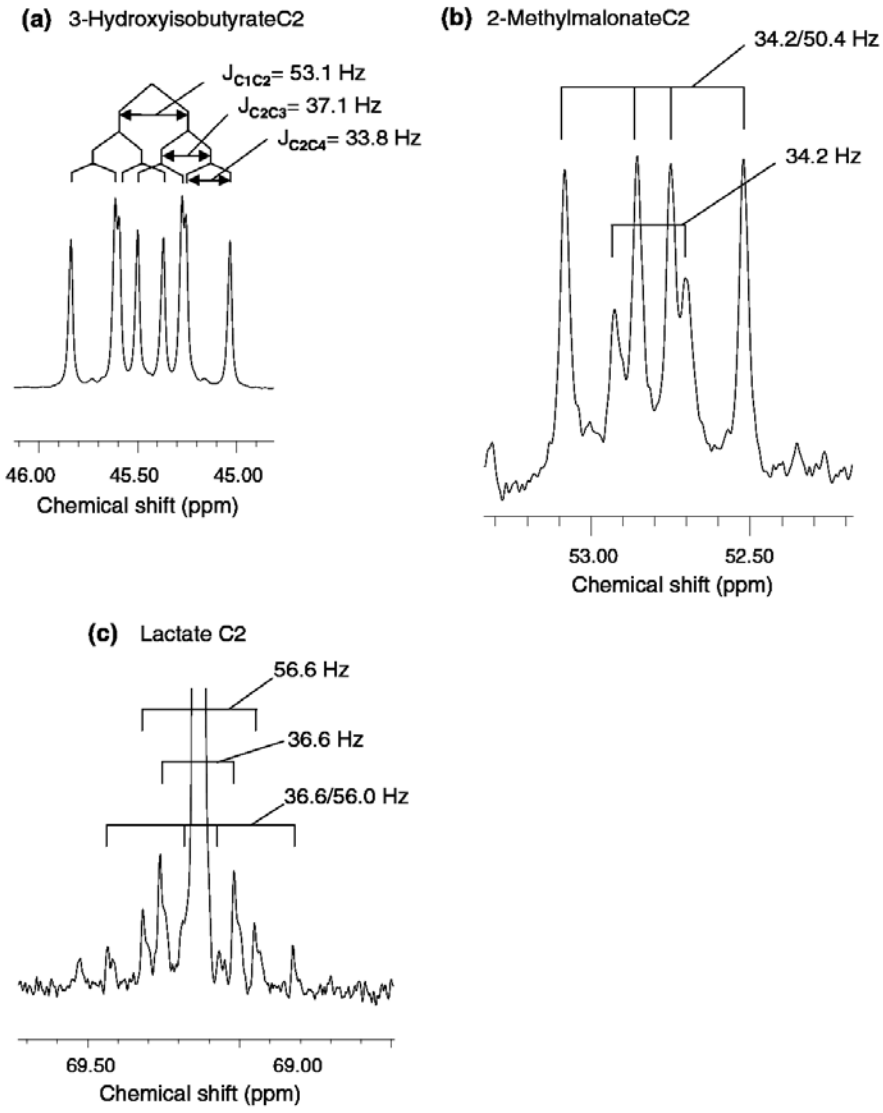

Fig. 4 Sections taken from the ^{13}C spectrum (Fig. 3) of the medium from a primary astrocyte culture that was incubated with [U-^{13}C]valine (0.8 mM) for 48 h. These sections show the multiplet structure at 3-hydroxyisobutyrate C2 (**a**; see Fig. 3, peak 14), 2-methylmalonate C2 (**b**; see Fig. 3, peak 15), and lactate C2 (**c**; see Fig. 3, peak 19)

respect to other released compounds. This is analogous to the release of 2-methylbutyrate, 3-hydroxy-2-methylbutyrate and propionate from astroglial cells when they are incubated with isoleucine [25]. The occurrence of isobutyrate in the incubation medium may not only be due to the hydrolysis of the thioester bond of isobutyryl-CoA and the subsequent release of the acylate from the cells, but may also be due to non-enzymic decarboxylation of 2-oxoisovalerate by reaction with hydrogen peroxide. Analogous to the 2-oxo-compounds pyruvate and 2-oxoglutarate [36, 37] 2-oxoisovalerate may react with H_2O_2 when it appears in cell culture media. This non-enzymatic mechanism underlies the protection of cultured neurons against hydrogen peroxide by pyruvate [38].

In addition to the compounds derived from intermediates of the valine degradative pathway and their metabolites, ^{13}C-labelled pyroglutamate, glutamine and lactate were detected in the media. Pyroglutamate may appear in media due to two distinct processes: (1) As a product of enzymatically catalized reactions such as the conversion of glutamate in glutathione metabolism [39] and the the action of pyroglutamyl-peptide hydrolase (EC 3.4.11.8; [40]), or more likely (2) as a product of the non-enzymatic conversion of glutamine during sample processing [41]. The presence of pyroglutamate and glutamine in the media indicates that APC are not only capable of degrading valine all the way to propionyl-CoA but apparently also of converting the latter into the TCA cycle member succinyl-CoA.

This conversion requires passing through the steps catalyzed by the enzymes propionyl-CoA carboxylase, methylmalonyl-CoA racemase and methyl-malonyl-CoA mutase (Fig. 1). The formation of succinyl-CoA could serve also an anaplerotic function. Succinyl-CoA proceeds in the TCA cycle to malate. This can undergo oxidative decarboxylation by malic enzyme giving rise to pyruvate [19], which on reduction by NADH becomes lactate. Further progression in the TCA cycle would lead to 2-oxoglutarate that could become the precursor of glutamate and glutamine. In brain, the carbon atoms of glutamate and glutamine are derived mainly from glucose but to a lesser extent also from other unspecified carbon sources [42, 43]. Relevant in this respect may be that BCAAs can be readily taken up into the brain [4] and that glial cells are capable of catabolizing them [15]. This catabolism results in the incorporation of their carbon atoms also into the glutamine molecules released into the extracellular space of the astrocytes [24, 25, present study]. Therefore it may be hypothesized that BCAAs serve as a minor source of the carbon atoms for the neural generation of glutamate and glutamine.

The reductionistic experimental conditions used for this study differ considerably from the physiological situation. The strongest bearings for glial metabolism may have the composition of the medium, the ratio of the volumes of the extracellular milieu and of the cell, and the lack of neuron-glia communication. Nevertheless, in view of the uptake and metabolism of branched-chain amino acids in brain described in the introduction, the results presented can be considered to reflect, at least qualitatively, the ability of astrocytes to catabolize valine and to release some of the metabolites thus generated into their extracellular milieu. However, the considerably more complex quantitative analysis of valine catabolism in astrocytes in situ remains still to be tackled. The astrocytic release of intermediates of BCAA catabolism [15, 18, 24, 25] is in agreement with the hypotheses that one of the roles of brain astrocytes may be to serve as "fuel processing plants" [19–21] and that BCAAs, including valine, can serve in brain energy metabolism as a minor fuel molecule.

References

1. Battistin L, Grynbaum A, Lajtha A (1971) The uptake of various amino acids by the mouse brain in vivo. Brain Res 29:85–99. doi:10.1016/0006-8993(71)90419-7
2. Oldendorf WH (1971) Brain uptake of radiolabeled amino acids, amines, and hexoses after arterial injection. Am J Physiol 221:1629–1639
3. Oldendorf WH (1971) Uptake of radiolabeled essential amino acids by brain following arterial injection. Proc Soc Exp Biol Med 136:385–386
4. Smith QR, Momma S, Aoyagi M et al (1987) Kinetics of neutral amino acid transport across the blood–brain barrier. J Neurochem 49:1651–1658. doi:10.1111/j.1471-4159.1987.tb01039.x
5. Swaiman KF, Milstein JM (1965) Oxidation of leucine, isoleucine and related ketoacids in developing rabbit brain. J Neurochem 12:981–986. doi:10.1111/j.1471-4159.1965.tb10257.x
6. Chaplin ER, Goldberg AL, Diamond I (1976) Leucine oxidation in brain slices and nerve endings. J Neurochem 26:701–707. doi:10.1111/j.1471-4159.1976.tb04440.x
7. Yudkoff M, Nissim I, Kim S et al (1983) [^{15}N]leucine as a source of [^{15}N]glutamate in organotypic cerebellar explants. Biochem Biophys Res Commun 115:174–179. doi:10.1016/0006-291X(83)90985-3
8. Yudkoff M (1997) Brain metabolism of branched-chain amino acids. Glia 21:92–98. doi:10.1002/(SICI)1098-1136(199709)21:1<92::AID-GLIA10>3.0.CO;2-W
9. Murín R, Hamprecht B (2008) Metabolic and regulatory roles of leucine in neural cells. Neurochem Res 33:279–284. doi:10.1007/s11064-007-9444-4
10. Yudkoff M, Daikhin Y, Nelson D et al (1996) Neuronal metabolism of branched-chain amino acids: flux through the aminotransferase pathway in synaptosomes. J Neurochem 66:2136–2145
11. Bixel MG, Hutson SM, Hamprecht B (1997) Cellular distribution of branched-chain amino acid aminotransferase isoenzymes among rat brain glial cells in culture. J Histochem Cytochem 45:685–694
12. Sweetman L, Williams JC (2001) Branched chain organic aciduria. In: Scriver C, Beaudet A, Sly W et al (eds) The metabolic and molecular basis of inherited disease. McGraw-Hill, Philadelphia, pp 2125–2163
13. Brand K (1981) Metabolism of 2-oxoacid analogues of leucine, valine and phenylalanine by heart muscle, brain and kidney of the rat. Biochim Biophys Acta 677:126–132
14. Yudkoff M, Daikhin Y, Lin ZP et al (1994) Interrelationships of leucine and glutamate metabolism in cultured astrocytes. J Neurochem 62:1192–1202
15. Bixel MG, Hamprecht B (1995) Generation of ketone bodies from leucine by cultured astroglial cells. J Neurochem 65:2450–2461
16. Honegger P, Braissant O, Henry H et al (2002) Alteration of amino acid metabolism in neuronal aggregate cultures exposed to hypoglycaemic conditions. J Neurochem 81:1141–1151. doi:10.1046/j.1471-4159.2002.00888.x
17. Bak LK, Johansen ML, Schousboe A et al (2007) Among the branched-chain amino acids, only valine metabolism is up-regulated in astrocytes during glutamate exposure. J Neurosci Res 85:3465–3470. doi:10.1002/jnr.21347
18. Murín R, Schaer A, Kowtharapu BS et al (2008) Expression of 3-hydroxyisobutyrate dehydrogenase in cultured neural cells. J Neurochem 105:1176–1186. doi:10.1111/j.1471-4159.2008.05298.x
19. Hamprecht B, Dringen R (1995) Energy metabolism. In: Kettenmann H, Ranson B (eds) Neuroglia. Oxford University Press, New York, pp 473–487
20. Zwingmann C, Leibfritz D (2003) Regulation of glial metabolism studied by ^{13}C NMR. NMR Biomed 16:370–399. doi:10.1002/nbm.850
21. Zwingmann C, Leibfritz D (2007) Glial-neuronal shuttle systems (chapter 1.2 brain energetics: integration of molecular and cellular processes). In: Gibson GE, Dienel G (Eds.) Handbook of Neurochemistry & molecular neurobiology 3rd Edn, vol 5. Springer, New York
22. Pellerin L, Magistretti PJ (1994) Glutamate uptake into astrocytes stimulates aerobic glycolysis: a mechanism coupling neuronal activity to glucose utilization. Proc Natl Acad Sci USA 91:10625–10629. doi:10.1073/pnas.91.22.10625

23. Bixel M, Shimomura Y, Hutson S et al (2001) Distribution of key enzymes of branched-chain amino acid metabolism in glial and neuronal cells in culture. J Histochem Cytochem 49:407–418
24. Bixel MG, Engelmann J, Willker W et al (2004) Metabolism of [U-(13)C]leucine in cultured astroglial cells. Neurochem Res 29:2057–2067. doi:10.1007/s11064-004-6879-8
25. Murín R, Mohammadi G, Leibfritz D, et al (2008) Glial metabolism of isoleucine. Neurochem Res. doi:10.1007/s11064-008-9840-4
26. Hamprecht B, Löffler F (1985) Primary glial cultures as a model for studying hormone action. Methods Enzymol 109:341–345. doi:10.1016/0076-6879(85)09097-8
27. Vassault A (1983) Lactate dehydrogenase: UV-method with pyruvate and NADH. In: Bergmeyer HU (ed) Methods of enzymatic analysis, vol 3. Verlag Chemie, Weinheim, pp 118–126
28. Dringen R, Hamprecht B (1996) Glutathione content as an indicator for the presence of metabolic pathways of amino acids in astroglial cultures. J Neurochem 67:1375–1382
29. Bradford MM (1976) A rapid and sensitive method for the quantification of microgram quantities of protein utilizing the principle of protein-dye binding. Anal Biochem 72:248–254. doi:10.1016/0003-2697(76)90527-3
30. Martin M, Portais JC, Labousse J et al (1993) [1-^{13}C]glucose metabolism in rat cerebellar granule cells and astrocytes in primary culture. Evaluation of flux parameters by ^{13}C- and ^{1}H-NMR spectroscopy. Eur J Biochem 217:617–625. doi:10.1111/j.1432-1033.1993.tb18284.x
31. Kupće E, Freeman R (1995) Stretched adiabatic pulses for broadband spin inversion. J Magn Reson A 117:246–256. doi:10.1006/jmra.1995.0750
32. Willker W, Engelmann J, Brand A et al (1996) Metabolite identification in cell extracts and culture media by proton-detected 2D-H, C-NMR spectroscopy. J Magn Reson Anal 2:21–32
33. Bröer S, Schneider HP, Bröer A et al (1998) Characterization of the monocarboxylate transporter 1 expressed in Xenopus laevis oocytes by changes in cytosolic pH. Biochem J 333:167–174
34. Pierre K, Pellerin L (2005) Monocarboxylate transporters in the central nervous system: distribution, regulation and function. J Neurochem 94:1–14. doi:10.1111/j.1471-4159.2005.03168.x
35. Wagenmakers AJ, Schepens JT, Veldhuizen JA et al (1984) The activity state of the branched-chain 2-oxo acid dehydrogenase complex in rat tissues. Biochem J 220:273–281
36. O'Donnell-Tormey J, Nathan CF, Lanks K et al (1987) Secretion of pyruvate. An antioxidant defense of mammalian cells. J Exp Med 165:500–514. doi:10.1084/jem.165.2.500
37. Nath KA, Ngo EO, Hebbel RP et al (1995) Alpha-ketoacids scavenge H_2O_2 in vitro and in vivo and reduce menadione-induced DNA injury and cytotoxicity. Am J Physiol 268:C227–C236
38. Desagher S, Glowinski J, Prémont J (1997) Pyruvate protects neurons against hydrogen peroxide-induced toxicity. J Neurosci 17:9060–9067
39. Meister A (1988) Glutathione metabolism and its selective modification. J Biol Chem 263:17205–17208
40. Awadé AC, Cleuziat P, Gonzalès T et al (1994) Pyrrolidone carboxyl peptidase (Pcp): an enzyme that removes pyroglutamic acid (pGlu) from pGlu-peptides and pGlu-proteins. Proteins 20:34–51. doi:10.1002/prot.340200106
41. Martin M, Portais JC, Voisin P et al (1995) Comparative analysis of ^{13}C-enriched metabolites released in the medium of cerebellar and cortical astrocytes incubated with [1–^{13}C]glucose. Eur J Biochem 231:697–703. doi:10.1111/j.1432-1033.1995.tb20750.x
42. Shen J, Petersen KF, Behar KL et al (1999) Determination of the rate of the glutamate/glutamine cycle in the human brain by in vivo ^{13}C NMR. Proc Natl Acad Sci USA 96:8235–8240. doi:10.1073/pnas.96.14.8235
43. Shen J, Rothman DL, Behar KL, et al (2008) Determination of the glutamate–glutamine cycling flux using two-compartment dynamic metabolic modeling is sensitive to astroglial dilution. J Cereb Blood Flow Metab. doi:10.1038/jcbfm.2008.102

Molecular structure of sulphonamide with caroanhydrase inhibitory effects

Topiramat (TPM)	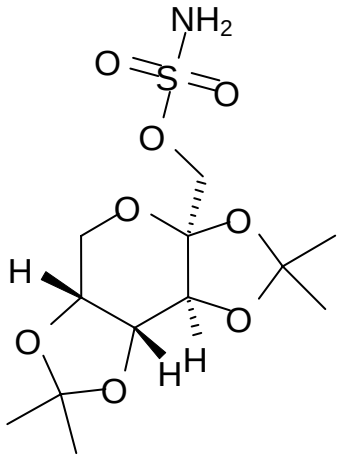
Acetazolamid (ACT)	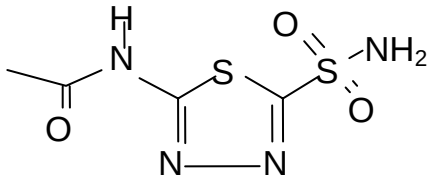
Ethoxzolamid ((ETZ)	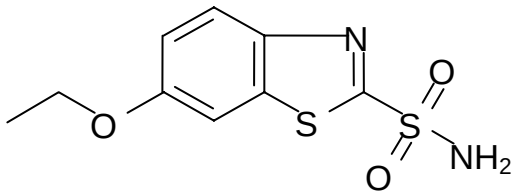
Compound **1**	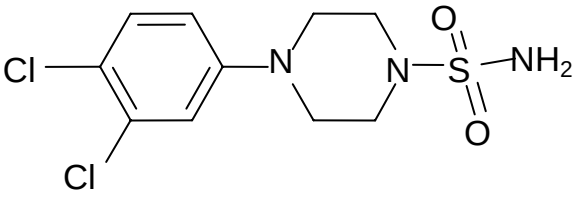
Compound **2**	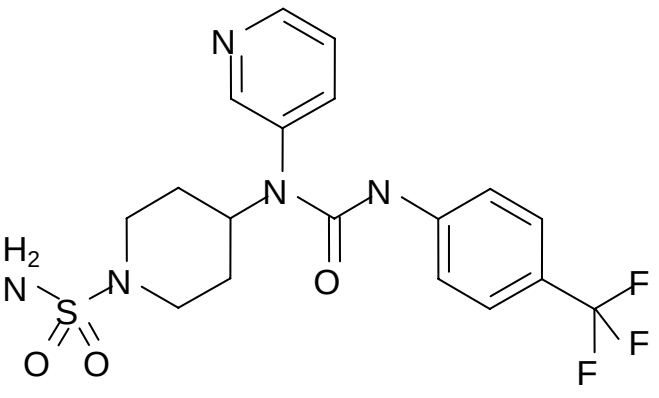

Compound **3**	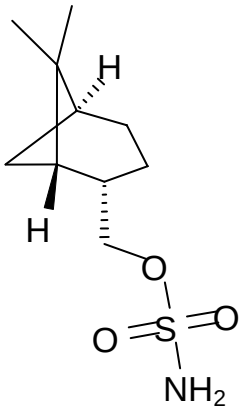
Compound **4**	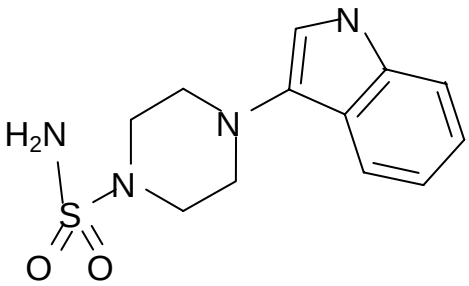
Compound **5**	NN